JBC Papers in Press. Published on November 17, 2016 as Manuscript M116.753053
The latest version is at http://www.jbc.org/cgi/doi/10.1074/jbc.M116.753053

Gibepyrone biosynthesis in the rice pathogen *Fusarium fujikuroi* is facilitated by a small polyketide synthase gene cluster

Slavica Janevska[1], Birgit Arndt[2], Eva-Maria Niehaus[1], Immo Burkhardt[3], Sarah M. Rösler[1,2], Nelson L. Brock[3], Hans-Ulrich Humpf[2], Jeroen S. Dickschat[3*], Bettina Tudzynski[1*]

[1] Institut für Biologie und Biotechnologie der Pflanzen, Westfälische Wilhelms-Universität Münster, Schlossplatz 8, D-48143 Münster
[2] Institut für Lebensmittelchemie, Westfälische Wilhelms-Universität Münster, Corrensstraße 45, D-48149 Münster
[3] Kekulé-Institut für Organische Chemie und Biochemie, Rheinische Friedrich Wilhelms-Universität Bonn, Gerhard-Domagk-Straße 1, D-53121 Bonn

Running title: Gibepyrone biosynthesis in *F. fujikuroi*

To whom correspondence should be addressed:
*Prof. Dr. J. S. Dickschat, fon: +49 228 73 5797, e-mail: dickschat@uni-bonn.de
*Prof. Dr. B. Tudzynski, fon: +49 251 83 24801, fax: +49 251 83 21601, e-mail: tudzynsb@uni-muenster.de

Keywords: Fungi, Secondary metabolism, Polyketide, Biosynthesis, Gene regulation**,** *Fusarium fujikuroi*, Gibepyrones

Abstract

The 2*H*-pyran-2-one gibepyrone A and its oxidized derivatives gibepyrones B-F have been isolated from the rice pathogenic fungus *Fusarium fujikuroi* already more than 20 years ago. However, these products have not been linked to the respective biosynthetic genes and therefore, their biosynthesis has not been analyzed on a molecular level so far.

Feeding experiments with isotopically labeled precursors clearly supported a polyketide origin for the formal monoterpenoid gibepyrone A, while the terpenoid pathway could be excluded. Targeted gene deletion verified that the *F. fujikuroi* polyketide synthase PKS13, designated Gpy1, is responsible for gibepyrone A biosynthesis. Next to Gpy1, the ATP-binding cassette transporter Gpy2 is encoded by the gibepyrone gene cluster. Gpy2 was shown to have only a minor impact on the actual efflux of gibepyrone A out of the cell. Instead, evidence was gained that Gpy2 is involved in gene regulation as it represses *GPY1* gene expression. Thus, *GPY1* was upregulated and gibepyrone A production was enhanced both extra- and intracellularly in Δ*gpy2* mutants. Furthermore, expression of *GPY* genes is strictly repressed by members of the fungal-specific *velvet* complex, Vel1, Vel2 and Lae1, while Sge1, a major regulator of secondary metabolism in *F. fujikuroi*, affects gibepyrone biosynthesis in a positive manner. The gibepyrone A derivatives gibepyrones B and D were shown to be produced by cluster-independent P450 monooxygenases, probably to protect the fungus from the toxic product. In contrast, the formation of gibepyrones E and F from gibepyrone A is a spontaneous process and independent of enzymatic activity.

Introduction

Fusarium fujikuroi is a member of the *Fusarium* (*Gibberella*) *fujikuroi* species complex which comprises some of the most detrimental fungal pathogens in agriculture (1, 2). It is the causative agent of the *bakanae* ("foolish seedling") disease of rice (3) that results in significant crop losses every year. The disease symptoms include the chlorotic hyperelongation of the internodes due to the fungus' ability to produce and secrete gibberellic acids, a group of highly bioactive, growth promoting plant hormones (4, 5). Indeed, their biosynthesis was the first to be elucidated on a molecular level among the secondary metabolites (SMs) produced by *F. fujikuroi* (6). Furthermore, the genes responsible for the biosynthesis of the pigments bikaverin and fusarubins (7, 8), the mycotoxins fusarins, fusaric acid, apicidin F, fumonisins and beauvericin (9-14), and the terpenes (+)-eremophilene, (-)-α-acorenol, (-)-guaia-6,10(14)-diene and (+)-koraiol (15, 16) have been recently characterized. The sequencing of the genome of *F. fujikuroi* IMI58289 revealed the presence of altogether 48 SM key genes, encoding 18 polyketide synthases (PKSs), among those one type III PKS, 16 nonribosomal peptide synthetases (NRPSs), twelve terpene cyclases and two dimethylallyltryptophan synthases (17). However, the majority of the corresponding products is still unknown.

Compounds with a 2*H*-pyran-2-one (α-pyrone) moiety (Fig. 1*A*) are highly abundant in animal, plant and microbial systems. Microbial 2*H*-pyran-2-one metabolites exhibit a wide range of interesting properties, including antibiotic, antifungal, cyto- and phytotoxic effects. Some of them are of medical importance displaying tumor- or HIV protease-inhibiting activities (18, 19). A diverse array of 2*H*-pyran-2-ones is produced by filamentous fungi, especially by species of the genera *Alternaria*, *Aspergillus*, *Penicillium*, *Trichoderma* and *Fusarium* (18). Structurally simple metabolites from this group include triacetic acid lactone (Fig. 1*B*) isolated from *Penicillium* spp. (20, 21) and 6-pentyl-2*H*-pyran-2-one (Fig. 1*C*) produced by *Trichoderma* spp. (22, 23), the latter compound being toxic to many fungal plant pathogens such as *Botrytis cinerea* (24). Its shorter and longer homologs 6-propyl-2*H*-pyran-2-one and 6-heptyl-2*H*-pyran-2-one, and the related unsaturated compounds (*E*)-6-(pent-1-en-1-yl)-2*H*-pyran-2-one and (*E*)-6-(hept-1-en-1-yl)-2*H*-pyran-2-one (Fig. 1*C*) are also known from *Trichoderma* spp. (25, 26). The 2*H*-pyran-2-ones isolated from species of the genus *Fusarium* include fusapyrone (27), acuminatopyrone (28), chlamydosporol (29), poaefusarin and sporofusarin (30), compounds exhibiting mainly mycotoxic properties.

Metabolites from *F. fujikuroi* with a 2*H*-pyran-2-one structure, gibepyrone A and its formal oxidation products gibepyrones B-F (Fig. 1*D*), were first reported by Barrero and co-workers (31). Gibepyrone A was also recently detected in *F. fujikuroi* headspace extracts (32, 33). Gibepyrones A and B exhibit a moderate

antimicrobial activity against Gram-positive bacteria (*Bacillus subtilis*, *Staphylococcus aureus*) and yeasts (*Saccharomyces cerevisiae*, *Candida albicans*) at a minimal inhibitory concentration of 100-200 µg/mL (31). Beside *F. fujikuroi*, gibepyrone A production was also reported for natural isolates of *Fusarium keratoplasticum* and *Fusarium petroliphilum*, two members of the *Fusarium solani* species complex (34). Gibepyrone D was found in cultures of endophytic isolates of *Fusarium oxysporum* and *Fusarium proliferatum* (35, 36), while gibepyrone F was detected in co-cultures of *Fusarium* sp./*Aspergillus clavatus* (37). Moreover, gibepyrone F was isolated from extracts of the South China Sea sponge *Jaspis stellifera* (38) which possibly originates also from a fungal symbiont, as described for other marine sponge-derived compounds (39, 40).

The (*Z*)-stereoisomer of gibepyrone A, fusalanipyrone (Fig. 1*E*), has been reported from *F. solani* and has antifungal and phytotoxic activities (41, 42). Based on its chemical structure, this C_{10} compound was first suggested to be of monoterpenoid origin, but subsequent feeding experiments with deuterated methionine provided evidence that fusalanipyrone could also represent a methylated polyketide product (41, 43). The phytotoxic methoxy derivatives nectriapyrone and pestalopyrone (Fig. 1*F*) were first isolated from *Gyrostroma missouriensis* and *Pestalotiopsis oenotherae*, respectively (44-47). Due to incorporation of radioactive labeling from [2-^{14}C]mevalonic acid, nectriapyrone was suggested to be a monoterpenoid, but this result is doubtful, because the "incorporation" of labeling into the widespread plasticizer *bis*-(2-ethylhexyl)phthalate, mistakenly identified as a natural product, was also reported in the same study (44). In an independent analysis, the incorporation of labeling from (1,2-$^{13}C_2$)acetate and (*methyl*-^{13}C)methionine was described, providing evidence for a polyketide origin of this compound (48).

Although gibepyrones A-F are well known SMs of *F. fujikuroi* IMI58289 (31), the genes and enzymes involved in their biosynthesis have not been identified so far. Here we present feeding experiments with isotopically labeled precursors that validated the polyketide nature of the gibepyrones as well as the identification and molecular characterization of their small PKS gene cluster. Gibepyrone A biosynthesis is regulated by members of the fungal-specific *velvet* complex (Vel1, Vel2, Lae1) and by Sge1, a major regulator of secondary metabolism in *F. fujikuroi*. Finally, the mechanisms for the formation of the oxidized gibepyrones B-F were elucidated, using a combination of chemical synthesis and gene knockout experiments.

Results

Chemical synthesis of gibepyrone A and its production by *F. fujikuroi*

Analysis of liquid cultures of *F. fujikuroi* IMI58289 by HPLC-high resolution mass spectrometry (HRMS) showed the presence of a SM with the exact mass of gibepyrone A. The same compound was also detected *via* GS-MS in headspace extracts from *F. fujikuroi* agar plate cultures as reported previously (32, 33). For unambiguous identification of gibepyrone A, the compound was synthesized *via* a known procedure by treating tigloyl chloride (**1**) with triethyl amine in dichloromethane (31). Its isomer 6-(but-3-en-2-yl)-3-methyl-2*H*-pyran-2-one (**2**) was also obtained in this reaction (Fig. 2). The synthetic gibepyrone A was identical to the detected SM in *F. fujikuroi* with respect to the HPLC-MS and GC-MS retention times (9 min and 28 min, respectively) and mass spectra (Fig. S1).

Feeding experiments on the biosynthesis of gibepyrone A

In order to exclude a terpenoid origin for gibepyrone A, a feeding experiment with (*methyl*-$^2H_3$)mevalonolactone was performed. No incorporation of labeling into gibepyrone A was detected (Fig. S2*A*), which contradicts a terpene biosynthetic pathway. Alternative feeding experiments were carried out to test for a polyketide origin of gibepyrone A. The formation of the carbon backbone from four acetate-derived C_2 building blocks and two *S*-adenosyl-L-methionine (SAM)-derived C_1 units seemed to be most likely, but the potential formation from two propionate-derived C_3 building blocks and two acetate-derived C_2 buildings blocks, though atypical for fungi, was addressed as well. Additionally, the possibility of a biosynthetic pathway *via* an isoleucine-derived (*E*)-2-methylbut-2-enoyl-CoA starter unit was evaluated. Feeding of (*methyl*-^{13}C)methionine resulted in the incorporation of up to two C_1 units with high rates (50%), as indicated by a 2 mass unit shift of the molecular ion of gibepyrone A,

while no incorporation of labeling from ($^2H_5$)propionate was observed (Fig. S2*A*). Up to four deuterium atoms were found in gibepyrone A in the feeding experiment with ($^2H_{10}$)isoleucine but only with a low incorporation rate (1.3%; Fig. S2*A*). This finding is in agreement with a degradation of ($^2H_{10}$)isoleucine to ($^2H_3$)acetyl-CoA and ($^2H_3$)propionyl-CoA along the isoleucine degradation pathway, followed by incorporation of ($^2H_3$)acetyl-CoA into gibepyrone A (Fig. S2*B*), but not with a hypothetical isoleucine-derived (*E*)-2-methylbut-2-enoyl-CoA starter-unit that would require incorporation of seven deuterium atoms. Indeed, feeding of (2-^{13}C)acetate resulted in an incorporation of up to four units with low incorporation rate (Fig. S2*A*). Taken together, these results confirmed that gibepyrone A is a tetraketide comprised of four acetate building blocks and two SAM-derived methyl groups.

PKS13 is responsible for gibepyrone A biosynthesis

After demonstrating the polyketide origin of gibepyrone A by the feeding experiments described above, we confirmed the PKS origin also on a genetic and enzymatic level. Therefore, the *F. fujikuroi* Δ*ppt1* deletion mutant as well as the complemented strain *PPT1*^{C} were analyzed for gibepyrone A production. The phosphopantetheinyl (Ppant) transferase encoded by *PPT1* is essential for the activation of the main proportion of fungal PKSs (and NRPSs) through post-translational attachment of the Ppant prosthetic group (49). Analysis of culture fluids by HPLC-MS/MS revealed the production of gibepyrone A by the wild-type (WT) strain and *PPT1*^{C}, but not by the Δ*ppt1* mutant (Fig. 3*A*), confirming the polyketide origin.

In the frame of an ongoing project to identify novel SMs produced by *F. fujikuroi*, deletion strains for all 18 PKS-encoding genes are currently generated. Targeted replacement of one of these genes (*PKS13*, *FFUJ_12020*) with the hygromycin B resistance cassette (Fig. S3) resulted in total loss of gibepyrone A biosynthesis in three independent deletion mutants. *In loco* complementation of one deletion mutant with the full-length *PKS13* gene resulted in full restoration of gibepyrone A formation (Fig. 3*B*; Fig. S4). Therefore, PKS13 is the key enzyme of gibepyrone biosynthesis, designated Gpy1.

The gibepyrone A biosynthetic gene cluster includes a transporter-encoding gene

In addition to the key enzyme-encoding gene, SM gene clusters often comprise genes encoding pathway-specific transcription factors (TFs), several tailoring enzymes such as methyltransferases, oxidoreductases or P450 monooxygenases and efflux transporters for the respective SM (50).

Upstream and downstream of *GPY1*, several genes were identified that might belong to a putative gibepyrone biosynthetic gene cluster (Fig. 4*A*). As summarized in Table 1, a methyltransferase-encoding gene (*FFUJ_12019*) was found upstream of *GPY1*, while two genes encoding an ATP-binding cassette (ABC) transporter (*FFUJ_12021*) and a fungal-specific $Zn(II)_2Cys_6$-type TF (*FFUJ_12023*) were detected downstream. The gene *FFUJ_12022* does not harbor any domains or motifs which might confer a specific function. Moreover, a genomic alignment of different *Fusarium* spp. (*F. proliferatum*, *F. mangiferae*, *F. verticillioides*, *F. oxysporum*) underlined that *GPY1* and further adjacent genes are conserved in these species, while the gene of unknown function, *FFUJ_12022*, is not always clustered with *GPY1* (Fig. S5). In order to assess the involvement of the other indicated genes in gibepyrone A biosynthesis, single deletion mutants were generated (Fig. S6, Fig. S7, Fig. S8). Deletion of the methyltransferase- and TF-encoding genes *FFUJ_12019* and *FFUJ_12023*, respectively, did not alter gibepyrone A yields, while deletion of the ABC transporter-encoding gene *FFUJ_12021* resulted in a significantly enhanced level of extracellular gibepyrone A (Fig. 4*B*). Thus, adjacent to *GPY1*, a second gene was identified with impact on gibepyrone A production, designated *GPY2*.

Next, overexpression mutants were generated for *GPY1* and the TF-encoding gene *FFUJ_12023* (Fig. S9*A*/*B*). While the OE::*GPY1* overexpression mutant showed significantly higher gibepyrone A production, overexpression of *FFUJ_12023* did not have any impact (Fig. 4*C*), indicating that the encoded putative TF does not represent a pathway-specific TF for gibepyrone biosynthesis.

The ABC transporter Gpy2 represses PKS gene expression

Beside the enhanced extracellular gibepyrone A levels upon deletion of the transporter-encoding gene *GPY2* (Fig. 4*B*), also

significantly elevated intracellular gibepyrone A levels were observed in the mutant compared to the WT (Fig. 5*A*). These increased product levels were in accordance with the upregulated expression of the PKS-encoding gene *GPY1* in Δ*gpy2* mutants (Fig. 5*B*). *GPY1* gene expression and gibepyrone A formation were elevated throughout the whole cultivation period of the Δ*gpy2* mutant, as shown for days 1-3 in Fig. 5*C/D*. The low-producing WT phenotype could be restored through *in loco* complementation with the full-length *GPY2* gene (Fig. S10; Fig. S11).

To study the potential regulatory role of *GPY2* in more detail, this ABC transporter-encoding gene was overexpressed in the WT and *GPY1* overexpression background (Fig. S9*C*). Interestingly, the overexpression of *GPY2* led to repression of *GPY1* gene expression and gibepyrone A product formation in the WT (native *GPY1* promoter), but not in the OE::*GPY1* background (OE::*GPY1*/OE::*GPY2*) (Fig. 5*A*/*B*). These data indicate that *GPY1* regulation by Gpy2 occurs on the level of gene expression.

While *GPY2* was equally expressed in the WT and Δ*gpy1* background (Fig. S12*A*), addition of 1 or 10 µg/mL synthetic gibepyrone A induced *GPY2* expression both in the WT and Δ*gpy1* (Fig. S12*B*). Interestingly, the PKS-encoding gene *GPY1* itself was also upregulated upon addition of gibepyrone A to the WT. In contrast, expression of the adjacent gene *FFUJ_12019* was not affected (Fig. S12*B*). Taken together, these data indicate that gibepyrone A is able to induce its own production by an elevated *GPY1* gene expression in a positive feedback loop (Fig. 5*D*; Fig. S12*B*). At the same time, expression of the ABC transporter-encoding gene *GPY2* is also induced (Fig. S12*B*), causing a downregulation of *GPY1* expression in a negative feedback loop.

Gibepyrone A is toxic to *F. fujikuroi*

The highly sophisticated regulatory mechanism described above led to the assumption that gibepyrone A might have a biological activity not only against bacterial and yeast strains (31), but also against the producing fungus itself. A plate assay using synthetic gibepyrone A against the WT strain and the mutants Δ*gpy1* and Δ*gpy2* was performed. Indeed, the growth of all three strains was equally inhibited as indicated by the reduced colony diameters to approximately 50% and 15% in the presence of 100 µg/mL and 200 µg/mL gibepyrone A, respectively (Fig. S13).

***C*-Methylation mechanism in the biosynthesis of gibepyrone A**

As underlined by feeding experiments with isotopically labeled precursors, gibepyrone A consists of a polyketide backbone that is modified by two methylation steps (Fig. S2*A*). Since deletion of the methyltransferase-encoding gene *FFUJ_12019* did not have an impact on gibepyrone A production (Fig. 4*B*), the *C*-methyltransferase domain within the highly reducing PKS Gpy1 might solely be responsible for attaching both methyl groups to the nascent polyketide backbone. In order to verify this hypothesis, an amino acid substitution was introduced into the catalytic center of the *C*-methyltransferase domain of Gpy1. Glycine at position 1443 was exchanged for valine (G1443V), as corresponding mutations in the *F. verticillioides* fumonisin synthase (Fum1) and *Phoma* sp. C2932 squalestatin tetraketide synthase (SQTKS) were described to sterically inhibit SAM substrate binding (51, 52). An amino acid alignment of the *C*-methyltransferase domains of Gpy1, Fum1 and SQTKS underlined the conserved position of this active site glycine (Fig. S14*A*). The Δ*gpy1* strain was complemented with this mutated *GPY1* variant yielding independent transformants of $GPY1^{G1443V}$. Although expression of $GPY1^{G1443V}$ was similar to $GPY1^{C}$, re-introduction of this point-mutated gene copy could not restore gibepyrone A production (Fig. S14*B*/*C*), suggesting that the PKS alone is able to condense the methylated polyketide gibepyrone A. Single-methylated or completely non-methylated gibepyrone A derivatives could not be identified in $GPY1^{G1443V}$ mutants by HPLC-HRMS analysis (Fig. S15).

Production of gibepyrone A derivatives

The initial report on gibepyrone A by Barrero and co-workers (31) also mentioned the presence of a series of oxygenated derivatives, gibepyrones B-F, in *F. fujikuroi* (Fig. 1*D*). All these compounds were assumed to have a common biosynthetic origin. In fact, gibepyrones B-D are characterized through oxidations at the methyl group C8, while gibepyrone E carries a 6,7-epoxide function in the side chain. Furthermore, gibepyrone F was hypothesized to be generated through oxidative cleavage of the C6-C7 double bond (31). No genes encoding oxidizing proteins were identified in close proximity to *GPY1* (Table 1), suggesting that independent enzymes encoded outside of the gene cluster might facilitate these reactions.

The oxidation of a single carbon atom, *e.g.* the conversion of gibepyrone A (methyl group) to gibepyrone D (acid group) *via* gibepyrone B (hydroxyl group) and gibepyrone C (aldehyde group), is a typical reaction sequence catalyzed by P450 monooxygenases. In order to test this hypothesis, WT cultures were compared to those of the Δ*cpr* mutant. *CPR* encodes the major NADPH-cytochrome P450 reductase in *F. fujikuroi* that is associated with P450 monooxygenases, being essential for the electron transfer from NADPH onto the prosthetic heme group of the P450s (53). Thus, in the Δ*cpr* mutant, the majority of all P450s is inhibited, which has been first demonstrated for the P450s encoded by the gibberellic acid gene cluster (53). To further examine the involvement of CPR in the biosynthesis of the oxidized gibepyrones, a chemical synthesis of gibepyrones B, C and E was performed (Fig. 2). Gibepyrone E was synthesized *via* epoxidation of gibepyrone A using *meta*-chlorobenzoic acid, while **2** was used as starting material for the synthesis of 6-(2-hydroxybut-3-en-2-yl)-3-methyl-2*H*-pyran-2-one (**3**) using modified Riley conditions (54). Compound **3** was converted into gibepyrone B *via* acidic rearrangement of the tertiary allylic hydroxy function function using methanesulfonic acid or to gibepyrone C *via* oxidative rearrangement using pyridinium chlorochromate (Fig. 2).

The synthetic compounds were used as standards to search for oxidized gibepyrones in the *F. fujikuroi* WT and mutant strains. Gibepyrones B and D were identified by HPLC-HRMS analysis in WT cultures and in increased amounts in the OE::*GPY1* strain, but not in the Δ*gpy1* mutant, linking the production of these metabolites to the gibepyrone PKS (Fig. 6; Fig. S16). In contrast, gibepyrone C was neither detected in WT cultures nor in the OE::*GPY1* mutant (Fig. S16). Comparison of WT and Δ*cpr* cultures revealed that gibepyrones B and D were missing in the mutant, while an accumulation of gibepyrone A was observed (Fig. 6). These data are in full agreement with the conversion of gibepyrone A to gibepyrones B and D by one or multiple CPR-dependent P450 monooxygenases encoded outside of the gibepyrone biosynthetic gene cluster.

The HPLC-HRMS analysis of an aged synthetic gibepyrone E standard showed a slow compound degradation in aqueous solution. Furthermore, gibepyrone E could not be detected in culture fluids, while two of its degradation products were present in cultures of the WT and the Δ*cpr* mutant (Fig. 6). Presumably, these two compounds represent diastereomeric diols that are formed from gibepyrone E by hydrolysis of its epoxide function in the presence of water (Fig. S17*A*). As the two compounds were also found in the Δ*cpr* mutant, the conversion of gibepyrone A into gibepyrone E must be independent of the P450 monooxygenase(s) involved in the formation of the other oxidized gibepyrones. Instead, gibepyrone E formation and its hydrolysis were also observed in an aqueous solution of synthetic gibepyrone A (Fig. S17*B*), indicating its autoxidation in the presence of molecular oxygen.

Gibepyrone F was only detected in headspace extracts of the *F. fujikuroi* WT *via* GC-MS, but not in liquid cultures *via* HPLC-HRMS. Similar to gibepyrone E, this compound was also formed spontaneously from synthetic gibepyrone A (Fig. S17*C*), and was also detectable in headspace extracts from the Δ*cpr* mutant strain (Fig. S18), indicating its formation independent of enzymatic activity.

Gibepyrone A production by *F. solani*

The reported structure of fusalanipyrone from *F. solani* DSM 62416 (41) represents the (*Z*)-stereoisomer of gibepyrone A. However, genome sequencing of the strain *F. solani* 77-13-4 (55) revealed that this organism encodes a PKS with the same domain organization and 84% amino acid identity compared to Gpy1 (17) (accession number NECHADRAFT_123282; Fig. S5). While a homolog of the ABC transporter-encoding gene *GPY2* cannot be found adjacent to the *F. solani GPY1* homolog, the methyltransferase-encoding border gene (a homolog of *FFUJ_12019*) is conserved in *F. solani*, highly suggesting that NECHADRAFT_123282 is the true Gpy1 homolog (Fig. S5). This bioinformatic analysis underlined that *F. solani* may also produce gibepyrone A, while the production of the stereoisomer fusalanipyrone by Gpy1 would be difficult to understand. Comparison of the NMR data reported for fusalanipyrone (41) to the NMR data of synthetic gibepyrone A (Experimental procedures) showed the identity of these compounds. Their identity was additionally verified by comparison of liquid culture extracts from *F. solani* DSM 62416 and *F. fujikuroi* IMI58289 to the synthetic gibepyrone A standard by GC-MS (Fig. S19). Therefore, the structure of

fusalanipyrone must be revised to that of gibepyrone A.

Regulation of gibepyrone A biosynthesis

F. fujikuroi SM biosynthesis was shown to be differentially regulated by global regulators such as members of the fungal-specific *velvet* complex (Vel1, Vel2, Lae1) (56), as well as Sge1, a recently characterized master regulator of several SM gene clusters in this fungus (57). To study their impact on gibepyrone A production, the yields were compared between the WT and the regulatory mutants. Gibepyrone A levels were elevated in deletion mutants of the *velvet* complex, Δ*vel1*, Δ*vel2* and Δ*lae1*, but downregulated in Δ*sge1* (Fig. 7*A*). Analysis of *GPY1* and *GPY2* expression by quantitative real-time PCR (qRT-PCR) verified these results (Fig. 7*B*). Besides *GPY1* and *GPY2*, no further adjacent genes were upregulated in the Δ*vel1* mutant (Fig. 7*C*), underlining that these two genes represent a co-regulated small biosynthetic gene cluster.

Discussion

Prior to this study, the biosynthetic origin of gibepyrone A and its oxidized derivatives was unknown. Therefore, this study focused on the biosynthetic pathway of gibepyrones A-F, the elucidation of their biosynthetic gene cluster and on the regulation of these genes in *F. fujikuroi*.

Biosynthesis of the polyketide gibepyrone A

In this work, evidence is provided for gibepyrone A biosynthesis by *F. fujikuroi* PKS13 (FFUJ_12020), designated Gpy1. Feeding experiments with isotopically labeled precursors and analysis of the Δ*ppt1* mutant ruled out a terpenoid origin for this compound. Although a polyketide biosynthetic pathway was suggested for the structurally related compounds fusalanipyrone and nectriapyrone (43, 48), unambiguous proof on a molecular level was lacking for this group of metabolites. By deleting *GPY1*, the responsible key gene of gibepyrone biosynthesis was identified, encoding a highly reducing PKS. A proposed biosynthetic pathway to gibepyrone A by Gpy1 uses an acetyl-CoA starter unit, three malonyl-CoA extender units and two SAM-dependent methylations to establish the gibepyrone A carbon backbone, followed by product release upon intramolecular cyclization (Fig. 8). Introduction of a loss-of-function mutation into the *C*-methyltransferase domain of Gpy1 and the non-effective deletion of a methyltransferase encoding gene adjacent to *GPY1* (*FFUJ_12019*) verified that both methylation steps are catalyzed by the PKS itself. It is unclear whether PKS biosynthesis in the GPY^{G1443V} mutant is blocked or results in an unidentified shunt product that may be unstable or quickly metabolized. The latter was suggested for *Phoma* sp. C2932 SQTKS (52), while for other systems, including the lovastatin PKS, the formation of defined non-methylated shunt products was shown by *in vitro* experiments in the absence of SAM (58).

Distribution of putative gibepyrone A biosynthetic genes among the genus *Fusarium*

Our bioinformatic analysis verified that *GPY1* is conserved among members of the *F. fujikuroi* species complex and can also be found in the closely related *F. oxysporum* and the distantly related *F. solani* species complexes (Fig. S5). These data are in agreement with the isolation of gibepyrone A from members of the *F. solani* species complex (34) and with our structural revision for fusalanipyrone from *F. solani* DSM 62416 that is identical to gibepyrone A. Conclusively, *GPY1* orthologs seem to be present within the whole genus *Fusarium*.

Moreover, we suggest that homologous PKSs are responsible for the biosynthesis of the related compounds nectriapyrone and pestalopyrone (Fig. 1*E*/*F*) from *G. missouriensis* and *P. oenotherae*, respectively (44, 45). Both nectria- and pestalopyrone harbor a methoxy group that is most likely introduced as hydroxyl group by the responsible PKS and modified in a second step by a cluster-encoded *O*-methyltransferase, as recently reported for fusarubin and bikaverin pigment biosyntheses by *F. fujikuroi* (8, 59). Furthermore, the desmethyl derivative pestalopyrone is most likely produced under the use of only one SAM unit by a PKS that is very similar to the gibepyrone PKS, which gives another example for the highly programmed fashion of tailoring domains in fungal iterative PKSs (60).

Gibepyrone A derivatives have both an enzymatic and non-enzymatic origin

Next to gibepyrone A, we analyzed the production of the derived compounds gibepyrones B-F. Gibepyrones B and D were shown to be produced from gibepyrone A by one

or multiple CPR-dependent P450 monooxygenases encoded by genes not clustered with *GPY1* and *GPY2*. A derivatization by P450s, encoded outside of the respective gene cluster, was also recently described for the *F. fujikuroi* SM fusaric acid. In this case, the conversion into the less toxic derivatives dehydrofusaric acid and fusarinolic acid represents a detoxification mechanism for the producing fungus (11). While gibepyrone A was shown to be moderately active against the Gram-positive bacteria *B. subtilis* and *S. aureus* as well as against the yeasts *S. cerevisiae* and *C. albicans*, gibepyrone B was only active against *S. aureus* and *S. cerevisiae* (31). As gibepyrone A has a toxic effect on the producing fungus itself, it is tempting to hypothesize that its derivatization into the oxidized compounds does represent a detoxification mechanism. In a comparable manner, incubation of the plant pathogen *B. cinerea* with the toxic compound 6-pentyl-2*H*-pyran-2-one (Fig. 1*C*) from *Trichoderma* spp. led to the formation of oxidized derivatives harboring hydroxyl and acid groups. These metabolized products were not toxic in a germination assay, while 6-pentyl-2*H*-pyran-2-one clearly was (61). The fact that gibepyrone D was also isolated from cultures of *F. oxysporum* and *F. proliferatum* indicates that this detoxification mechanism would not be specific to *F. fujikuroi* (35, 36).

Gibepyrone C, which represents the intermediate between gibepyrones B and D, was identified by Barrero and co-workers (31), but was not found in our liquid cultures comparing with the synthetic gibepyrone C. Reasons for this contrasting result could be different cultivation procedures or the fact that gibeyprone C, harboring an aldehyde group, is a highly reactive metabolite that might be quickly processed into gibepyrone D, maybe even by the same P450 catalyzing the conversion to gibepyrone B.

Furthermore, we could establish that gibepyrones E and F are generated spontaneously, in the absence of enzymatic activity, based on spontaneous oxidation of synthetic gibepyrone A in the presence of air. For the formation of these compounds, a reaction pathway can be proposed starting with the addition of molecular oxygen to the C6-C7 double bond of gibepyrone A (Fig. S20). Under neat conditions, the resulting dioxetane may decompose to gibepyrone F and acetaldehyde, while the dioxetane can be attacked by water in aqueous solution to decompose to gibepyrone E and hydrogen peroxide (Fig. S20). No degradation of clean synthetic gibepyrone A was observed over several months, when stored at -20 °C in the dark.

The special role of the ABC transporter Gpy2

In *F. fujikuroi*, an ABC transporter-encoding gene, *GPY2*, belongs to the gibepyrone gene cluster besides *GPY1*. This gene was found to be co-regulated with *GPY1* in the regulatory mutant Δ*vel1*. Furthermore, the generation of *GPY2* deletion and overexpression mutants clearly verified its impact on gibepyrone A production. Our data suggest that Gpy2 plays only a minor or no role at all in the actual transport of gibepyrone A out of the cell. We propose that at least one other transporter is involved in metabolite efflux, as gibepyrone A was found both in the culture fluid and mycelium of Δ*gpy2* mutants. Our data indicate that Gpy2 is able to regulate the expression of the PKS-encoding gene *GPY1*. *GPY1* expression and gibepyrone A production were significantly elevated in the Δ*gpy2* mutant, but downregulated in the OE::*GPY2* mutants. This highly sophisticated Gpy2-mediated regulatory mechanism allows a fine-tuning of gibepyrone A biosynthesis, probably protecting the producing fungus from the toxic effect of its own product.

There are several examples where deletion of a transporter-encoding gene negatively affected SM production and in all of these cases, it was highly anticipated that the SMs are toxic to the producing fungi. Such SM-specific transporters conferring self-protection are major facilitator superfamily (MFS) transporters as encoded by the *Aspergillus fumigatus* gliotoxin cluster (GliA) (62), the *Fusarium graminearum* trichothecene cluster (Tri12) (63) and the *Fusarium* spp. fusaric acid cluster (Fub11) (11, 64). Deletion of *gliA* and *FUB11* resulted in a reduced intra- and extracellular accumulation of gliotoxin and fusaric acid, respectively, most likely due to the detoxification of these compounds *via* derivatization, while cluster gene expression was not affected (11, 62, 64). Similarly, deletion of *TRI12* led to diminished trichothecene levels *via* a yet unknown mechanism (63).

Far less SM gene clusters harbor ABC transporter-encoding genes. Examples are the *F. verticilliodes* fumonisin cluster (Fum19) (65), the *Leptosphaeria maculans* sirodesmin cluster (SirA) (66) and the *F. fujikuroi* beauvericin cluster (14). Upon disruption of *FUM19*, little impact was detected on extracellular fumonisin contents and the authors assumed that other transporters are able to compensate for Fum19

(65). To the best of our knowledge, only two reports on enhanced extracellular SM contents upon deletion of a transporter-encoding gene have been described before, a phenotype that would be comparable to the one observed for *F. fujikuroi* Δ*gpy2*. Thus, the *L. maculans* sirodesmin NRPS-encoding gene *sirP* was upregulated in Δ*sirA* ABC transporter mutants. Unfortunately, the authors did not quantify intracellular sirodesmin levels but did find enhanced extracellular sirodesmin in Δ*sirA* mutants (66). Additionally, an upregulation of NRPS gene expression and SM product formation was observed upon deletion of *F. fujikuroi BEA3*, encoding the beauvericin ABC transporter that we recently analyzed (14).

It is tempting to hypothesize that this regulatory role of SM transporters is specific to ABC transporters, however, further research is needed to proof this. A transporter, which has been implicated in having a sensing function in addition to its transport function, is the *S. cerevisiae* general amino acid permease Gap1 (67). The authors were able to introduce C-terminal truncations that only affected the sensing function but not the transport efficiency of Gap1, establishing that the signaling pathway is mediated *via* protein kinase A (67). A potential signal transduction pathway which might be responsible for *GPY1* repression *via* the ABC transporter Gpy2 as well as its biological function remain to be elucidated.

Global regulatory mechanisms controlling gibepyrone A biosynthesis

As no cluster-specific TF is encoded by the small gene cluster, we evaluated the impact of global regulators on gibepyrone A biosynthesis. Thus, members of the fungal-specific *velvet* complex, Vel1, Vel2 and Lae1, represent repressors of gibepyrone A biosynthesis, while Sge1 acts as positive regulator.

In addition to the pigment bikaverin, gibepyrone A represents the second SM that is influenced in a negative manner by members of the *velvet* complex in *F. fujikuroi*. In the case of bikaverin, however, only Vel1 and Vel2 act as repressors, while Lae1 does not (56). The mode of action of the *velvet* complex is still not fully understood. While homologs of the *velvet* domain proteins Vel1 and Vel2 have been described to have DNA-binding properties (68), the putative histone methyltransferase Lae1 has been implicated to act on the highest hierarchical level of chromatin remodeling (69). Furthermore, the complex may vary in its conformation when regulating different aspects of differentiation and secondary metabolism (70). Notably, this is the first example that all three members of the *velvet* complex seem to work together to repress gibepyrone A biosynthesis in *F. fujikuroi*.

Sge1 was shown to be a major positive regulator of secondary metabolism in *F. fujikuroi* (57) which also held true for gibepyrone A biosynthesis. Also for Sge1, the mode of action is not fully resolved. While the yeast Sge1-homologs in *C. albicans* and *Histoplasma capsulatum* have been described to bind the promoters of their target genes (71, 72), no common DNA-binding motif has been identified in filamentous fungi so far. In fact, Sge1 in *F. fujikuroi* was suggested to act on a high hierarchical level, also regulating genes encoding histone-modifying enzymes on a transcriptional level (57).

In conclusion, this work provides a comprehensive overview on the biosynthesis and regulation of gibepyrone A and its derivatives in *F. fujikuroi*, applying feeding experiments, chemical synthesis of gibepyrone standards, gene knockout and overexpression strategies as well as regulatory mutants. As summarized in Fig. 9, the PKS Gpy1 is responsible for the production of gibepyrone A while one or several cluster-independent P450 monooxygenases account for the production of gibepyrones B and D. Furthermore, gibepyrones E and F are gained in the absence of enzymatic activity. Evidence was provided that the ABC transporter Gpy2 represses expression of the PKS-encoding gene *GPY1 via* a yet unknown mechanism. Finally, gibepyrone biosynthesis underlies global regulatory mechanisms, as verified for Sge1 and the *velvet* complex that affect gibepyrone A biosynthesis in a positive and negative manner, respectively.

Experimental procedures

Fungal strains, media and growth conditions

The WT strain *F. fujikuroi* IMI58289 (Commonwealth Mycological Institute, Kew, United Kingdom) was used as parental strain for the generation of deletion and overexpression mutants. Concerning the analysis of gene expression as well as product formation, the following strains were applied additionally: Δ*ppt1*, $PPT1^{C}$ (49), Δ*cpr* (53), Δ*vel1*, Δ*vel2*, Δ*lae1* (56), Δ*sge1* (57) and *F. solani* DSM 62416 (41).

For all experiments in liquid culture, the fungal strains were pre-incubated for three days in 300 mL-Erlenmeyer flasks containing 100 mL Darken medium (73) on a rotary shaker at 180 rpm and 28 °C in the dark. 500 µL of this pre-culture were transferred into 100 mL synthetic ICI medium (Imperial Chemical Industries Ltd., United Kingdom) (74) supplemented with 6 mM glutamine as sole nitrogen source. This main culture was incubated under indicated conditions for additional one to seven days. Feeding experiments in liquid culture were performed under the addition of 0, 1, 10 µg/mL synthetic gibepyrone A to a two day-old 30 mL ICI culture. After two hours of induction, the mycelium was harvested and used for the isolation of RNA. For protoplasting *F. fujikuroi*, 500 µL of the pre-culture were transferred into 100 mL ICI medium with 10 g/L fructose instead of glucose as well as 0.5 g/L $(NH_4)_2SO_4$ as nitrogen source and shaken for no longer than 16 h. The general maintenance of the fungal strains was carried out on solidified complete medium (CM) (75) while, prior to DNA isolation, the strains were incubated on CM covered with cellophane for two to four days at 28 °C in the dark. Hyphal growth of fungal strains was assessed on solidified CM medium supplemented with 0-200 µg/mL synthetic gibepyrone A. Plates were incubated for four days at 28 °C in the dark. The solvent (ethanol absolute) was added as control, not resulting in an inhibition of fungal growth (data not shown).

Plasmid constructions

The cloning of deletion, complementation and overexpression constructs was accomplished under the use of yeast recombinational cloning (76, 77). For targeted gene deletion, ca. 0.6-1 kb large upstream (5') and downstream (3') regions of the gene of interest were amplified with the primer pairs 5F/5R and 3F/3R, respectively (Table S1). The hygromycin resistance cassette *hphR*, consisting of the hygromycin B phosphotransferase gene *hph* and the strong *trpC* promoter from *Aspergillus nidulans*, was amplified with hph_F/hph_R from the template pCSN44 (78). *S. cerevisiae* FY834 (79) was transformed with the obtained fragments as well as with the *Eco*RI/*Xho*I restricted shuttle vector pRS426 (80) resulting in the deletion vectors p∆*12019*, p∆*gpy1*, p∆*gpy2* and p∆*12023*.

For *in loco* complementation of the PKS13-encoding gene *GPY1* (*FFUJ_12020*), the full-length gene was amplified in three overlapping fragments using a proof-reading polymerase and primer pairs 12020_c_F1/12020_c_R1, 12020_c_F2/12020_c_R2 and 12020_c_F3/12020_c_R3 (Table S2). It was cloned upstream of the glucanase terminator *Tgluc* from *B. cinerea* B05.10 that was amplified with BcGlu_Term_F2/Tgluc_Nat1_R. The nourseothricin resistance cassette *natR*, including the strong *A. nidulans trpC* promoter, served as resistance marker and was amplified with hph_R/hph_R2 from the template pZPnat1 (GenBank accession no. AY631958.1). *GPY1* 5' and 3' sequences were gained as indicated above. *S. cerevisiae* FY834 was transformed with the obtained fragments as well as with the *Eco*RI/*Xho*I restricted vector pRS426 yielding the complementation vector p*GPY1*^{C} (Fig. S4*A*). For introducing the G1443V mutation into the Gpy1 *C*-methyltransferase domain (51, 52), a modified *in loco* complementation vector was cloned, p*GPY1*^{G1443V}. Using overlapping primers that harbor the nucleotide exchange, *GPY1* was amplified in four overlapping fragments, two of which were based on the novel primer combinations 12020_c_F2/12020_G1443V_R and 12020_G1443V_F/12020_c_R2 (Table S2). Furthermore, for *in loco* complementation of the ABC transporter-encoding gene *GPY2* (*FFUJ_12021*), the following gene-specific fragments were amplified: 12021_5F/12021_c_R1, 12021_c_F2/12021_c_R2, 12021_3F/12021_3R (Table S2). *S. cerevisiae* FY834 was transformed with the obtained fragments, *Tgluc*, *natR*, as well as with the *Eco*RI/*Xho*I restricted vector pRS426 yielding the complementation vector p*GPY2*^{C} (Fig. S10*A*).

Overexpression of *GPY1* was achieved through fusion to the strong *oliC* promoter from *A. nidulans*. Thus, *GPY1* was again amplified in three overlapping fragments using a proof-reading polymerase, in this case with 12020_OE_F/12020_c_R1, 12020_c_F2/12020_c_R2 and 12020_c_F3/12020_OE_R (Table S2). The latter primer combination included ca. 300 bp of the *GPY1* terminator sequence. *S. cerevisiae* was transformed with these fragments as well as with the *Nco*I/*Sac*II restricted plasmid pNDN-OGG (77) resulting in pOE::*GPY1* (Fig. S9*A*). Similarly, for overexpressing *FFUJ_12023 via PoliC*, the gene of interest was amplified with the primer pair 12023_OE_F/12023_OE_R (Table S2). The *Nco*I/*Not*I restricted plasmid pNAH-OGG (77) served as plasmid backbone yielding pOE::*12023* (Fig. S9*B*). And for

overexpression of *GPY2* in the WT and OE::*GPY1* overexpression backgrounds, the first 1.4 kb of *GPY2* were amplified with the primer pair 12021_OE_F/12021_OE_R (Table S2). The fragment was fused to the *Nco*I/*Sac*II restricted plasmid pNAH-GGT harboring the strong *glnA* promoter from *F. fujikuroi* (11) resulting in pOE::*GPY2* (Fig. S9*C*). The correct assembly of all complementation and overexpression vectors was verified by sequencing with primers listed in Table S2.

Fungal transformations and analysis of transformants

Protoplast transformation of *F. fujikuroi* was carried out as previously described (81). About 10^7 protoplasts were transformed with the amplified replacement cassettes to generate deletion mutants. Amplification was achieved with primer combination 5F/3R (Table S1) while the circular deletion vectors served as DNA templates. For *in loco* complementation of Δ*gpy1* T5 with p*GPY1*^{C} (Fig. S4*A*) or p*GPY1*^{G1443V}, 30 µg of the vectors was linearized with *Apa*I prior to transformation. Similarly, for *in loco* complementation of Δ*gpy2* T9 with p*GPY2*^{C} (Fig. S10*A*), 30 µg of the vector was linearized with *Ase*I. Furthermore, 15 µg of the overexpression vectors pOE::*GPY1* (Fig. S9*A*), pOE::*12023* (Fig. S9*B*) and pOE::*GPY2* (Fig. S9*C*) was introduced in a circular manner. Selection of transformants was achieved under the use of 100 µg/mL hygromycin B (Calbiochem, Darmstadt, Germany) or 100 µg/mL nourseothricin (Werner-Bioagents, Jena, Germany) depending on the resistance marker.

Homologous integration of the resistance cassettes and absence of the WT genes was verified in Southern blot analyses as well as diagnostic PCR. In the latter case, the following primer combinations were applied: 5diag/trpC_T (5'), 3diag/trpC_P2 (3'), WT_F/WT_R (untransformed nuclei). Diagnostic PCRs for three independent transformants of Δ*12019*, Δ*gpy1*, Δ*gpy2* and Δ*12023*, respectively, can be found in Fig. S3 and Fig. S6-Fig. S8. Concerning the *in loco* complementation, transformants unable to grow on hygromycin B (deletion phenotype) but able to grow on nourseothricin (complementation phenotype) were additionally analyzed for the homologous integration of the complementation constructs: 5diag/c_diag (5'), 3diag/nat1_R1 (3'), 5diag/trpC_T (untransformed nuclei). Diagnostic PCRs for three independent transformants of *GPY1*^{C} are depicted in Fig. S4*C*; further three transformants of *GPY1*^{G1443V} showed the same signals (data not shown). Diagnostic PCRs for two independent transformants of *GPY2*^{C} are shown in Fig. S10*C*. Finally, the presence of the overexpression vectors was verified using PoliC_Seq_F2/12020_OE_diag for two independent transformants of OE::*GPY1* (Fig. S9*A*), PoliC_Seq_F2/12023_WT_R for three independent transformants of OE::*12023* (Fig. S9*B*) as well as GS_Prom_M/OE_12021_diag for three independent transformants of OE::*GPY2* and one transformant of OE::*GPY1*/OE::*GPY2* (Fig. S9*C*).

Standard molecular methods

For DNA isolation from *F. fujikuroi*, lyophilized mycelium was ground in the presence of liquid nitrogen and extracted following the protocol of Cenis (82). Generated deletion mutants were analyzed *via* Southern blot (83) regarding ectopically integrated replacement cassettes. Thus, their genomic DNA was digested with an appropriate restriction enzyme (Fermentas, St. Leon-Rot, Germany) whereupon it was separated in a 1% (w/v) agarose gel and transferred onto a nylon membrane (Nytran™ SPC, Whatman, Sanford, USA) by downward alkali blotting (84). Hybridization was performed with ^{32}P-labeled probes that were generated with the random oligomer-primer method (85). Amplified 5' or 3' sequences served as templates for probe generation (Table S1). Southern blot analyses of Δ*gpy1* and Δ*gpy2* can be found in Fig. S3 and Fig. S7, respectively. Plasmid DNA from *S. cerevisiae* as well as *E. coli* Top10 F' (Invitrogen, Darmstadt, Germany) was isolated with the NucleoSpin® Plasmid Kit (Machery-Nagel, Düren, Germany). Concerning DNA amplification by PCR, BioTherm™ DNA Polymerase (GeneCraft, Lüdinghausen, Germany) was chosen for standard applications, especially diagnostic PCR, and handled according to the manufacturer's instructions. For the purpose of amplifying long fragments, TaKaRa LA Taq® DNA Polymerase (Takara Bio, Saint-Germain-en-Laye, France) was used, while Phusion® High-Fidelity DNA Polymerase (Finnzymes, Vantaa, Finland) was applied in case proof-reading was essential.

RNA isolation was carried out under the use of the TRI Reagent™ (Sigma-Aldrich, Steinheim, Germany). For expressional analyses by Northern blot (86), 20 µg of total RNA was separated in a 1% (w/v) denaturating agarose gel (85). Upon

transfer of the separated RNA onto a nylon membrane (Nytran™ SPC, Whatman, Sanford, USA), it was hybridized with ^{32}P-labeled probes as indicated above (85). Ca. 1 kb fragments of *GPY1* and *FFUJ_12023* served as templates for probe generation and were amplified with primer pairs 12020_WT_F/12020_WT_R and 12023_WT_F/12023_WT_R, respectively (Table S1). Prior to expressional analyses by qRT-PCR, 1 µg of total RNA was treated with DNase I (Fermentas, St. Leon-Rot, Germany) and transcribed into cDNA using oligo dT primers and SuperScript® II Reverse Transcriptase (Invitrogen, Darmstadt, Germany) according to the manufacturer's instructions. Subsequently, qRT-PCR was performed with iQ SYBR Green Supermix (Bio-Rad, München, Germany) and cDNA as template using an iCycler iQ Real-Time PCR System (Bio-Rad). The annealing temperature was 60 °C and the primer efficiencies were between 90-110%. The ΔΔCt-method was used for calculating the results (87). For quantification of mRNA levels of the desired genes (*FFUJ_12019*, *GPY1*, *GPY2*, *FFUJ_12022*, *FFUJ_12023*) and the constitutively expressed reference genes (*FFUJ_07710*, a GDP mannose transporter gene; *FFUJ_05652*, a related actin gene; *FFUJ_08398*, a ubiquitin gene), the primers listed in Table S3 were used. The experiments were performed in two technical replicates and at least two biological repeats.

Quantitative analysis of gibepyrone A and its derivatives by HPLC-MS/MS and HPLC-HRMS

For quantifying gibepyrone A in the supernatant as sensitive as possible, a QTRAP 6500 MS system (SCIEX, Darmstadt, Germany) coupled to a 1260 Infinity LC system (Agilent, Waldbronn, Germany) was used. Seven day-old cultures were filtered using 0.45 µm membrane filters (BGB Analytik, Schloßböckelheim, Germany). Metabolite extraction from the mycelium was performed with a modified method described by Niehaus and co-workers (12). Briefly, 0.1 g of harvested, washed and lyophilized mycelium was mixed thoroughly with 1.5 mL ethyl acetate:MeOH:dichlormethane (3:2:1, v/v) for 2 h. 0.75 mL of the extract was evaporated to dryness and taken up in 0.75 mL 15% (v/v) MeOH.

For relative quantification of gibepyrone A *via* HPLC-MS, methylparaben (MePa) was used as internal standard and chromatographic separation was carried out on a 150 mm x 2.1 mm i.d., 5 µm, Eclipse XDB-C_{18} column (Agilent Technologies, Waldbronn, Germany) with MeOH + 1% formic acid (FA) as solvent A and H_2O + 1% FA as solvent B. The column was tempered to 40 °C. After isocratic running for 3 min at 15% A, the gradient rose up to 100% A in 10 min. With the concentration of solvent A, the flow rate also rose from 400 µL to 450 µL. After holding these conditions for 2 min, the column was equilibrated for 3 min. A divert valve was used to discard polar substances from the medium in the first 3 min of the run. For MS/MS analysis with electrospray ionization (ESI), the following parameters were used: The curtain gas (nitrogen) was set to 30 psi, the nebulizer gas (zero-grade air) to 35 psi and the drying gas (zero-grade air) to 40 psi. The ion spray voltage was set to +5500 V in the positive and to -4500 V in the negative mode. Nitrogen was also used as collision gas in medium mode. Gibepyrone A was analyzed with a declustering potential (DP) of 56 V, an entrance potential (EP) of 10 V and a cell exit potential (CXP) of 12 V. The collision energy (CE) was adjusted for every Multiple Reaction Monitoring, respectively. The proton adduct of gibepyrone A was used as parent ion for gibepyrone A analysis and the following transitions were applied: Quantifier gibepyrone A $(M+H)^+$: *m/z* 165/91 (CE +31 V), qualifier 1 gibepyrone A: *m/z* 165/77 (CE +47 V), qualifier 2 gibepyrone A: *m/z* 165/67 (CE +27 V). For MePa analysis, negative polarity was used. The DP was set to -50 V while the CE and the CXP varied for each transition. Quantifier MePa $(M-H)^-$: *m/z* 151.0/92.0 (CE -23 V, CXP -11 V), qualifier MePa: *m/z* 151.0/121.0 (CE -28 V, CXP -11 V).

For the identification of gibepyrone A derivatives, HPLC-HRMS measurements were carried out on a HPLC system (Accela LC with Accela pump 60057-60010 and Accela autosampler 60057-60020, Thermo Scientific, Dreieich, Germany) coupled to a Fourier transform mass spectrometer with a heated ESI source (LTQ Orbitrap XL, Thermo Scientific, Dreieich, Germany). The HPLC column used was a 150 mm × 2.00 mm i.d., 5 µm, Gemini C_{18} with a 4 mm × 2 mm Gemini NX C_{18} guard column (Phenomenex, Aschaffenburg, Germany). The MS parameters were set as described elsewhere (17) with a change in capillary temperature from 275 °C to 300 °C. 1% FA in MeOH (v/v, solvent A) and 1% FA in H_2O (v/v, solvent B) were used as solvents with a flow rate of 250 µL/min. The gradient started with 10% A, holding this condition for 5 min. Until 15 min, the

gradient rose up to 100% A. Then, the column was equilibrated again with 10% A for 10 min. The injection volume was set to 10 µL. For HPLC-HRMS measurements, standard substances were dissolved in ethyl acetate and diluted with MeOH (1:10, v/v). A 10 µg/mL solution (in MeOH:H_2O (1:10, v/v)) was applied for the measurements. For analyzing the non-enzymatic conversion of gibepyrone A into gibepyrone E, 20 µg of gibepyrone A standard was incubated in 1 mL H_2O at 28 °C and 180 rpm for seven days.

Calculated *m/z* ratios of the different gibepyrone derivatives (Fig. 1*D*) are as follows: *m/z* gibepyrone A $(M+H)^+$ 165.0910, *m/z* gibepyrone B $(M+H)^+$ 181.0859, *m/z* gibepyrone C $(M+H)^+$ 178.0630, *m/z* gibepyrone D $(M+H)^+$ 195.0652, *m/z* gibepyrone E $(M+H)^+$ 181.0859, *m/z* gibepyrone F $(M+H)^+$ 153.0546. To differentiate between gibepyrones B and E, data dependent fragmentation (most intense ion from mass list) of gibepyrone derivatives was applied. Therefore, higher-energy collisional dissociation (HCD) with 50% normalized collision energy was used.

Gibepyrone B (*m/z* 181.0859, $(M+H)^+$, retention time (RT) 11.7 min) @HCD 50%: 109.0648 [$(M+H)^+$-$C_3H_4O_2$, 100%], 107.0855 [$(M+H)^+$-$C_2H_2O_3$, 61%], 137.0599 [$(M+H)^+$-, C_2H_4O; 41%], 181.0862 [$(M+H)^+$, 29%], 135.0806 [$(M+H)^+$-CH_2O_2, 25%], 105.0689 [$(M+H)^+$-$C_2H_4O_3$, 17%], 117.0699 [$(M+H)^+$-CH_4O_3, 10%], 115.0543 [$(M+H)^+$-CH_6O_3, 6%], 163.0756 [$(M+H)^+$-H_2O, 6%], 111.0805 [$(M+H)^+$-$C_3H_2O_2$, 3%], 107.0491 [$(M+H)^+$-$C_3H_6O_2$, 2%], 125.0961 [$(M+H)^+$-C_2O_2, 2%], 151.0756 [$(M+H)^+$-CH_2O, 2%].

Gibepyrone E 1 (presumably diol 1) (*m/z* 181.0859, $(M+H)^+$, RT 8.4 min) @HCD 50%: 109.0284 [$(M+H)^+$-C_4H_8O, 100%], 139.0755 [$(M+H)^+$-C_2H_2O, 70%], 111.0804 [$(M+H)^+$-$C_3H_2O_2$, 30%], 138.0677 [$(M+H)^+$-C_2H_3O, 12%], 109.0647 [$(M+H)^+$-C_3H_4O, 6%], 121.0649 [$(M+H)^+$-$C_2H_4O_2$, 5%], 181.0863 [$(M+H)^+$, 4%], 152.0834 [$(M+H)^+$-CHO, 4%], 135.0806 [$(M+H)^+$-CH_2O_2, 3%], 111.0440 [$(M+H)^+$-C_4H_6O, 2%].

Gibepyrone E 2 (presumably diol 2) (*m/z* 181.0859, $(M+H)^+$, RT 9.1 min) @HCD 50%: 109.0284 [$(M+H)^+$-C_4H_8O, 100%], 139.0755 [$(M+H)^+$-C_2H_2O, 72%], 111.0804 [$(M+H)^+$-$C_3H_2O_2$, 30%], 138.0677 [$(M+H)^+$-C_2H_3O, 12%], 121.0649 [$(M+H)^+$-$C_2H_4O_2$, 5%], 181.0863 [$(M+H)^+$, 4%], 152.0834 [$(M+H)^+$-CHO-4%], 109.0647 [$(M+H)^+$-$C_3H_4O_2$, 4%], 111.0440 [$(M+H)^+$-C4H6O, 3%].

Gibepyrone E (main peak of standard substance) (*m/z* 181.0857, $(M+H)^+$, RT 11.9 min) @HCD 50%: 109.0280, [$(M+H)^+$-C_4H_8O, 100%], 139.0750 [$(M+H)^+$-C_2H_2O, 67%], 111.0801 [$(M+H)^+$-$C_3H_2O_2$, 28%], 109.0647 [$(M+H)^+$-$C_3H_4O_2$, 16%], 138.0672 [$(M+H)^+$-C_2H_3O, 11%],152.0829 [$(M+H)^+$-CHO, 9%], 135.0806 [$(M+H)^+$-CH_2O_2, 8%], 181.0863 [$(M+H)^+$, 8%], 121.0649 [$(M+H)^+$-$C_2H_4O_2$, 6%].

General synthetic and analytical methods

Chemicals were purchased from Acros Organics (Geel, Belgium) or Sigma-Aldrich (Steinheim, Germany) and used without purification. Commercially available isotopically labeled compounds were purchased from Euriso-Top (Saarbrücken, Germany) or Sigma-Aldrich. Thin-layer chromatography was performed with 0.2 mm pre-coated plastic sheets Polygram® Sil G/UV254 (Machery-Nagel, Düren, Germany). Normal phase column chromatography was carried out using Merck silica gel 60 (70-200 mesh). Reversed phase column chromatography was carried out using Merck Lichroprep RP-18 silica gel (40-63 µm). ^{1}H NMR and ^{13}C NMR spectra were recorded on Bruker AV I (300 MHz), AV I (400 MHz) and AV III HD Prodigy (500 MHz) spectrometers and were referenced against $CDCl_3$ (δ = 7.26 ppm), C_6D_6 (δ = 7.16 ppm) and CD_2Cl_2 (δ = 5.32 ppm) for ^{1}H-NMR and $CDCl_3$ (δ = 77.01 ppm), C_6D_6 (δ = 128.06 ppm), CD_2Cl_2 (δ = 53.84 ppm) for ^{13}C-NMR. Analyses *via* GC-MS were carried out with a HP 7890B gas chromatograph connected to a HP 5977A inert mass detector fitted with a HP5-MS fused silica capillary column (30 m, 0.25 mm i.d., 0.50 µm film). The instrumental parameters were (1) inlet pressure, 77.1 kPa, He 23.3 mL min^{-1}, (2) injection volume, 2 µL, (3) transfer line, 250 °C, and (4) electron energy, 70 eV. The GC was programmed as follows for synthetic samples: 5 min at 50 °C increasing at 10 °C min^{-1} to 320 °C, and operated in split mode (50:1, 60 s valve time). For headspace analysis, autoxidation experiments and analysis of liquid culture extracts, the GC program was as follows: 5 min at 50 °C increasing at 5 °C min^{-1} to 320 °C, and operated in split mode (10:1, 60 s valve time). The carrier gas was He at 1 mL min^{-1}. Retention indices (*I*) were determined from a homologous series of n-alkanes (C_8-C_{40}). IR spectra were recorded on a Bruker Alpha ATR spectrometer.

UV/Vis spectra were recorded on an Agilent Cary 100 spectrometer.

Synthetic procedures

Gibepyrone A: A solution of triethyl amine (8.96 g, 88.6 mmol, 1.05 eq) in dichloromethane (10 mL) was added dropwise over 15 min to a solution of tigloyl chloride (10.0 g, 84.3 mmol, 1.0 eq) in dichloromethane (80 mL) under argon atmosphere at room temperature. The solution changed colors immediately from colorless to deep red and was stirred for 18 h at room temperature. The solvent was removed *in vacuo* and the solid residue was taken up in Et_2O. The insoluble material was removed by filtration and the filtrate was concentrated *in vacuo*, giving a red oil, which was subjected to column chromatography on reversed phase silica gel (H_2O:MeOH, 1:1 changing to 2:1). The product yielding fractions were collected, concentrated to an aqueous suspension and extracted with dichloromethane (3x). The combined organic layers were dried over $MgSO_4$ and the solvent was evaporated, giving gibepyrone A (1.26 g, 7.67 mmol, 18%) as a colorless highly viscous oil and its isomer 6-(but-3-en-2-yl)-3-methyl-2*H*-pyran-2-one (**2**, 1.18 g, 7.22 mmol, 17%) as a yellow oil.

TLC (pentane:Et_2O, 5:1): R_f = 0.29. GC (HP-5): I = 1523. ^{1}H-NMR (400 MHz, CD_2Cl_2): δ = 7.12 (dq, $^3J_{H,H}$ = 6.9 Hz, $^4J_{H,H}$ = 1.2 Hz, 1H, CH), 6.54 (q, $^3J_{H,H}$ = 6.9 Hz, 1H, CH), 6.06 (d, $^3J_{H,H}$ = 6.9 Hz, 1H, CH), 2.04 (s, 3H, CH_3), 1.85 (d, $^4J_{H,H}$ = 1.1 Hz, 3H, CH_3), 1.83 (d, $^3J_{H,H}$ = 6.9 Hz, 3H, CH_3) ppm. ^{13}C-NMR (100 MHz, CD_2Cl_2): δ = 163.4 (C_q), 160.1 (C_q), 140.2 (CH), 128.0 (CH), 127.5 (C_q), 123.4 (C_q), 100.9 (CH), 16.7 (CH_3), 14.3 (CH_3), 12.2 (CH_3) ppm. IR (ATR): $\tilde{\nu}$ = 3040 (w), 2978 (w), 2920 (w), 2856 (w), 1697 (s), 1645 (s), 1559 (s), 1449 (m), 1381 (m), 1322 (w), 1210 (w), 1130 (m), 1111 (m), 1050 (s), 1016 (m), 992 (m), 958 (m), 884 (w), 801 (s), 740 (s), 696 (m), 557 (w), 529 (m), 471 (w) cm^{-1}. UV/Vis (MeOH): λ_{max} (lg ε): 331 (1.602), 240 (1.642) nm. EI-MS (70 eV): *m*/*z* (%) = 164 (100), 136 (64), 121 (77), 109 (62), 93 (22), 91 (15), 82 (7), 77 (11), 55 (14), 53 (40). High resolution electron ionization mass spectrometry (HREIMS) calculated for $C_{10}H_{12}O_2^{\bullet+}$: 164.0832, found: 164.0823.

Pyrone **2**: TLC (cyclohexane:EtOAc, 2:1) R_f = 0.65. GC (HP-5): I = 1240. ^{1}H-NMR (400 MHz, C_6D_6): δ = 6.25 (dq, $^3J_{H,H}$ = 6.6 Hz, $^4J_{H,H}$ = 1.2 Hz, 1H, CH), 5.65 (ddd, $^3J_{H,H}$ = 17.3 Hz, $^3J_{H,H}$ = 10.0 Hz, $^3J_{H,H}$ = 7.1 Hz, 1H, CH), 4.91 (ddd, $^4J_{H,H}$ = 1.2 Hz, $^3J_{H,H}$ = 17.4 Hz, $^2J_{H,H}$ = 1.4 Hz, 1H, CH), 4.90 (ddd, $^4J_{H,H}$ = 1.3 Hz, $^3J_{H,H}$ = 10.2, $^2J_{H,H}$ = 1.4 Hz, 1H, CH), 2.85 (dq $^3J_{H,H}$ = 7.0 Hz, $^3J_{H,H}$ = 7.0 Hz, 1H, CH), 1.84 (d, $^4J_{H,H}$ = 1.2 Hz, 3H, CH_3), 1.02 (d, $^3J_{H,H}$ = 7.0 Hz, 3H, CH_3) ppm. ^{13}C-NMR (100 MHz, C_6D_6): δ = 165.1 (C_q), 162.9 (C_q), 138.7 (CH), 138.5 (CH), 123.0 (C_q), 115.8 (CH_2), 100.9 (CH), 41.8 (CH), 17.6 (CH_3), 16.7 (CH_3). IR (ATR): $\tilde{\nu}$ = 3084 (w), 2973 (w), 2937 (w), 2924 (w), 2886 (w), 1706 (vs), 1642 (s), 1580 (s), 1453 (w), 1434 (w), 1417 (w), 1380 (m), 1360 (m), 1228 (w), 1216 (w), 1108 (s), 1075 (w), 1042 (m), 995 (m), 920 (m), 817 (m), 732 (m), 691 (w), 673 (w), 543 (w), 531 (w). UV/Vis (dichlormethane): λ_{max} (lg ε): 297 (2.657), 202 (3.737) nm. EI-MS (70 eV): *m*/*z* (%) = 164 (45), 136 (18), 121 (16), 109 (100), 93 (5), 91 (5), 81 (12), 53 (51), 39 (5). HREIMS calculated for $C_{10}H_{12}O_2^{\bullet+}$: 164.0832, found: 164.0826.

Gibepyrone E: To a solution of gibepyrone A (300 mg, 1.83 mmol, 1.0 eq) in dichloromethane, *meta*-chloroperbenzoic acid (70% in H_2O, 541 mg, 2.20 mmol, 1.2 eq) was added. The reaction was quenched after 30 min by adding $NaHCO_3$ (aq., sat.). The mixture was extracted with dichloromethane (3x) and the combined organic layers were dried over $MgSO_4$. The solvent was removed *in vacuo* and the oily residue was subjected to column chromatography on reversed phase silica gel (H_2O:MeOH, 2:1). The product yielding fractions were collected, concentrated to an aqueous suspension and extracted with dichloromethane (3x). The combined organic layers were dried over $MgSO_4$ and the solvent was evaporated, yielding gibepyrone E (245 mg, 1.36 mmol, 74%) as a colorless, viscous oil.

TLC (H_2O:MeOH, 2:1) R_f = 0.27. GC (HP-5): I = 1471. ^{1}H-NMR (300 MHz, C_6D_6): δ = 6.21 (dq, $^3J_{H,H}$ = 6.7 Hz, $^4J_{H,H}$ = 1.5 Hz, 1H, CH), 5.69 (d, $^3J_{H,H}$ = 6.7 Hz, 1H, CH), 2.68 (q, $^3J_{H,H}$ = 5.4 Hz, 1H, CH), 1.82 (d, $^4J_{H,H}$ = 1.3 Hz, 3H, CH_3), 1.23 (s, 3H, CH_3), 0.88 (d, $^3J_{H,H}$ = 5.4 Hz, 3H, CH_3) ppm. ^{13}C-NMR (75 MHz, C_6D_6): δ = 163.0 (C_q), 162.3 (C_q), 138.8 (CH), 123.9 (C_q), 99.9 (CH), 61.3 (CH), 57.4 (C_q), 16.8 (CH_3), 13.9 (CH_3), 13.7 (CH_3) ppm. IR (ATR): $\tilde{\nu}$ = 3458 (w, br), 3099 (w), 3052 (w), 2978 (w), 2950 (w), 2922 (w), 1704 (vs), 1643 (s), 1578 (s), 1375 (m), 1281 (m), 1222 (w), 1169 (w), 1124 (s), 1081 (m), 1053 (s), 1027 (s), 811 (s), 756 (s), 739 (m), 669 (w),653 (m), 548 (m), 522 (w), 481 (m), 450 (m) cm^{-1}. UV/Vis (dichlormethane): λ_{max} (lg ε): 299 (3.517), 238 (2.964) nm. EI-MS (70 eV): *m*/*z* (%) = 180 (20), 164 (6), 153 (3), 136 (45), 121 (100), 109 (20), 108 (19), 107 (18), 93 (11), 81 (16), 79

(22), 65 (11), 53 (37), 43 (31), 39 (8). HREIMS calculated for $C_{10}H_{12}O_3^{\bullet+}$: 180.0781, found: 180.0781.

6-(2-Hydroxybut-3-en-2-yl)-3-methyl-2*H*-pyran-2-one (**3**): *t*-BuOOH (70% in H_2O, 1.96 g, 15.3 mmol, 2.50 eq) was added to a suspension of SeO_2 (372 mg, 3.36 mmol, 0.55 eq) in dichloromethane (45 mL). The resulting mixture was stirred for 20 min at room temperature. After addition of a solution of pyrone **2** (1.00 g, 6.10 mmol, 1.00 eq) in dichloromethane (10 mL), the resulting solution was heated under reflux for six days. The reaction was cooled to 0 °C and diluted with H_2O and dichloromethane. The layers were separated and the H_2O layer was extracted with dichloromethane (3x). The combined organic layers were dried with $MgSO_4$ and the solvent was removed *in vacuo*. The crude product was subjected to column chromatography (Florisil, petroleum ether:Et_2O, 5:1 to 2:1), yielding hydroxypyrone **5** (380 mg, 2.11 mmol, 35%).

TLC (cyclohexane:EtOAc, 2:1) R_f = 0.19. GC (HP-5) I = 1471. ^{1}H-NMR (400 MHz, C_6D_6): δ = 6.30 (dq, $^3J_{H,H}$ = 6.7 Hz, $^4J_{H,H}$ = 1.2 Hz, 1H, CH), 5.99 (dd, $^3J_{H,H}$ = 10.6 Hz, $^3J_{H,H}$ = 17.2 Hz, 1H, CH), 5.92 (d, $^3J_{H,H}$ = 6.7 Hz, 1H, CH), 5.34 (dd, $^3J_{H,H}$ = 17.2 Hz, $^2J_{H,H}$ = 1.1 Hz, 1H, CH), 4.98 (dd, $^3J_{H,H}$ = 10.6 Hz, $^2J_{H,H}$ = 1.1 Hz, 1H, CH), 1.79 (d, $^4J_{H,H}$ = 1.2 Hz, 3H, CH_3), 1.42 (s, 3H, CH_3) ppm. ^{13}C-NMR (100 MHz, C_6D_6): δ = 165.7 (C_q), 162.9 (C_q), 141.5 (CH), 139.3 (CH), 123.2 (C_q), 114.0 (CH), 100.0 (CH_2), 73.3 (C_q), 26.7 (CH_3), 16.6 (CH_3). IR (ATR): $\tilde{\nu}$ = 3520 (m, br), 3049 (w), 2981 (w), 2927 (w), 1692 (s), 1638 (s), 1577 (s), 1452 (w), 1410 (w), 1382 (w), 1363 (m), 1338 (m), 1199 (m),1107 (s), 1046 (s), 994 (s), 928 (s), 827 (s), 761 (s), 538 (m) cm^{-1}. UV/Vis (dichlormethane): λ_{max} (lg ε): 298 (3.756), 201 (3.604) nm. EI-MS (70 eV): *m*/*z* (%) = 180 (10), 165 (5), 137 (64), 135 (7), 125 (16), 109 (100), 91 (5), 82 (14), 81 (20), 71 (33), 55 (17), 53 (90), 43 (39), 41 (7), 39 (7). HREIMS calculated for $C_{10}H_{12}O_3^{\bullet+}$: 180.0781, found: 180.0772.

Gibepyrone B: A mixture of tetrahydrofuran (3 mL) and H_2O (0.7 mL) was degassed by an argon stream for 60 min. Hydroxypyrone **3** (110 mg, 0.67 mmol, 1.00 eq) and methanesulfonic acid (118 mg, 1.22 mmol, 2 eq) were added subsequently under argon atmosphere at room temperature and the resulting mixture was stirred at room temperature for 25 days in the dark. The reaction mixture was diluted with H_2O and extracted with EtOAc (3x). The combined organic layers were dried with $MgSO_4$, the solvent was removed *in vacuo* and the crude product was subjected to column chromatography on silica gel (cyclohexane:EtOAc, 1:2), yielding gibepyrone B (35 mg, 0.19 mmol, 29%) as a pale yellow viscous oil.

TLC (cyclohexane:EtOAc, 2:1) R_f = 0.11. GC (HP-5) I = 1817. ^{1}H-NMR (400 MHz, CD_2Cl_2): δ = 7.04 (dq, $^3J_{H,H}$ = 6.9 Hz, $^4J_{H,H}$ = 1.2 Hz, 1H, CH), 6.46 (tq, $^3J_{H,H}$ = 6.5 Hz, $^4J_{H,H}$ = 1.1 Hz, 1H, CH), 6.05 (d, $^3J_{H,H}$ = 6.9 Hz, 1H, CH), 4.27 (d, $^3J_{H,H}$ = 6.5 Hz, 2H, CH_2), 1.96 (br s, 3H, CH_3), 1.78 (br s, 3H, CH_3). ^{13}C-NMR (125 MHz, CD_2Cl_2): 163.3 (C_q), 159.2 (C_q), 140.0 (CH), 131.7 (CH), 127.9 (C_q), 124.5 (C_q), 102.1 (CH), 59.8 (CH_2), 16.7 (CH_3), 12.7 (CH_3). IR (ATR): $\tilde{\nu}$ = 3472 (br m), 3044 (w), 2922 (w), 2863 (w), 1669 (vs), 1642 (vs), 1615 (s), 1552 (vs), 1454 (m), 1382 (m), 1226 (m), 1203 (w), 1115 (s), 1069 (s), 1009 (s), 908 (w), 812 (s), 760 (s), 594 8m), 556 (m), 532 (m), 489 (m) cm^{-1}. UV/Vis (dichlormethane): λ_{max} (lg ε): 324 (3.900), 235 (3.911), 213 (3.981) nm. EI-MS (70 eV): *m*/*z* (%) = 180 (20), 151 (100), 123 (5), 109 (19), 107 (5), 105 (6), 95 (8), 91 (9), 81 (6), 79 (6), 77 (6), 53 (24), 43 (10), 41 (6), 39 (6). HREIMS calculated for $C_{10}H_{12}O_3^{\bullet+}$: 180.0781, found: 180.0778.

Gibepyrone C: Pyridinium chlorochromate (242 mg, 1.12 mmol, 2.0 eq) was added to a solution of hydroxypyrone **3** (100 mg, 0.56 mmol, 1.0 eq) in dichloromethane under argon atmosphere at room temperature. The mixture was heated to reflux for 6 h, followed by addition of another portion of pyridinium chlorochromate (242 mg, 1.12 mmol, 2.0 eq). Heating was continued for 3 h. The reaction mixture was cooled to room temperature, diluted with Et_2O and filtrated over a short pad of silica gel. The solvents were evaporated and the crude product was subjected to column chromatography (petroleum ether:EtOAc, 1:2) yielding gibepyrone C (10 mg, 0.056 mmol, 10%) as a yellow solid.

TLC (petrolium ether:EtOAc, 2:1) R_f = 0.16. GC (HP-5) I = 1740. ^{1}H-NMR (500 MHz, $CDCl_3$): 10.19 (d, $^3J_{H,H}$ = 7.4 Hz, 1H, CH), 7.19 (d, $^3J_{H,H}$ = 6.9 Hz, 1H, CH), 6.80 (d, $^3J_{H,H}$ = 7.4 Hz, 1H, CH), 6.53 (d, $^3J_{H,H}$ = 6.8 Hz, 1H, CH), 2.37 (s, 3H, CH_3), 2.16 (s, 3H, CH_3) ppm. ^{13}C-NMR (125 MHz, $CDCl_3$): 191.0 (CH), 162.0 (C_q), 157.0 (C_q), 144.3 (C_q), 138.5 (CH), 128.7 (C_q), 127.2 (CH), 106.2 (CH), 17.2 (CH_3), 12.8 (CH_3) ppm. EI-MS (70 eV): *m*/*z* (%) = 178 (90), 163 (7), 150 (100), 149 (19), 135 (44), 133 (11), 122 (50), 121 (20), 109 (58), 108 (21), 107 (55), 96 (63), 91 (20), 82 (25), 81 (16), 79 (38), 77 (27), 69 (16),

68 (42), 53 (91), 52 (14), 51 (16), 43 (19), 41 (14), 39 (23). HREIMS calculated for $C_{10}H_{10}O_3^{\bullet+}$: 178.0625, found: 178.0621.

GC-MS analysis and feeding experiments

For analysis of emitted volatile compounds, the fungal strains were inoculated on solid CM medium using a small piece of pre-culture grown on the same medium and grown for seven days at 28 °C in the dark, before collection of the volatiles on charcoal filter traps by use of a closed-loop stripping apparatus (CLSA), followed by analysis of headspace extracts by GC-MS, as described previously (32).

For the comparative analysis of gibepyrone A production by *F. fujikuroi* IMI58289 and *F. solani* DSM 62416, both strains were cultivated in liquid ICI medium (6 mM glutamine) and in the medium used for the isolation of fusalanipyrone (41) for seven days at 28 °C and 180 rpm. After filtration through a cotton cloth and centrifugation, 45 mL of the respective culture supernatant was extracted with EtOAc (2x 5 mL). The combined organic layers were dried over $MgSO_4$ and subjected directly to GC-MS analysis.

Autoxidation of gibepyrone A to gibepyrone F was performed by solving 0.5 mg gibepyrone A in Et_2O (1.5 mL) and analysis by GC-MS. Then the solvent was allowed to evaporate at room temperature and the dry sample was kept at ambient conditions for seven days before being solved in Et_2O (1.5 mL) and analyzed by GC-MS again.

The mutant strain *F. fujikuroi* Δ*vel1* (56) was used for all feeding experiments and was pre-cultured on CM solid medium. For the feeding experiments, (*methyl*-^{13}C)methionine (2 mM), ($^2H_{10}$)isoleucine (2 mM), (2-^{13}C)acetate (2 mM), ($^2H_5$)propionate (3 mM) or (6,6,6-$^2H_3$)mevalonolactone (2 mM) (88) were added to CM solid medium after autoclaving. The agar plates were inoculated with about 0.25 cm^2 of the pre-culture, incubated for four days at 28 °C and used for CLSA/GC-MS headspace analysis. Incorporation rates were calculated from integrated peak areas using ion trace chromatograms of the respective molecular ion for each isotopomer.

Acknowledgments

This work was supported by the German Research Foundation (project numbers TU101/16-2 and HU730/9-3) and by the Collaborative Research Centre SFB 813 “Chemistry at Spin Centres”.

Conflict of interest

The authors declare that they have no conflicts of interest with the contents of this article.

Author contributions

Conceived and designed the experiments: SJ, BA, IB, HH, JD, BT; Performed the experiments: SJ, BA, EN, IB, SR, NB; Analyzed the data: SJ, BA, EN, IB, SR, NB, HH, JD, BT; Contributed materials: HH, JD, BT; Wrote the paper: SJ, BA, JD, BT

References

1. Nirenberg, H.I., and O'Donnell, K. (1998) New *Fusarium* species and combinations within the *Gibberella fujikuroi* species complex. *Mycologia.* **90,** 434-458

2. Leslie, J.F., and Summerell, B.A. (2006) *Fusarium* laboratory workshops - A recent history. *Mycotoxin Research.* **22,** 73-74

3. Sun, S., and Snyder, W.C. (1981) The *bakanae* disease of the rice plant. In: Nelson, P.E., Toussoun, T.A., and Cook, R.J. (ed) *Fusarium*: Diseases, Biology and Taxonomy. The Pennsylvania State University Press, University Park, pp 104-113

4. Tudzynski, B. (2005) Gibberellin biosynthesis in fungi: Genes, enzymes, evolution, and impact on biotechnology. *Appl.Microbiol.Biotechnol.* **66,** 597-611

5. Bömke, C., and Tudzynski, B. (2009) Diversity, regulation, and evolution of the gibberellin biosynthetic pathway in fungi compared to plants and bacteria. *Phytochemistry.* **70,** 1876-1893

6. Tudzynski, B., and Hölter, K. (1998) Gibberellin biosynthetic pathway in *Gibberella fujikuroi*: Evidence for a gene cluster. *Fungal Genet.Biol.* **25,** 157-170

7. Wiemann, P., Willmann, A., Straeten, M., Kleigrewe, K., Beyer, M., Humpf, H., and Tudzynski, B. (2009) Biosynthesis of the red pigment bikaverin in *Fusarium fujikuroi*: Genes, their function and regulation. *Mol.Microbiol.* **72,** 931-946

8. Studt, L., Wiemann, P., Kleigrewe, K., Humpf, H., and Tudzynski, B. (2012) Biosynthesis of fusarubins accounts for pigmentation of *Fusarium fujikuroi* perithecia. *Appl.Environ.Microbiol.* **78,** 4468-4480

9. Niehaus, E., Kleigrewe, K., Wiemann, P., Studt, L., Sieber, C.M.K., Connolly, L.R., Freitag, M., Güldener, U., Tudzynski, B., and Humpf, H. (2013) Genetic manipulation of the *Fusarium fujikuroi* fusarin gene cluster yields insight into the complex regulation and fusarin biosynthetic pathway. *Chem.Biol.* **20,** 1055-1066

10. Niehaus, E., von Bargen, K.W., Espino, J.J., Pfannmüller, A., Humpf, H., and Tudzynski, B. (2014) Characterization of the fusaric acid gene cluster in *Fusarium fujikuroi*. *Appl.Microbiol.Biotechnol.* **98,** 1749-1762

11. Studt, L., Janevska, S., Niehaus, E., Burkhardt, I., Arndt, B., Sieber, C.M.K., Humpf, H., Dickschat, J.S., and Tudzynski, B. (2016) Two separate key enzymes and two pathway-specific transcription factors are involved in fusaric acid biosynthesis in *Fusarium fujikuroi*. *Environ.Microbiol.* **18,** 936-956

12. Niehaus, E., Janevska, S., von Bargen, K.W., Sieber, C.M.K., Harrer, H., Humpf, H., and Tudzynski, B. (2014) Apicidin F: Characterization and genetic manipulation of a new secondary metabolite gene cluster in the rice pathogen *Fusarium fujikuroi*. *PLoS ONE.* **9,** e103336

13. Rösler, S.M., Sieber, C.M.K., Humpf, H., and Tudzynski, B. (2016) Interplay between pathway-specific and global regulation of the fumonisin gene cluster in the rice pathogen *Fusarium fujikuroi*. *Appl.Microbiol.Biotechnol.* **13,** 5869–5882

14. Niehaus, E., Studt, L., von Bargen, K.W., Kummer, W., Humpf, H., Reuter, G., and Tudzynski, B. (2016) Sound of silence: the beauvericin cluster in *Fusarium fujikuroi* is controlled by cluster-specific

and global regulators mediated by H3K27 modification. *Environ.Microbiol.* Accepted article, doi: 10.1111/1462-2920.13576

15. Brock, N.L., Huss, K., Tudzynski, B., and Dickschat, J.S. (2013) Genetic dissection of desquiterpene biosynthesis by *Fusarium fujikuroi. ChemBioChem.* **14,** 311-315

16. Burkhardt, I., Siemon, T., Henrot, M., Studt, L., Rösler, S., Tudzynski, B., Christmann, M., and Dickschat, J.S. (2016) Mechanistic characterization of two sesquiterpene cyclases from the plant pathogenic fungus *Fusarium fujikuroi. Angew.Chem.Int.Ed.* **55,** 8748-8751

17. Wiemann, P., Sieber, C.M.K., von Bargen, K.W., Studt, L., Niehaus, E., Espino, J.J., Huß, K., Michielse, C.B., Albermann, S., Wagner, D., Bergner, S.V., Connolly, L.R., Fischer, A., Reuter, G., Kleigrewe, K., Bald, T., Wingfield, B.D., Ophir, R., Freeman, S., Hippler, M., Smith, K.M., Brown, D.W., Proctor, R.H., Münsterkötter, M., Freitag, M., Humpf, H., Güldener, U., and Tudzynski, B. (2013) Deciphering the cryptic genome: Genome-wide analyses of the rice pathogen *Fusarium fujikuroi* reveal complex regulation of secondary metabolism and novel metabolites. *PLoS Pathog.* **9,** e1003475

18. Dickinson, J.M. (1993) Microbial pyran-2-ones and dihydropyran-2-ones. *Nat.Prod.Rep.* **10,** 71-98

19. McGlacken, G.P., and Fairlamb, I.J.S. (2005) 2-Pyrone natural products and mimetics: Isolation, characterisation and biological activity. *Nat.Prod.Rep.* **22,** 369-385

20. Light, R.J., Harris, T.M., and Harris, C.M. (1966) Metabolism of triacetic acid and triacetic acid lactone. *Biochemistry (N.Y.).* **5,** 4037-4043

21. Bentley, R., and Zwitkowits, P.M. (1967) Biosynthesis of tropolones in *Penicillium stipitatum*. VII. The formation of polyketide lactones and other nontropolone compounds as a result of ethionine inhibition. *J.Am.Chem.Soc.* **89,** 676-680

22. Collins, R.P., and Halim, A.F. (1972) Characterization of the major aroma constituent of the fungus *Trichoderma viride* (Pers.). *J.Agric.Food Chem.* **20,** 437-438

23. Ghisalberti, E.L., Narbey, M.J., Dewan, M.M., and Sivasithamparam, K. (1990) Variability among strains of *Trichoderma harzianum* in their ability to reduce take-all and to produce pyrones. *Plant Soil.* **121,** 287-291

24. Claydon, N., Allan, M., Hanson, J.R., and Avent, A.G. (1987) Antifungal alkyl pyrones of *Trichoderma harzianum. Trans.Br.Mycol.Soc.* **88,** 503-513

25. Moss, M.O., Jackson, R.M., and Rogers, D. (1975) The characterization of 6-(pent-1-enyl)-α-pyrone from *Trichoderma viride. Phytochemistry.* **14,** 2706-2708

26. Wickel, S.M., Citron, C.A., and Dickschat, J.S. (2013) 2*H*-pyran-2-ones from *Trichoderma viride* and *Trichoderma asperellum. Eur.J.Org.Chem.* 2906-2913

27. Evidente, A., Conti, L., Altomare, C., Bottalico, A., Sindona, G., Segre, A.L., and Logrieco, A. (1994) Fusapyrone and deoxyfusapyrone, two antifungal α-pyrones from *Fusarium semitectum. Nat.Toxins.* **2,** 4-13

28. Visconti, A., Solfrizzo, M., Fruchier, A., and Apsimon, J.W. (1994) Acuminatopyrone: Revised structure and production by *Fusarium chlamydosporum* and *Fusarium tricinctum. J.Nat.Prod.* **57,** 695-699

29. Abbas, H.K., Mirocha, C.J., and Shier, W.T. (1992) Isolation, identification and biological activity of chlamydosporol from *Fusarium culmorum* HM-8. *Mycopathologia.* **118,** 115-123

30. Joffe, A.Z. (1969) Toxic properties and effects of *Fusarium poae* (Peck) Wr., *F. sporotrichioides* Sherb. and *Aspergillus flavus* Link. *J.Stored Prod.Res.* **5,** 211-218

31. Barrero, A.F., Oltra, J.E., Herrador, M.M., Cabrera, E., Sanchez, J.F., Quilez, J.F., Rojas, F.J., and Reyes, J.F. (1993) Gibepyrones: α-Pyrones from *Gibberella fujikuroi. Tetrahedron.* **49,** 141-150

32. Brock, N.L., Tudzynski, B., and Dickschat, J.S. (2011) Biosynthesis of sesqui- and diterpenes by the gibberellin producer *Fusarium fujikuroi. ChemBioChem.* **12,** 2667-2676

33. Dickschat, J.S. (2014) Capturing volatile natural products by mass spectrometry. *Nat.Prod.Rep.* **31,** 838-861

34. Short, D.P.G., O'Donnell, K., Thrane, U., Nielsen, K.F., Zhang, N., Juba, J.H., and Geiser, D.M. (2013) Phylogenetic relationships among members of the *Fusarium solani* species complex in human infections and the descriptions of *F. keratoplasticum* sp. nov. and *F. petroliphilum* stat. nov. *Fungal Genet.Biol.* **53,** 59-70

35. Wang, Q., Li, S., Zhao, F., Dai, H., Bao, L., Ding, R., Gao, H., Zhang, L., Wen, H., and Liu, H. (2011) Chemical constituents from endophytic fungus *Fusarium oxysporum. Fitoterapia.* **82,** 777-781

36. Liu, D., Li, X., Li, C., and Wang, B. (2013) Sesterterpenes and 2*H*-pyran-2-ones (=α-pyrones) from the mangrove-derived endophytic fungus *Fusarium proliferatum* MA-84. *Helv.Chim.Acta.* **96,** 437-444

37. Bertrand, S., Azzollini, A., Schumpp, O., Bohni, N., Schrenzel, J., Monod, M., Gindro, K., and Wolfender, J. (2014) Multi-well fungal co-culture for *de novo* metabolite-induction in time-series studies based on untargeted metabolomics. *Mol.Biosyst.* **10,** 2289-2298

38. Tang, S., Xu, R., Lin, W., and Duan, H. (2012) Jaspiferin A and B: Two new secondary metabolites from the South China Sea sponge *Jaspis stellifera. Records of Natural Products.* **6,** 398-401

39. Abrell, L.M., Cheng, X., and Crews, P. (1994) New nectriapyrones by salt water culture of a fungus separated from an Indo-Pacific sponge. *Tetrahedron Lett.* **35,** 9159-9160

40. Hentschel, U., Piel, J., Degnan, S.M., and Taylor, M.W. (2012) Genomic insights into the marine sponge microbiome. *Nat.Rev.Microbiol.* **10,** 641-654

41. Abraham, W., and Arfmann, H. (1988) Fusalanipyrone, a monoterpenoid from *Fusarium solani. Phytochemistry.* **27,** 3310-3311

42. Shimizu, B., Saito, F., Miyagawa, H., Watanabe, K., Ueno, T., Sakata, K., and Ogawa, K. (2005) Phytotoxic components produced by pathogenic *Fusarium* against morning glory. *J.Bioscience.* **60,** 862-866

43. Abraham, W., Knoch, I., and Witte, L. (1990) Biosynthesis of the terpenoidic polyketide fusalanipyrone. *Phytochemistry.* **29,** 2877-2878

44. Nair, M.S.R., and Carey, S.T. (1975) Metabolites of phyrenomycetes II: Nectriapyrone, an antibiotic monoterpenoid. *Tetrahedron Lett.* **16,** 1655-1658

45. Venkatasubbaiah, P., and van Dyke, C.G. (1991) Phytotoxins produced by *Pestalotiopsis oenotherae*, a pathogen of evening primrose. *Phytochemistry.* **30,** 1471-1474

46. Lee, J.C., Yang, X., Schwartz, M., Strobel, G., and Clardy, J. (1995) The relationship between an endangered North American tree and an endophytic fungus. *Chem.Biol.* **2,** 721-727

47. Türkkan, M., Andolfi, A., Zonno, M.C., Erper, I., Perrone, C., Cimmino, A., Vurro, M., and Evidente, A. (2011) Phytotoxins produced by *Pestalotiopsis guepinii*, the causal agent of hazelnut twig blight. *Phytopathol.Mediterr.* **50,** 154-158

48. Avent, A.G., Hanson, J.R., and Truneh, A. (1992) The biosynthesis of nectriapyrone and vermopyrone. *Phytochemistry.* **31,** 3447-3449

49. Wiemann, P., Albermann, S., Niehaus, E., Studt, L., von Bargen, K.W., Brock, N.L., Humpf, H., Dickschat, J.S., and Tudzynski, B. (2012) The Sfp-type 4′-phosphopantetheinyl transferase Ppt1 of *Fusarium fujikuroi* controls development, secondary metabolism and pathogenicity. *PLoS ONE.* **7,** e37519

50. Keller, N.P., Turner, G., and Bennett, J.W. (2005) Fungal secondary metabolism - From biochemistry to genomics. *Nat.Rev.Microbiol.* **3,** 937-947

51. Yu, F., Zhu, X., and Du, L. (2005) Developing a genetic system for functional manipulations of *FUM1*, a polyketide synthase gene for the biosynthesis of fumonisins in *Fusarium verticillioides*. *FEMS Microbiol.Lett.* **248,** 257-264

52. Skellam, E.J., Hurley, D., Davison, J., Lazarus, C.M., Simpson, T.J., and Cox, R.J. (2010) Mutation of key residues in the *C*-methyltransferase domain of a fungal highly reducing polyketide synthase. *Mol.Biosyst.* **6,** 680-682

53. Malonek, S., Rojas, M.C., Hedden, P., Gaskin, P., Hopkins, P., and Tudzynski, B. (2004) The NADPH-cytochrome P450 reductase gene from *Gibberella fujikuroi* is essential for gibberellin biosynthesis. *J.Biol.Chem.* **279,** 25075-25084

54. Umbreit, M.A., and Sharpless, K.B. (1977) Allylic oxidation of olefins by catalytic and stoichiometric selenium dioxide with *tert*-butyl hydroperoxide. *J.Am.Chem.Soc.* **99,** 5526-5528

55. Coleman, J.J., Rounsley, S.D., Rodriguez-Carres, M., Kuo, A., Wasmann, C.C., Grimwood, J., Schmutz, J., Taga, M., White, G.J., Zhou, S., Schwartz, D.C., Freitag, M., Ma, L., Danchin, E.G.J., Henrissat, B., Coutinho, P.M., Nelson, D.R., Straney, D., Napoli, C.A., Barker, B.M., Gribskov, M., Rep, M., Kroken, S., Molnár, I., Rensing, C., Kennell, J.C., Zamora, J., Farman, M.L., Selker, E.U., Salamov, A., Shapiro, H., Pangilinan, J., Lindquist, E., Lamers, C., Grigoriev, I.V., Geiser, D.M., Covert, S.F., Temporini, E., and van Etten, H.D. (2009) The genome of *Nectria haematococca*: Contribution of supernumerary chromosomes to gene expansion. *PLoS Genet.* **5,** e1000618

56. Wiemann, P., Brown, D.W., Kleigrewe, K., Bok, J.W., Keller, N.P., Humpf, H., and Tudzynski, B. (2010) FfVel1 and Fflae1, components of a *velvet*-like complex in *Fusarium fujikuroi*, affect differentiation, secondary metabolism and virulence. *Mol.Microbiol.* **77,** 972-994

57. Michielse, C.B., Studt, L., Janevska, S., Sieber, C.M.K., Arndt, B., Espino, J.J., Humpf, H., Güldener, U., and Tudzynski, B. (2015) The global regulator FfSge1 is required for expression of secondary metabolite gene clusters but not for pathogenicity in *Fusarium fujikuroi. Environ.Microbiol.* **17,** 2690-2708

58. Ma, S.M., Li, J.W., Choi, J.W., Zhou, H., Lee, K.K.M., Moorthie, V.A., Xie, X., Kealey, J.T., Da Silva, N.A., Vederas, J.C., and Tang, Y. (2009) Complete reconstitution of a highly reducing iterative polyketide synthase. *Science.* **326,** 589-592

59. Arndt, B., Studt, L., Wiemann, P., Osmanov, H., Kleigrewe, K., Köhler, J., Krug, I., Tudzynski, B., and Humpf, H. (2015) Genetic engineering, high resolution mass spectrometry and nuclear magnetic resonance spectroscopy elucidate the bikaverin biosynthetic pathway in *Fusarium fujikuroi*. *Fungal Genet.Biol.* **84,** 26-36

60. Cacho, R.A., Thuss, J., Xu, W., Sanichar, R., Gao, Z., Nguyen, A., Vederas, J.C., and Tang, Y. (2015) Understanding programming of fungal iterative polyketide synthases: The biochemical basis for regioselectivity by the methyltransferase domain in the lovastatin megasynthase. *J.Am.Chem.Soc.* **137,** 15688-15691

61. Cooney, J.M., Lauren, D.R., Poole, P.R., and Whitaker, G. (1997) Microbial transformation of the *Trichoderma* metabolite 6-*n*-pentyl-2*H*- pyran-2-one. *J.Nat.Prod.* **60,** 1242-1244

62. Wang, D., Toyotome, T., Muraosa, Y., Watanabe, A., Wuren, T., Bunsupa, S., Aoyagi, K., Yamazaki, M., Takino, M., and Kamei, K. (2014) GliA in *Aspergillus fumigatus* is required for its tolerance to gliotoxin and affects the amount of extracellular and intracellular gliotoxin. *Med.Mycol.* **52,** 504-516

63. Menke, J., Dong, Y.N., and Kistler, H.C. (2012) *Fusarium graminearum* Tri12p influences virulence to wheat and trichothecene accumulation. *Mol.Plant-Microbe Interact.* **25,** 1408-1418

64. Crutcher, F.K., Liu, J., Puckhaber, L.S., Stipanovic, R.D., Bell, A.A., and Nichols, R.L. (2015) FUBT, a putative MFS transporter, promotes secretion of fusaric acid in the cotton pathogen *Fusarium oxysporum* f. sp. *vasinfectum. Microbiology.* **161,** 875-883

65. Proctor, R.H., Brown, D.W., Plattner, R.D., and Desjardins, A.E. (2003) Co-expression of 15 contiguous genes delineates a fumonisin biosynthetic gene cluster in *Gibberella moniliformis. Fungal Genet.Biol.* **38,** 237-249

66. Gardiner, D.M., Jarvis, R.S., and Howlett, B.J. (2005) The ABC transporter gene in the sirodesmin biosynthetic gene cluster of *Leptosphaeria maculans* is not essential for sirodesmin production but facilitates self-protection. *Fungal Genet.Biol.* **42,** 257-263

67. Donaton, M.C.V., Holsbeeks, I., Lagatie, O., van Zeebroeck, G., Crauwels, M., Winderickx, J., and Thevelein, J.M. (2003) The Gap1 general amino acid permease acts as an amino acid sensor for activation of protein kinase A targets in the yeast *Saccharomyces cerevisiae. Mol.Microbiol.* **50,** 911-929

68. Ahmed, Y.L., Gerke, J., Park, H., Bayram, Ö., Neumann, P., Ni, M., Dickmanns, A., Kim, S.C., Yu, J., Braus, G.H., and Ficner, R. (2013) The velvet family of fungal regulators contains a DNA-binding domain structurally similar to NF-κB. *PloS Biol.* **11,** e1001750

69. Bok, J.W., Noordermeer, D., Kale, S.P., and Keller, N.P. (2006) Secondary metabolic gene cluster silencing in *Aspergillus nidulans. Mol.Microbiol.* **61,** 1636-1645

70. Bayram, Ö., and Braus, G.H. (2012) Coordination of secondary metabolism and development in fungi: The velvet family of regulatory proteins. *FEMS Microbiol.Rev.* **36,** 1-24

71. Nguyen, V.Q., and Sil, A. (2008) Temperature-induced switch to the pathogenic yeast form of *Histoplasma capsulatum* requires Ryp1, a conserved transcriptional regulator. *Proc.Natl.Acad.Sci.U.S.A.* **105,** 4880-4885

72. Lohse, M.B., Zordan, R.E., Cain, C.W., and Johnson, A.D. (2010) Distinct class of DNA-binding domains is exemplified by a master regulator of phenotypic switching in *Candida albicans*. *Proc.Natl.Acad.Sci.U.S.A.* **107,** 14105-14110

73. Darken, M.A., Jensen, A.L., and Ahu, P. (1959) Production of gibberellic acid by fermentation. *Appl.Microbiol.* **7,** 301-303

74. Geissman, T.A., Verbiscar, A.J., Phinney, B.O., and Cragg, G. (1966) Studies on the biosynthesis of gibberellins from (-)-kaurenoic acid in cultures of *Gibberella fujikuroi*. *Phytochemistry.* **5,** 933-947

75. Pontecorvo, G., Roper, J.A., Chemmons, L.M., Macdonald, K.D., and Bufton, A.W.J. (1953) The Genetics of *Aspergillus nidulans. Adv.Genet.* **5,** 141-238

76. Colot, H.V., Park, G., Turner, G.E., Ringelberg, C., Crew, C.M., Litvinkova, L., Weiss, R.L., Borkovich, K.A., and Dunlap, J.C. (2006) A high-throughput gene knockout procedure for *Neurospora* reveals functions for multiple transcription factors. *Proc.Natl.Acad.Sci.U.S.A.* **103,** 10352-10357

77. Schumacher, J. (2012) Tools for *Botrytis cinerea*: New expression vectors make the gray mold fungus more accessible to cell biology approaches. *Fungal Genet.Biol.* **49,** 483-497

78. Staben, C., Jensen, B., Singer, M., Pollock, J., Schechtmann, M., Kinsey, J., and Selker, E. (1989) Use of a bacterial hygromycin B resistance gene as a dominant selectable marker in *Neurospora crassa* transformation. *Fungal Genet Newslett.* **36,** 79-81

79. Winston, F., Dollard, C., and Ricupero-Hovasse, S.L. (1995) Construction of a set of convenient *Saccharomyces cerevisiae* strains that are isogenic to S288C. *Yeast.* **11,** 53-55

80. Christianson, T.W., Sikorski, R.S., Dante, M., Shero, J.H., and Hieter, P. (1992) Multifunctional yeast high-copy-number shuttle vectors. *Gene.* **110,** 119-122

81. Tudzynski, B., Homann, V., Feng, B., and Marzluf, G.A. (1999) Isolation, characterization and disruption of the *areA* nitrogen regulatory gene of *Gibberella fujikuroi*. *Mol.Gen.Genet.* **261,** 106-114

82. Cenis, J.L. (1992) Rapid extraction of fungal DNA for PCR amplification. *Nucleic Acids Res.* **20,** 2380

83. Southern, E.M. (1975) Detection of specific sequences among DNA fragments separated by gel electrophoresis. *J.Mol.Biol.* **98,** 503-517

84. Ausubel, F.M., Brent, R., Kingston, R.E., Moore, D.D., Seidman, J.G., Smith, J.A., and Struhl, K. (1987) Current protocols in molecular biology. Wiley, New York

85. Sambrook, J., Fritsch, E.F., and Maniatis, T. (1989) Molecular cloning: A laboratory manual, 2nd Ed. Cold Spring Harbor, New York

86. Church, G.M., and Gilbert, W. (1984) Genomic sequencing. *Proc.Natl.Acad.Sci.U.S.A.* **81,** 1991-1995

87. Pfaffl, M.W. (2001) A new mathematical model for relative quantification in real-time RT-PCR. *Nucleic Acids Res.* **29,** e45

88. Dickschat, J.S., Citron, C.A., Brock, N.L., Riclea, R., and Kuhz, H. (2011) Synthesis of deuterated mevalonolactone isotopomers. *Eur.J.Org.Chem.* 3339-3346

Footnotes

The abbreviations used are: SM, secondary metabolite; PKS, polyketide synthase; NRPS, nonribosomal peptide synthetase; HRMS, high resolution mass spectrometry; SAM, *S*-adenosyl-L-methionine; Ppant, phosphopantetheinyl; WT, wild-type; TF, transcription factor; ABC, ATP-binding cassette; SQTKS, squalestatin tetraketide synthase; qRT-PCR, quantitative real-time PCR; MFS, major facilitator superfamily; ICI, Imperial Chemical Industries; CM, complete medium; MePa, methylparaben; FA, formic acid; ESI, electrospray ionization; DP, declustering potential; EP, entrance potential; CXP, cell exit potential; CE, collision energy; HCD, higher-energy collisional dissociation; HREIMS, high resolution electron ionization mass spectrometry; CLSA, closed-loop stripping apparatus

Tables

Table 1. Gene names, gene/protein lengths (in base pairs, bp/amino acids, aa) and predicted functions of gibepyrone cluster genes *GPY1* and *GPY2* as well as of adjacent genes.

Gene name (accession number)	Length [bp]	Length [aa]	Domains and motifs	Predicted function
FFUJ_12019	1,798	438	IPR029063 *S*-adenosyl-L-methionine-dependent methyltransferase	Methyltransferase; does probably not belong to the cluster
GPY1 (*FFUJ_12020*)	8,438	2,543	IPR020841 PKS, β-ketoacyl synthase domain IPR020801 PKS, acyl transferase domain IPR020807 PKS, dehydratase domain IPR029063 *S*-adenosyl-L-methionine-dependent methyltransferase IPR020843 PKS, enoylreductase domain IPR013968 PKS, ketoreductase domain IPR020806 PKS, phosphopantetheine-binding domain	PKS (polyketide synthase)
GPY2 (*FFUJ_12021*)	5,007	1,432	IPR011527 ABC transporter type 1, transmembrane domain IPR003593 AAA+ ATPase domain	ABC (ATP-binding cassette) transporter
FFUJ_12022	1,132	244	/	Unknown function; does probably not belong to the cluster
FFUJ_12023	2,362	725	IPR001138 Zn(2)-C6 fungal-type DNA-binding domain	$Zn(II)_2Cys_6$-type transcription factor; does probably not belong to the cluster

Figures and figure legends

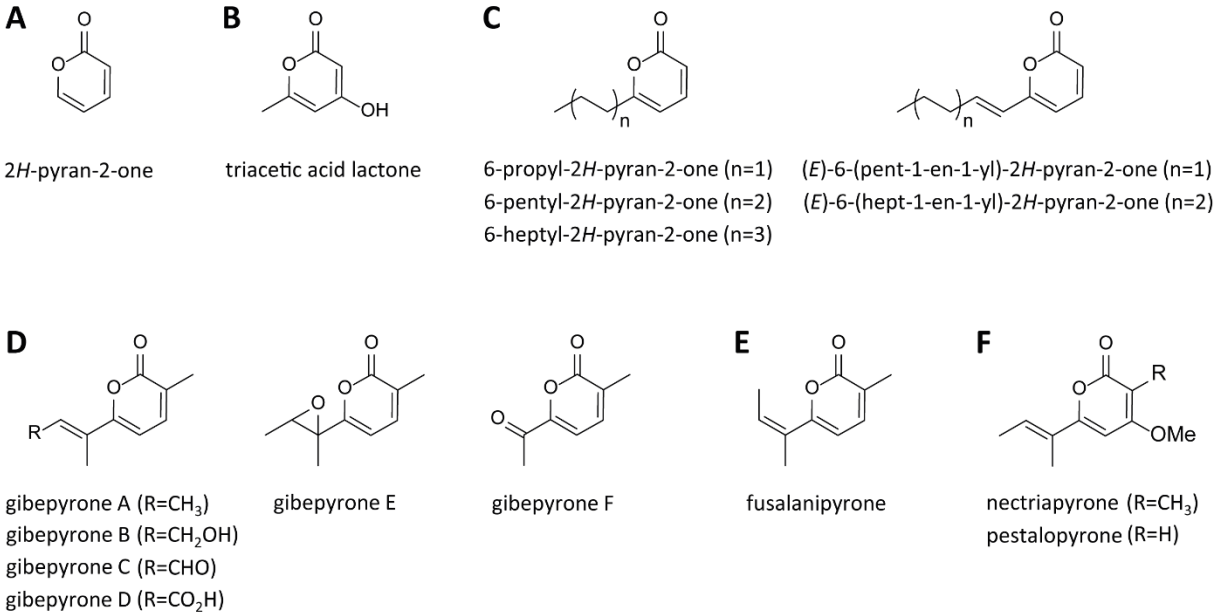

Figure 1. Chemical structures of 2*H*-pyran-2-ones. Structures of the parent compound 2*H*-pyran-2-one (*A*), the fungal metabolites triacetic acid lactone (*B*), 6-pentyl-2*H*-pyran-2-one, its shorter and longer homologs and derivatives with unsaturated side chain (*C*), gibepyrones A-F (*D*), fusalanipyrone (*E*), nectriapyrone and pestalopyrone (*F*).

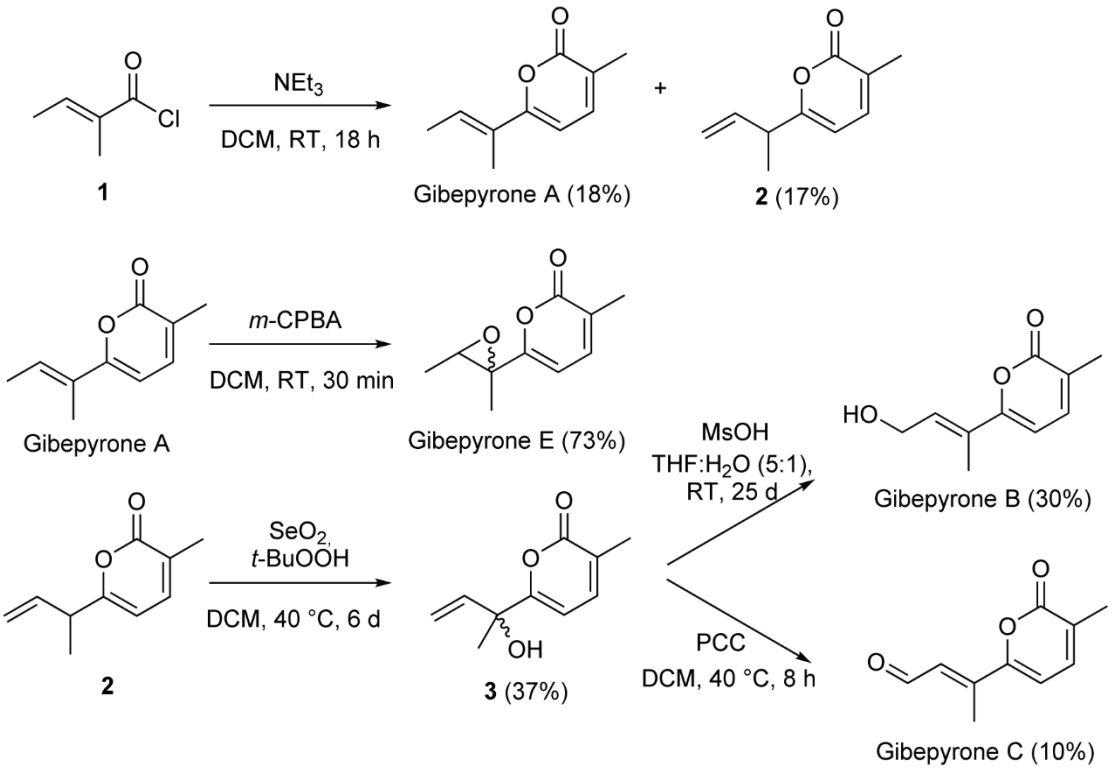

Figure 2. Synthesis of gibepyrones A, B, C and E. Abbreviations: NEt_3, triethyl amine; DCM, dichloromethane; *m*-CPBA, *meta*-chlorperbenzoic acid; MsOH, methanesulfonic acid; THF, tetrahydrofurane; PCC, pyridinium chlorochromate; SeO_2, selenium dioxide; *t*-BuOOH, *tert*-butyl hydroperoxide; RT, room temperature.

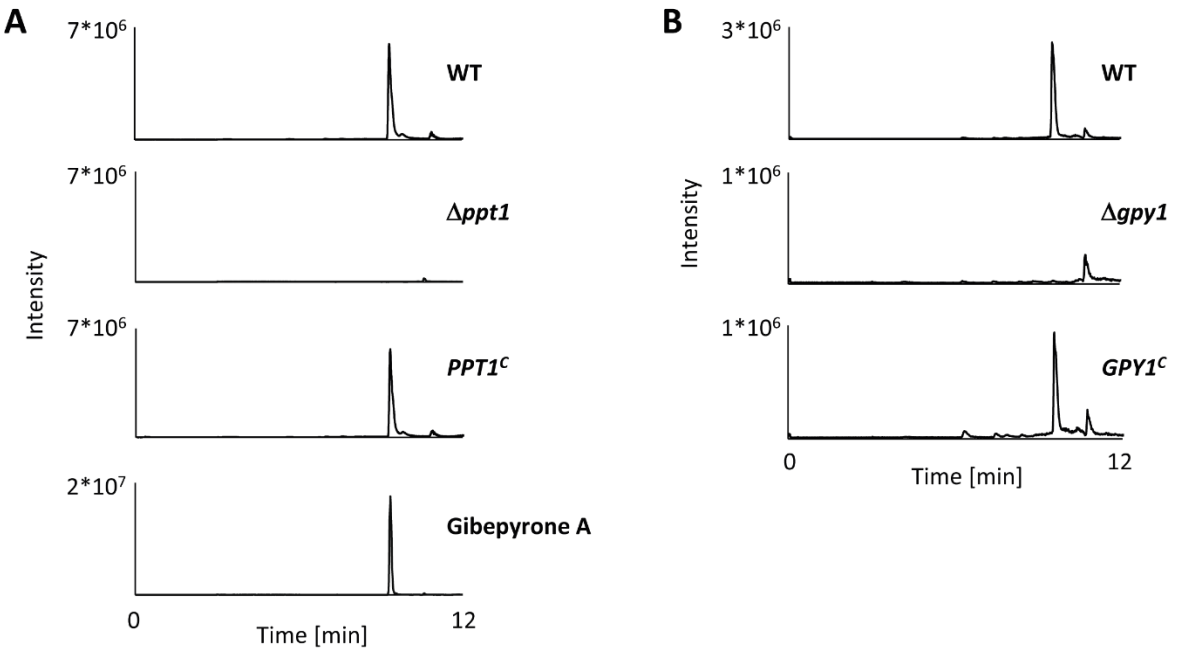

Figure 3. Gibepyrone A production depends on the presence of Ppt1 (*A*) and the SM biosynthetic key enzyme PKS13, designated Gpy1 (*B*). *A*, HPLC-MS/MS analysis of culture fluids of the wild type (WT), Δ*ppt1*and *PPT1*^{C}. The strains were grown in the presence of 6 mM glutamine for seven days. The gibepyrone A peak was verified through comparison with the synthesized chemical standard. *B*, The WT, the Δ*gpy1* deletion mutant as well as the complemented strain *GPY1*^{C} were grown and analyzed as described above.

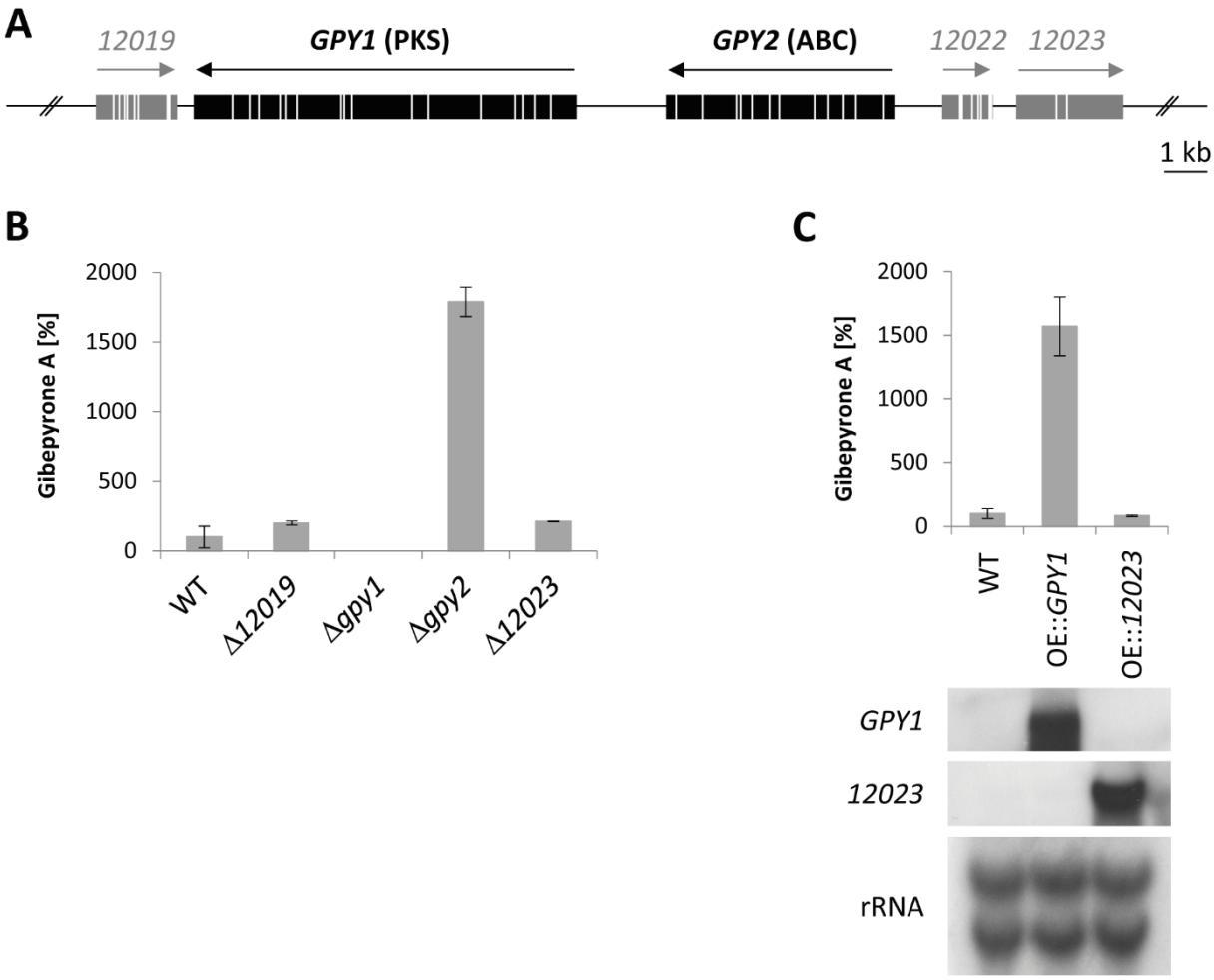

Figure 4. The gibepyrone biosynthetic gene cluster comprises a PKS- and an ABC transporter-encoding gene, *GPY1* and *GPY2*, respectively. *A*, Schematic representation of *GPY1* (*FFUJ_12020*), *GPY2* (*FFUJ_12021*) as well as neighboring, non-cluster genes (gray). Arrows indicate the direction of transcription and white bars the introns. *B*, HPLC-MS/MS analysis of culture fluids of the wild type (WT) and indicated deletion mutants. The strains were grown in triplicates in the presence of 6 mM glutamine for seven days with product formation of the WT being set to 100%. *C*, HPLC-MS/MS and Northern blot expressional analysis of the WT and the overexpression mutants of *GPY1* and *FFUJ_12023* (TF). The strains were grown and analyzed as described above for gibepyrone A quantification while cell harvest was carried out after three days for expressional analysis. In the latter case, *GPY1* and *FFUJ_12023* were used as probes.

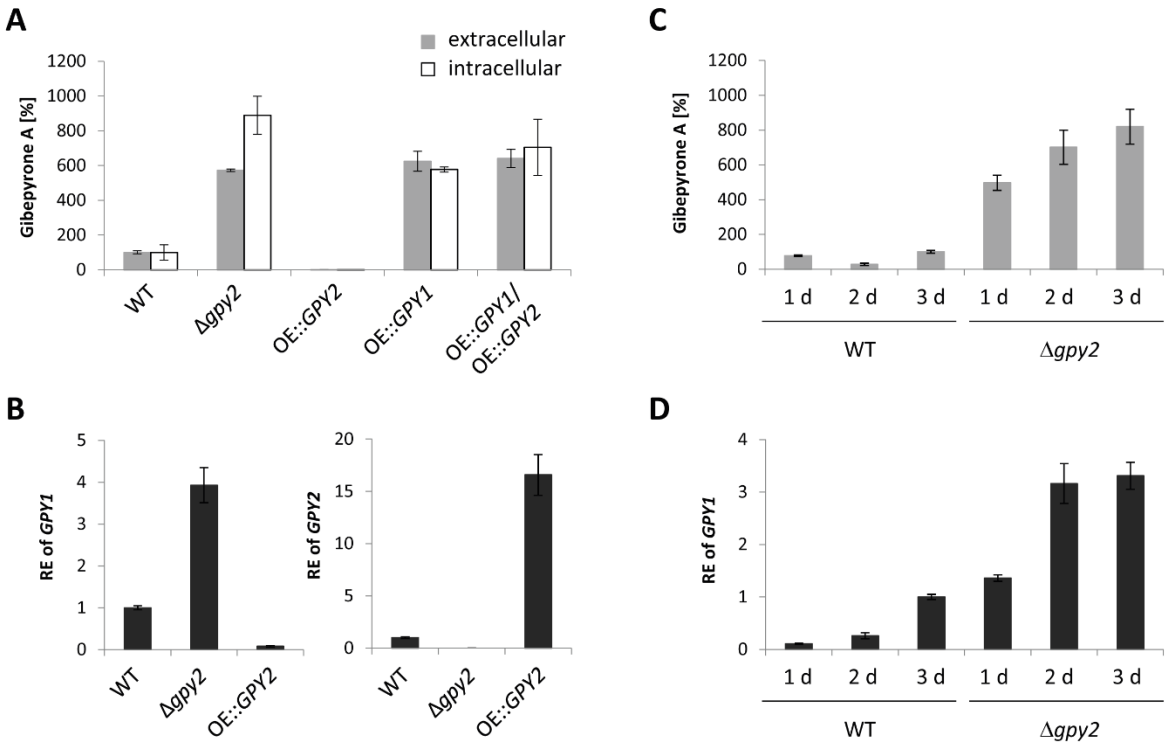

Figure 5. The ABC transporter Gpy2 represses expression of the PKS-encoding gene *GPY1*. *A*, HPLC-MS/MS analysis of extra- and intracellular gibepyrone A. The wild type (WT) and indicated deletion and overexpression mutants were grown in the presence of 6 mM glutamine for seven days. Culture fluids were directly measured for extracellular gibepyrone A contents, while metabolite extraction from washed mycelium was applied prior to quantifying intracellular levels. The cultivation was carried out in triplicates and product formation of the WT was set to 100%. *B*, qRT-PCR analysis of the relative expression (RE) of *GPY1* and *GPY2* using the ΔΔCt method. The WT, Δ*gpy2* and OE::*GPY2* mutants were cultivated for three days whereupon total RNA was isolated from the harvested mycelium. Error bars (±SD) originate from a technical replicate and expression of the WT was arbitrarily set to 1. *C*, HPLC-MS/MS analysis of extracellular gibepyrone A. The WT and Δ*gpy2* were grown in the presence of 6 mM glutamine for 1-3 days (d). The cultivation was carried out in triplicates and product formation of the WT at 3 d was set to 100%. *D*, qRT-PCR analysis of the RE of *GPY1* using the ΔΔCt method. The WT and Δ*gpy2* were cultivated for 1-3 d whereupon total RNA was isolated from the harvested mycelium. Error bars (±SD) originate from a technical replicate and expression of the WT at 3 d was arbitrarily set to 1.

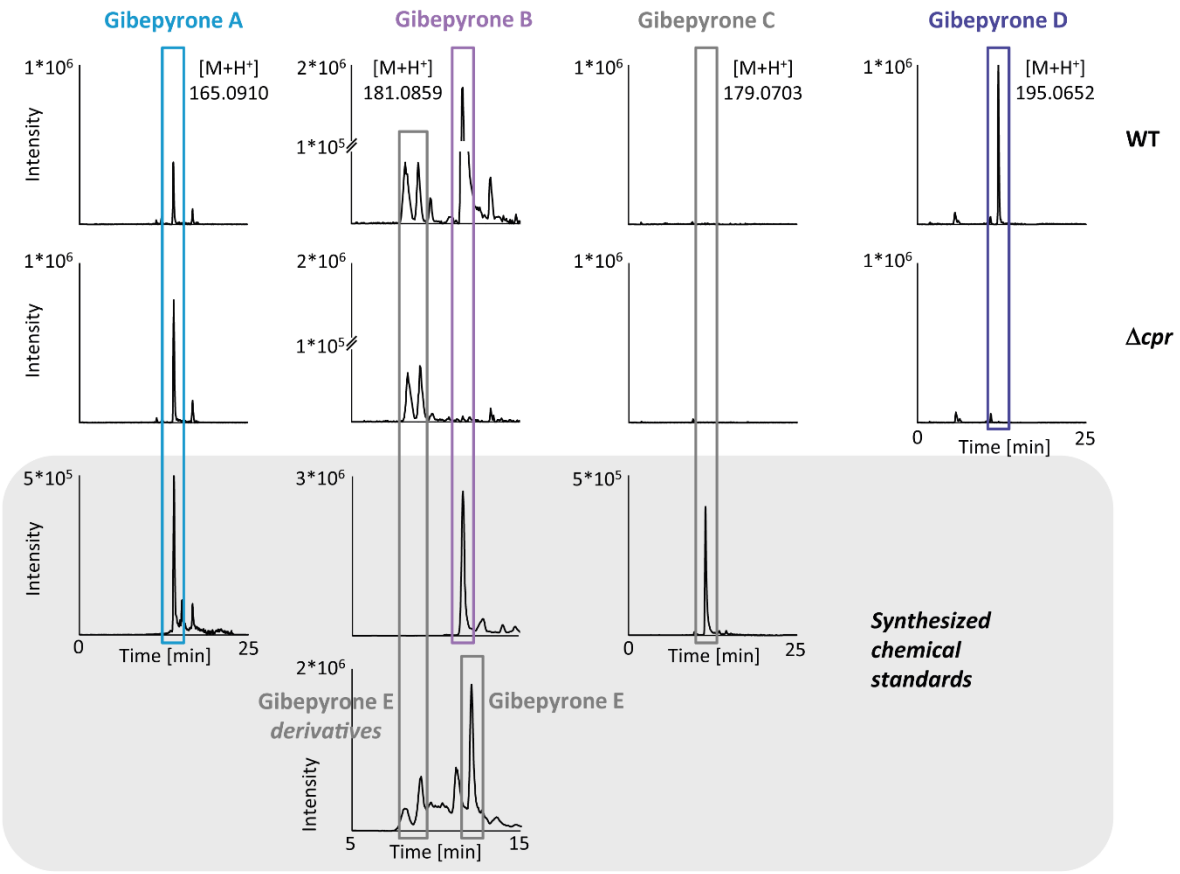

Figure 6. Production of gibepyrone A derivatives, gibepyrones B-E. HPLC-HRMS analysis of culture fluids of the wild type (WT) and the Δ*cpr* mutant. The strains were grown in the presence of 6 mM glutamine for seven days and the supernatant was analyzed without further processing. Shown are extracted ion chromatograms for the calculated masses of gibepyrones A-E for the two strains as well as for the synthesized chemical standards. The gibepyrone E peak cannot be found in the cultures. However, in the presence of water, both the cultures and the standard show an identical double peak, designated gibepyrone E derivatives.

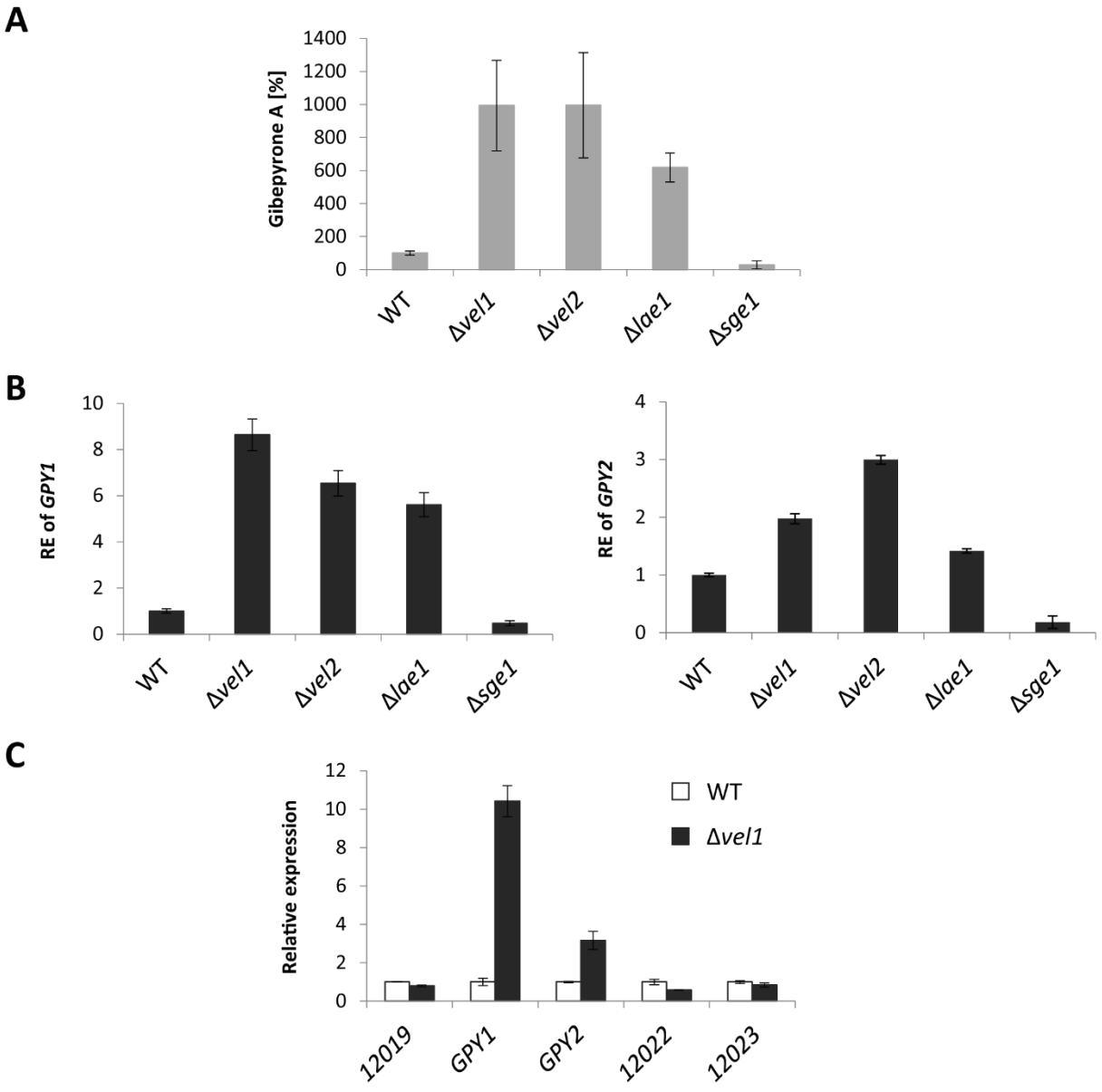

Figure 7. Regulation of gibepyrone A biosynthesis. *A*, HPLC-MS/MS analysis of culture fluids of the wild type (WT) and indicated deletion mutants. The strains were grown in triplicates in the presence of 6 mM glutamine for seven days with product formation of the WT being set to 100%. *B*, qRT-PCR analysis of the relative expression (RE) of *GPY1* and *GPY2* using the ΔΔCt method. The strains were cultivated for three days whereupon total RNA was isolated from the harvested mycelium. Error bars (±SD) originate from a technical replicate and expression of the WT was arbitrarily set to 1. *C*, qRT-PCR analysis of the relative expression of indicated genes using the ΔΔCt method. The WT and Δ*vel1* mutant were cultivated for three days whereupon total RNA was isolated from the harvested mycelium. Error bars (±SD) originate from a technical replicate and expression of each gene in the WT was arbitrarily set to 1.

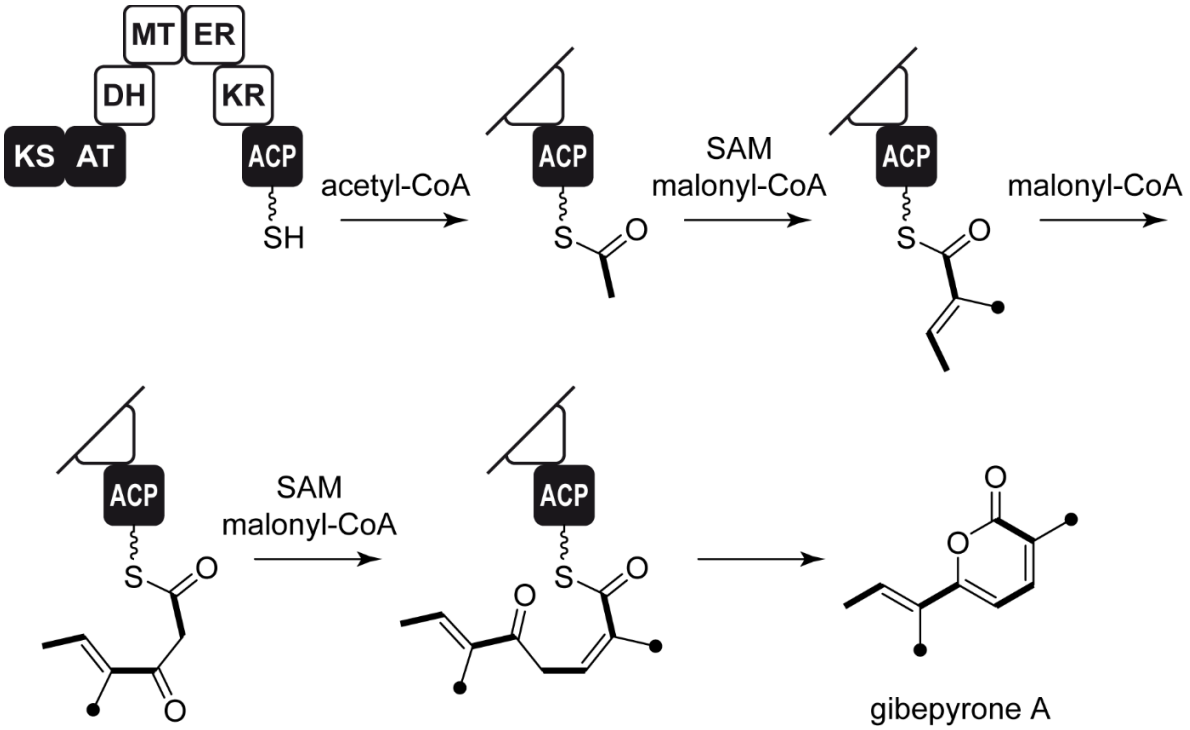

Figure 8. Proposed pathway for gibepyrone A biosynthesis by the PKS Gpy1. As first step, the acetyl-CoA starter unit is bound to the acyl carrier (ACP) domain of Gpy1 as thioester. It is condensed with three malonyl-CoA extender units under the release of carbon dioxide through the activities of the β-ketoacyl synthase (KS) and acyl transferase (AT) domains. Experimental evidence was gained that the methyltransferase (MT) domain of Gpy1 is responsible for the *C*-methylation of the polyketide backbone during two of the elongation steps using *S*-adenosyl-L-methionine (SAM) as precursor. Finally, gibepyrone A is released upon intramolecular cyclization. Bold lines indicate C_2 units from acetate/malonate, while black circles represent methyl groups originating from SAM.

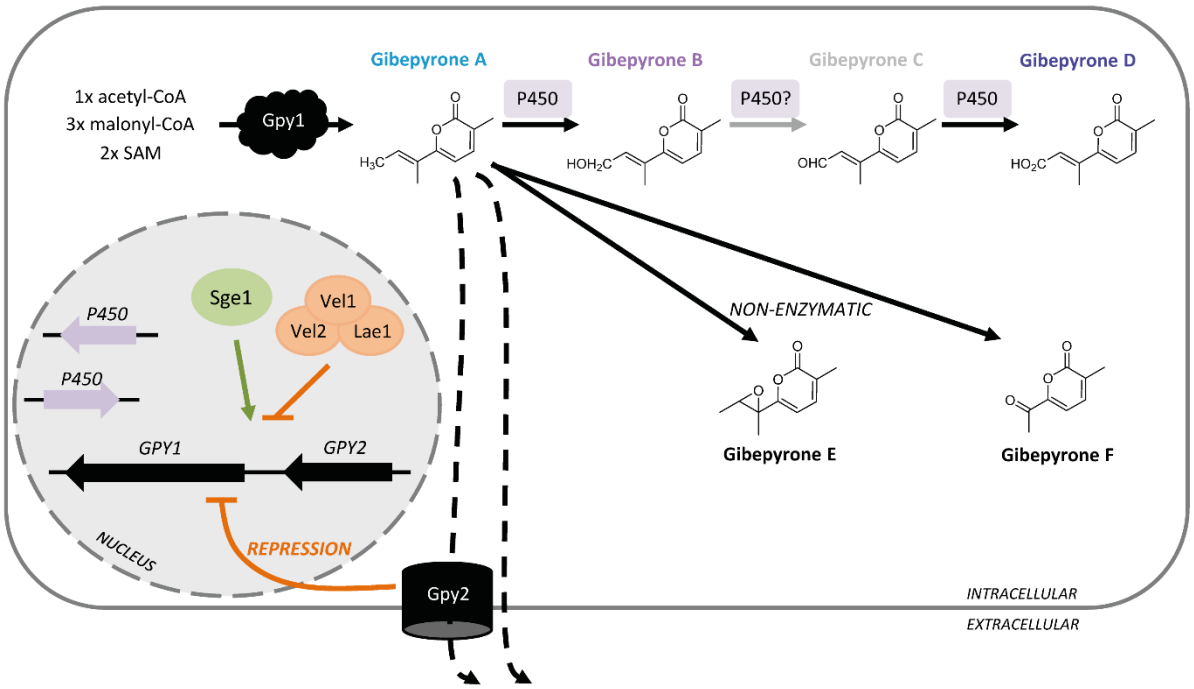

Figure 9. Biosynthesis and regulation of gibepyrone A and its derivatives in *F. fujikuroi*. The PKS Gpy1 facilitates the condensation of the C_{10} compound gibepyrone A. Next to the PKS, an ABC transporter-encoding gene, *GPY2*, belongs to the cluster. However, Gpy2 seems to have a minor impact on the efflux of gibepyrone A out of the cell, but was shown to repress expression of the key gene *GPY1*. Furthermore, members of the *velvet* complex, Vel1, Vel2 and Lae1, negatively affect cluster gene expression and gibepyrone A product formation, while Sge1 represents a positive regulator of gibepyrone biosynthesis. The oxidized compounds gibepyrones B and D are derived from gibepyrone A through the activity of cluster-independent, CPR-dependent P450 monooxygenases, while gibepyrones E and F are formed in the absence of enzymatic activity.

Gibepyrone biosynthesis in the rice pathogen *Fusarium fujikuroi* is facilitated by a small polyketide synthase gene cluster

Slavica Janevska[1], Birgit Arndt[2], Eva-Maria Niehaus[1], Immo Burkhardt[3], Sarah M. Rösler[1,2], Nelson L. Brock[3], Hans-Ulrich Humpf[2], Jeroen S. Dickschat[3*], Bettina Tudzynski[1*]

[1] Institut für Biologie und Biotechnologie der Pflanzen, Westfälische Wilhelms-Universität Münster, Schlossplatz 8, D-48143 Münster
[2] Institut für Lebensmittelchemie, Westfälische Wilhelms-Universität Münster, Corrensstraße 45, D-48149 Münster
[3] Kekulé-Institut für Organische Chemie und Biochemie, Rheinische Friedrich Wilhelms-Universität Bonn, Gerhard-Domagk-Straße 1, D-53121 Bonn

Running title: Gibepyrone biosynthesis in *F. fujikuroi*

To whom correspondence should be addressed:
*Prof. Dr. J. S. Dickschat, fon: +49 228 73 5797, e-mail: dickschat@uni-bonn.de
*Prof. Dr. B. Tudzynski, fon: +49 251 83 24801, fax: +49 251 83 21601, e-mail: tudzynsb@uni-muenster.de

Keywords: Fungi, Secondary metabolism, Polyketide, Biosynthesis, Gene regulation**,** *Fusarium fujikuroi*, Gibepyrones

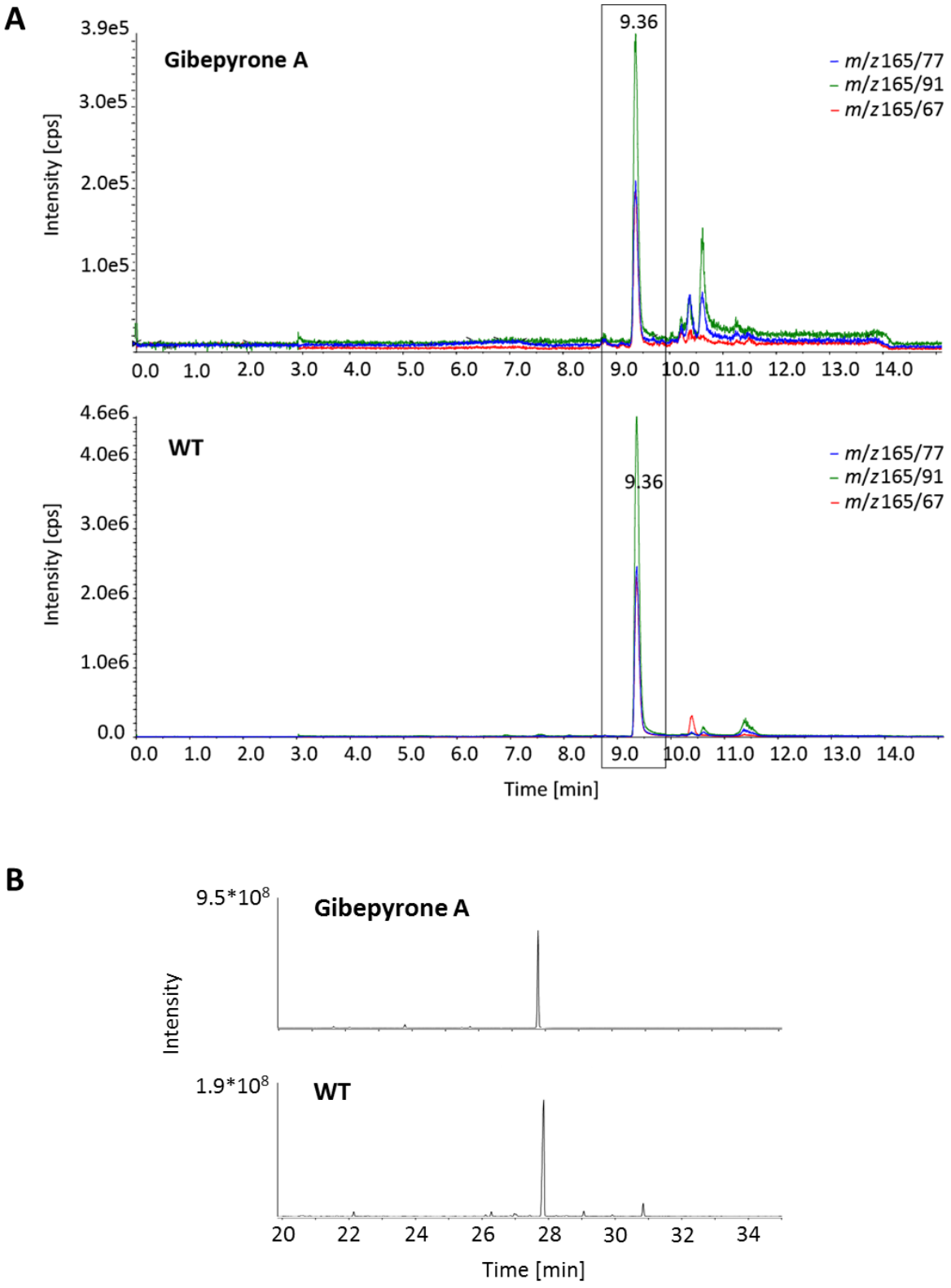

Figure S1. Comparison of gibepyrone A produced by the wild type (WT) with the synthesized chemical standard. *A*, Fingerprint of the fragmentation pattern of gibepyrone A upon analysis *via* HPLC-MS/MS. Chromatograms depict different transitions of gibepyrone A, including the quantifier Multiple Reaction Monitoring transition *m*/*z* 165/91 and the two qualifier transitions *m*/*z* 165/77 and *m*/*z* 165/67. cps, counts per second. *B*, Comparison of WT culture extracts and synthetic gibepyrone A *via* GC-MS. In both cases, the culture fluid of the WT was analyzed upon growth in the presence of 6 mM glutamine for seven days.

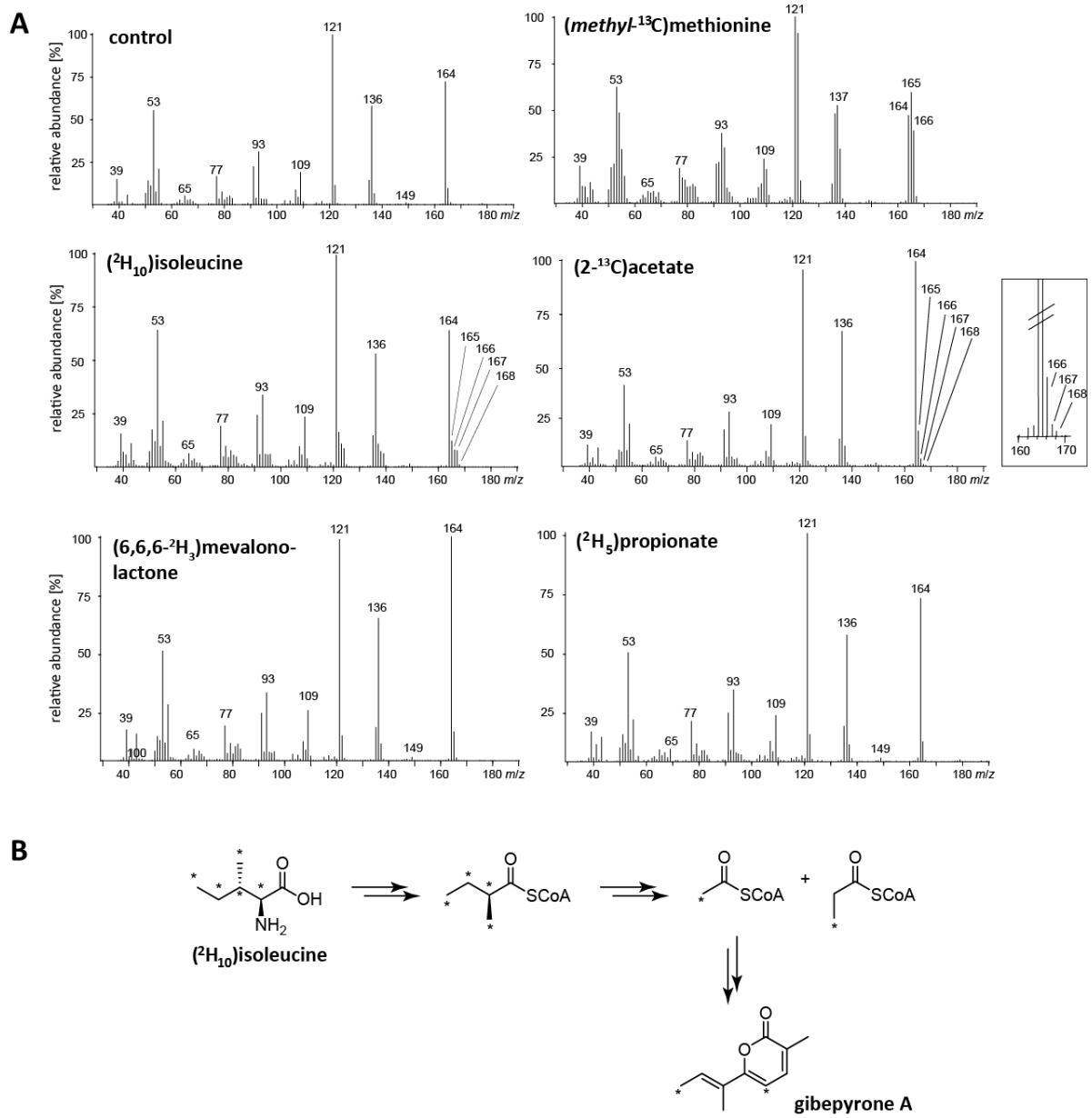

Figure S2. Feeding experiments with labeled precursors for elucidating gibepyrone A biosynthesis. *A*, EI mass spectra of naturally occurring gibepyrone A (control), [$^{13}C_2$]gibepyrone A after feeding of (*methyl*-^{13}C)methionine (incorporation rate: 50%), and [$^{2}H_4$]gibepyrone A after feeding of ($^{2}H_{10}$)isoleucine (the fragment ion at *m*/*z* 168 is 20% higher as expected for the ^{13}C isotope peak of *m*/*z* 167, pointing to incorporation of up to four deuterium atoms) and [$^{13}C_4$]gibepyrone A after feeding of (2-^{13}C)acetate (the fragment ion at *m*/*z* 168 is 10% higher as expected for the ^{13}C isotope peak of *m*/*z* 167 showing incorporation of up to four ^{13}C atoms). Mass spectra of gibepyrone A after feeding of (6,6,6-$^{2}H_3$)mevalonolactone and ($^{2}H_5$)propionate do not show incorporation of deuterium atoms. *B*, Deuterium label of ($^{2}H_{10}$)isoleucine can be recovered in gibepyrone A due to its degradation to acetyl- and propionyl-CoA. The asterisks designate fully deuterated carbon atoms. For both experiments, the Δ*vel1* mutant, which produces larger amounts of gibepyrone A compared to the wild type, was cultivated on supplemented CM solid medium and subsequently subjected to CLSA/GC-MS analysis.

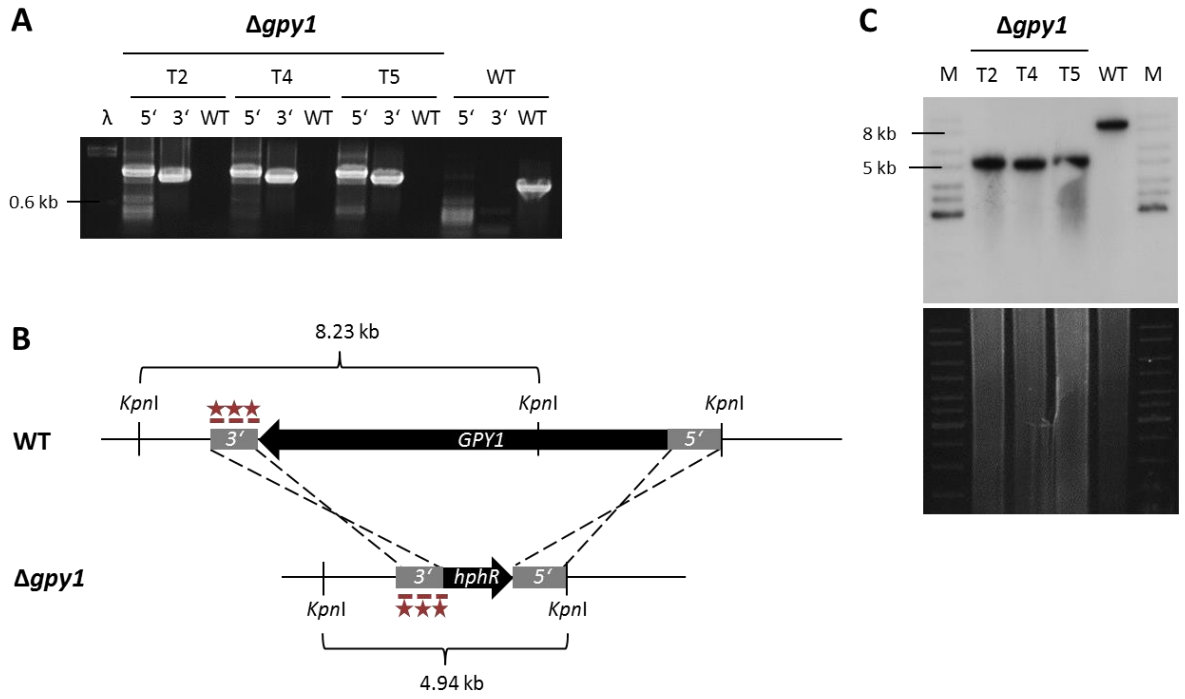

Figure S3. Verification of Δ*gpy1* (*FFUJ_12020*) deletion mutants by diagnostic PCR and Southern blot. Deletion *via* homologous recombination (*A*) with the hygromycin B resistance cassette (*hphR*) was underlined with the amplification of 5' (12020_5diag/trpC_T; 1.35 kb) and 3' (12020_3diag/trpC_P2; 1.19 kb) sequences but no amplification of wild-type signal (WT; 12020_WT_F/12020_WT_R; 0.99 kb) for independent transformants (T). For analyzing ectopic integration of deletion constructs, genomic DNA of transformants and WT was digested with *Kpn*I (*B*) whereupon the 3' sequence was applied for probing. Detected signals match the expected 4.94 kb for Δ*gpy1* as well as 8.23 kb for the WT (*C*). λ: λ/*Hin*dIII, M: GeneRuler DNA Ladder Mix.

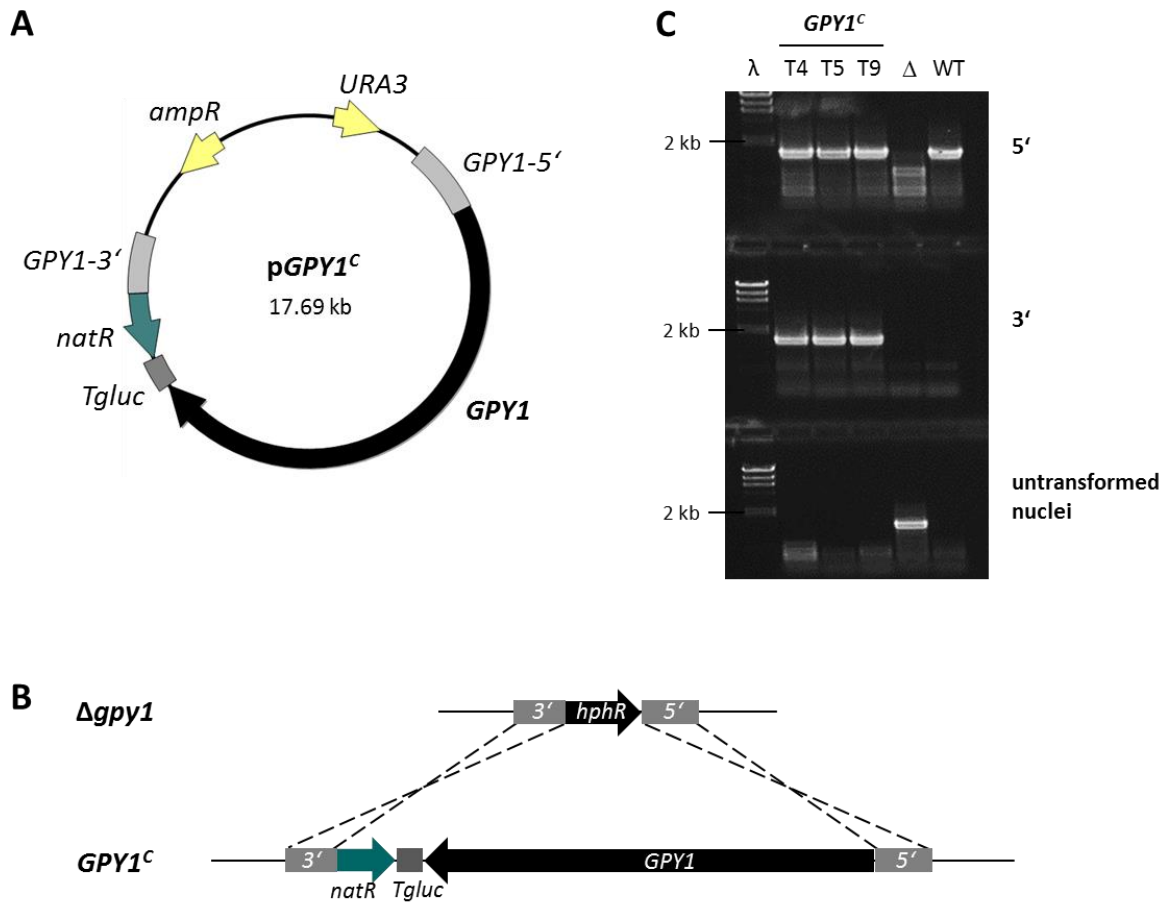

Figure S4. *In loco* complementation of *GPY1* encoding the key enzyme, the PKS. The deletion mutant Δ*gpy1* T5 was transformed with *Apa*I digested p*GPY1*^{C} harboring the full-length gene *GPY1* driven by its native promoter as well as the nourseothricin resistance cassette *natR* (*A*). The homologous integration of the construct (*B*) in the complemented transformants (T) was checked using primer pairs 12020_5diag/12020_c_diag (5‘), 12020_3diag/nat1_R1 (3‘) and 12020_5diag/trpC_T (untransformed nuclei) giving fragments of 1.47 kb, 1.57 kb and 1.34 kb, respectively (*C*). λ: λ/*Hin*dIII, Δ: Δ*gpy1* T5, WT: wild type *F. fujikuroi* IMI58289.

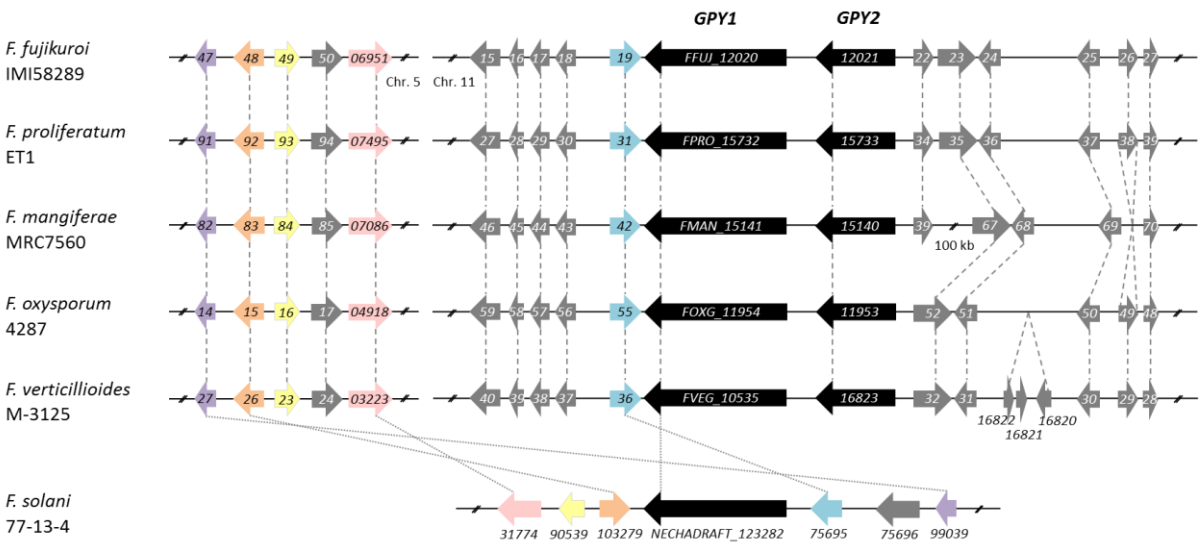

Figure S5. Schematic representation of homologous genomic regions of *F. fujikuroi*, closely related fungi of the *F. fujikuroi* species complex (*F. proliferatum*, *F. mangiferae*, *F. verticillioides*), *F. oxysporum* and *F. solani* (*Nectria haematococca*). The two gibepyrone cluster genes *GPY1* (*FFUJ_12020*) and *GPY2* (*FFUJ_12021*), encoding a PKS and an ABC transporter, respectively, are represented by black arrows. The respective gene accession numbers are shown and dotted lines indicate the synteny. Genome sequences of *F. proliferatum* ET1 and *F. mangiferae* MRC7560 represent unpublished data.

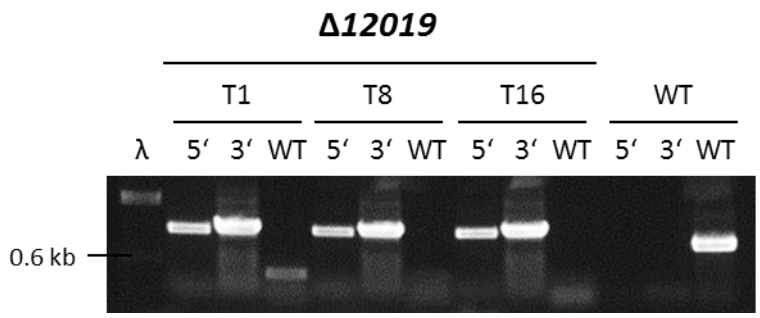

Figure S6. Verification of Δ*12019* deletion mutants by diagnostic PCR. Deletion *via* homologous recombination with the hygromycin B resistance cassette was underlined with the amplification of 5' (12019_5diag/trpC_T; 1.19 kb) and 3' (12019_3diag/trpC_P2; 1.22 kb) sequences but no amplification of wild-type signal (WT; 12019_WT_F/12019_WT_R; 0.86 kb) for independent transformants (T). λ: λ/*Hin*dIII.

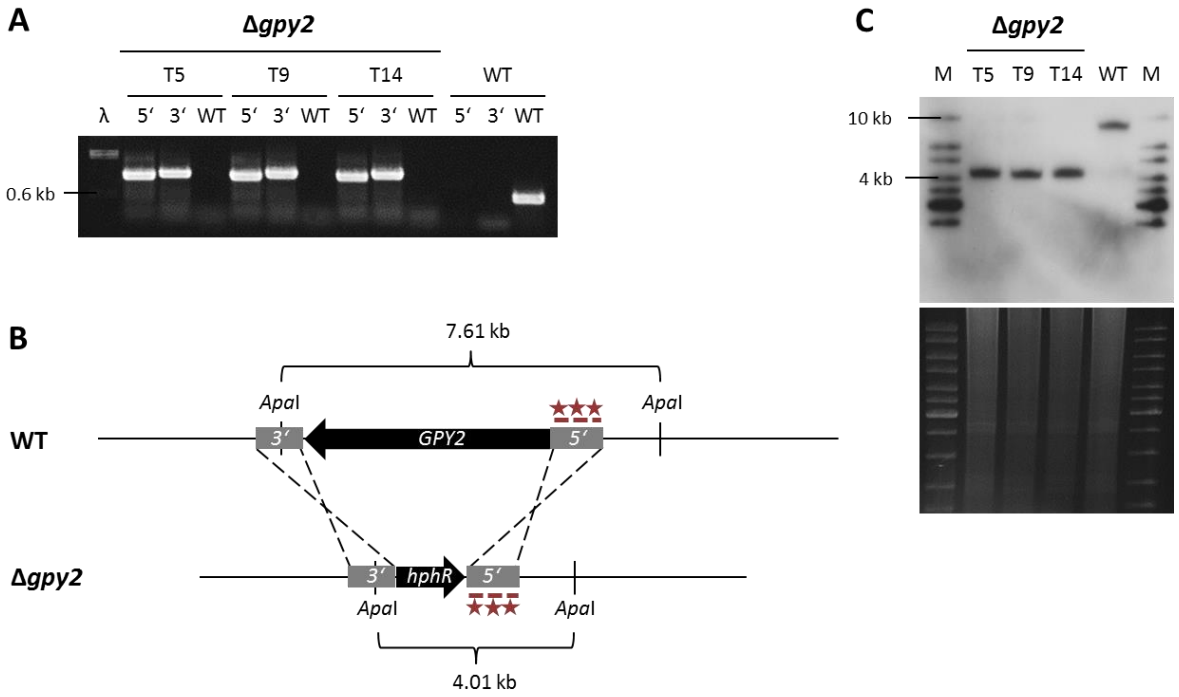

Figure S7. Verification of Δ*gpy2* (*FFUJ_12021*) deletion mutants by diagnostic PCR and Southern blot. Deletion *via* homologous recombination (*A*) with the hygromycin B resistance cassette (*hphR*) was underlined with the amplification of 5' (12021_5diag/trpC_T; 1.12 kb) and 3' (12021_3diag/trpC_P2; 1.19 kb) sequences but no amplification of wild-type signal (WT; 12021_WT_F/12021_WT_R; 0.58 kb) for independent transformants (T). For analyzing ectopic integration of deletion constructs, genomic DNA of transformants and WT was digested with *Apa*I (*B*) whereupon the 5' sequence was applied for probing. Detected signals match the expected 4.01 kb for Δ*gpy2* as well as 7.61 kb for the WT (*C*). λ: λ/*Hin*dIII, M: GeneRuler DNA Ladder Mix.

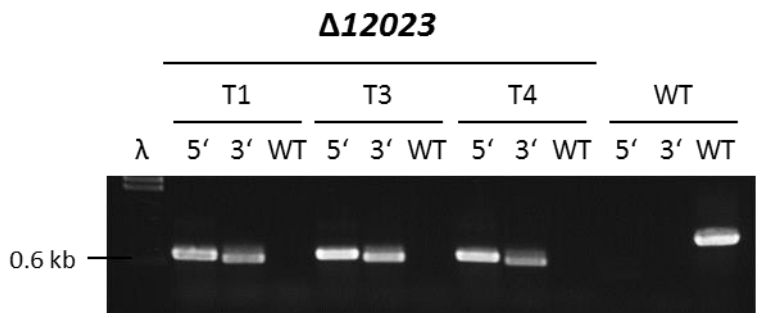

Figure S8. Verification of Δ*12023* deletion mutants by diagnostic PCR. Deletion *via* homologous recombination with the hygromycin B resistance cassette was underlined with the amplification of 5' (12023_5diag/trpC_T; 0.67 kb) and 3' (12023_3diag/trpC_P2; 0.63 kb) sequences but no amplification of wild-type signal (WT; 12023_WT_F/12023_WT_R; 0.91 kb) for independent transformants (T). λ: λ/*Hin*dIII.

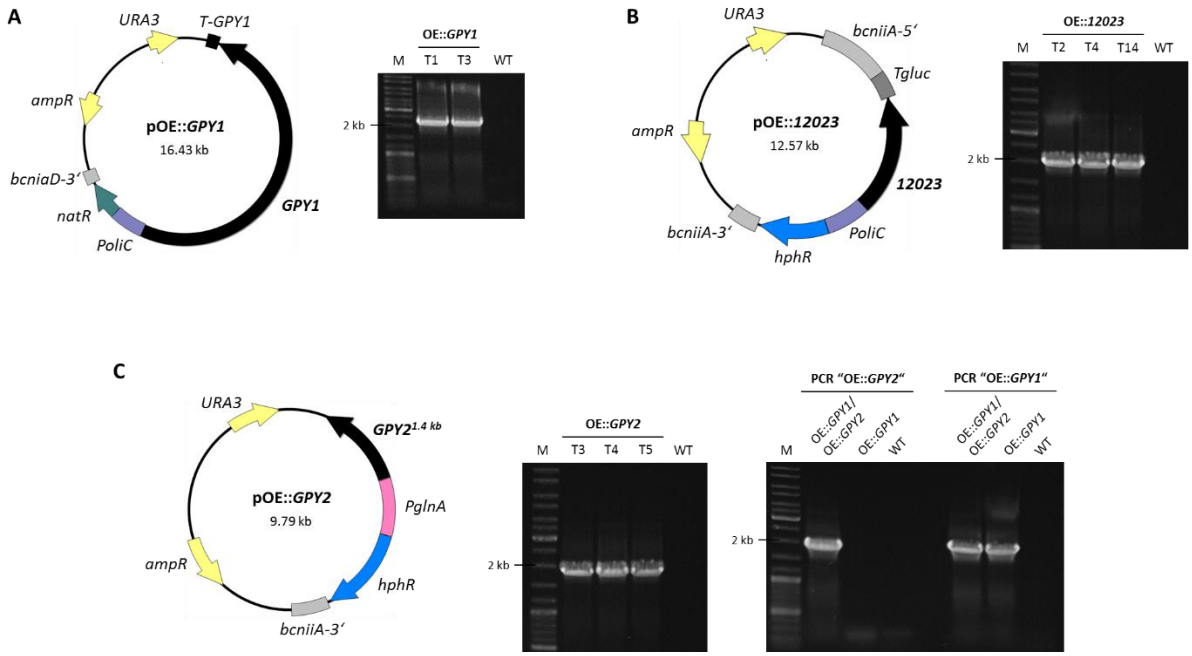

Figure S9. Overexpression of *GPY1* and *FFUJ_12023 via* constitutive *oliC* promoter from *A. nidulans* as well as overexpression of *GPY2 via PglnA* from *F. fujikuroi*. *A*, The full-length *GPY1* gene including ca. 300 bp of the native terminator sequence (*T-GPY1*) was cloned into *Nco*I/*Sac*II restricted pNDN-OGG conferring nourseothricin resistance (*natR*). The presence of pOE::*GPY1* in the overexpression transformants (T) was checked using primer pair PoliC_Seq_F2/12020_OE_diag (2.15 kb). *B*, The full-length *FFUJ_12023* gene was cloned into *Nco*I/*Not*I restricted pNAH-OGG conferring hygromycin B resistance (*hphR*). The presence of pOE::*12023* in the overexpression transformants (T) was checked using primer pair PoliC_Seq_F2/12023_WT_R (2.04 kb). *C*, The first 1.4 kb of *GPY2* (*GPY2*$^{1.4\ kb}$) were cloned into *Nco*I/*Sac*II restricted pNAH-GGT conferring hygromycin B resistance (*hphR*). The *in loco* integration of pOE::*GPY2* in the single overexpression mutants OE::*GPY2* T3-5 was checked using primer pair GS_Prom_M/12021_OE_diag (1.88 kb). Furthermore, the OE::*GPY1*/OE::*GPY2* double mutant was checked for the presence of both overexpression vectors as described above (PCR "OE::*GPY2*" and PCR "OE::*GPY1*"). M: GeneRuler DNA Ladder Mix, WT: wild type *F. fujikuroi* IMI58289.

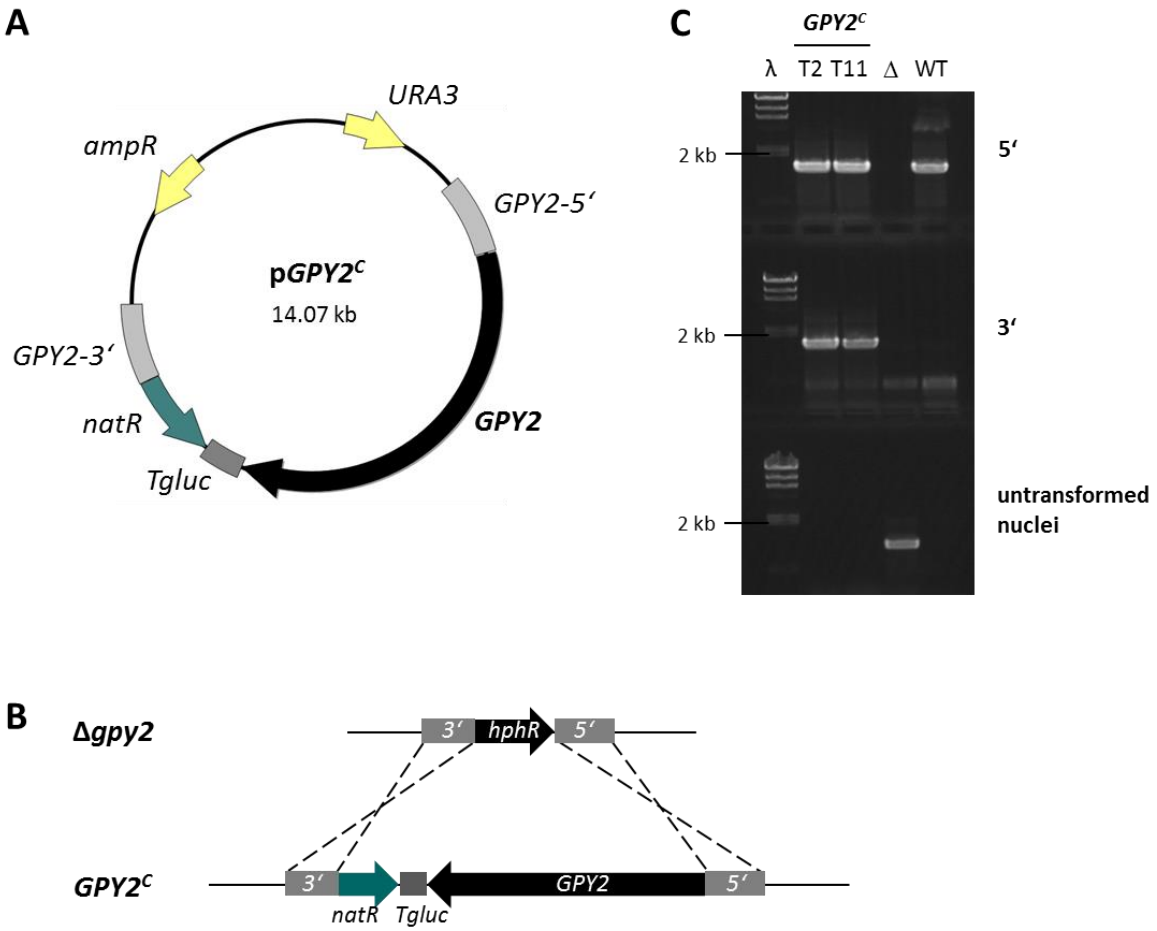

Figure S10. *In loco* complementation of *GPY2* encoding an ABC transporter. The deletion mutant Δ*gpy2* T9 was transformed with *Ase*I digested p*GPY2*^{C} harboring the full-length gene *GPY2* driven by its native promoter as well as the nourseothricin resistance cassette *natR* (*A*). The homologous integration of the construct (*B*) in the complemented transformants (T) was checked using primer pairs 12021_5diag/12021_c_diag (5‘), 12021_3diag/nat1_R1 (3‘) and 12021_5diag/trpC_T (untransformed nuclei) giving fragments of 1.42 kb, 1.55 kb and 1.12 kb, respectively (*C*). λ: λ/*Hin*dIII, Δ: Δ*gpy2* T9, WT: wild type *F. fujikuroi* IMI58289.

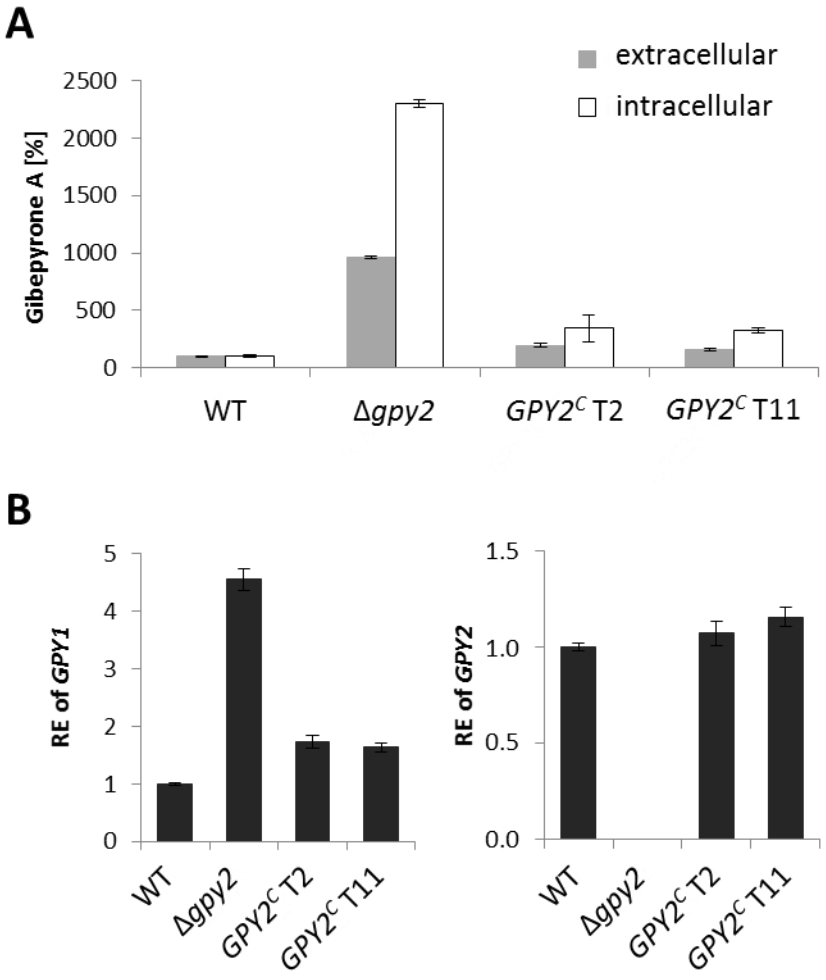

Figure S11. *In loco* complementation of the ABC transporter deletion mutant Δ*gpy2* restores wild-type *GPY1* expression and gibepyrone A product formation. *A*, HPLC-MS/MS analysis of extra- and intracellular gibepyrone A. The wild type (WT), Δ*gpy2* and the complemented transformants (T) were grown in the presence of 6 mM glutamine for seven days. Culture fluids were directly measured for extracellular gibepyrone A contents, while metabolite extraction from washed mycelium was applied prior to quantifying intracellular levels. The cultivation was carried out in triplicates and product formation of the WT was set to 100%. *B*, qRT-PCR analysis of the relative expression (RE) of *GPY1* and *GPY2* using the ΔΔCt method. Indicated strains were cultivated for three days whereupon total RNA was isolated from the harvested mycelium. Error bars (±SD) originate from a technical replicate and expression of the WT was arbitrarily set to 1.

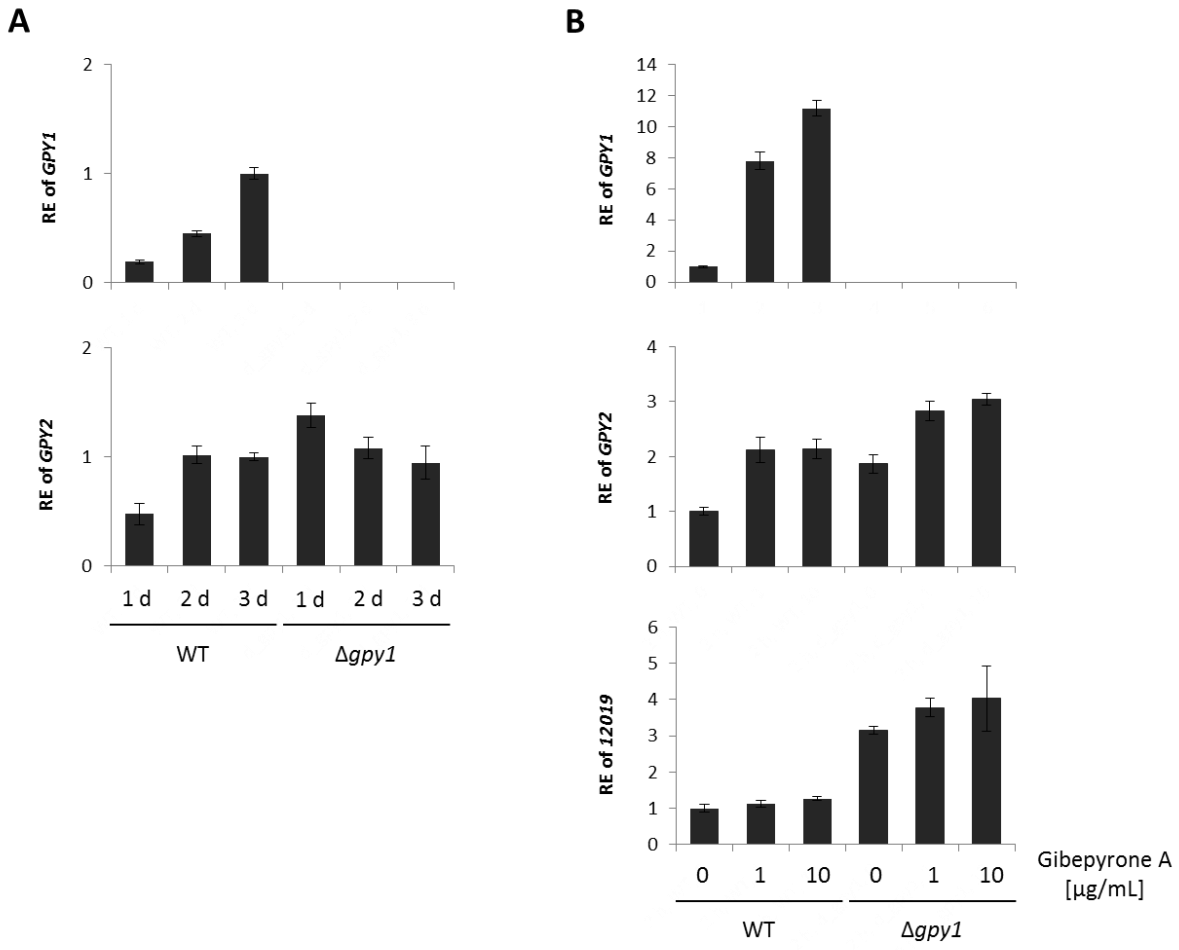

Figure S12. Expression of *GPY2* in the Δ*gpy1* mutant. *A*, qRT-PCR analysis of the relative expression (RE) of *GPY1* (PKS) and *GPY2* (ABC transporter) using the ΔΔCt method. The wild type (WT) and Δ*gpy1* were cultivated in the presence of 6 mM glutamine for 1-3 days (d) whereupon total RNA was isolated from the harvested mycelium. Error bars (±SD) originate from a technical replicate and expression of the WT at 3 d was arbitrarily set to 1. *B*, qRT-PCR analysis of the RE of *GPY1*, *GPY2* and *12019* (methyltransferase) using the ΔΔCt method. The WT and Δ*gpy1* were cultivated in the presence of 6 mM glutamine for 2 d whereupon indicated amounts of synthetic gibepyrone A were added for two additional hours. Total RNA was isolated from the harvested mycelium. Error bars (±SD) originate from a technical replicate and expression of the WT without supplement was arbitrarily set to 1.

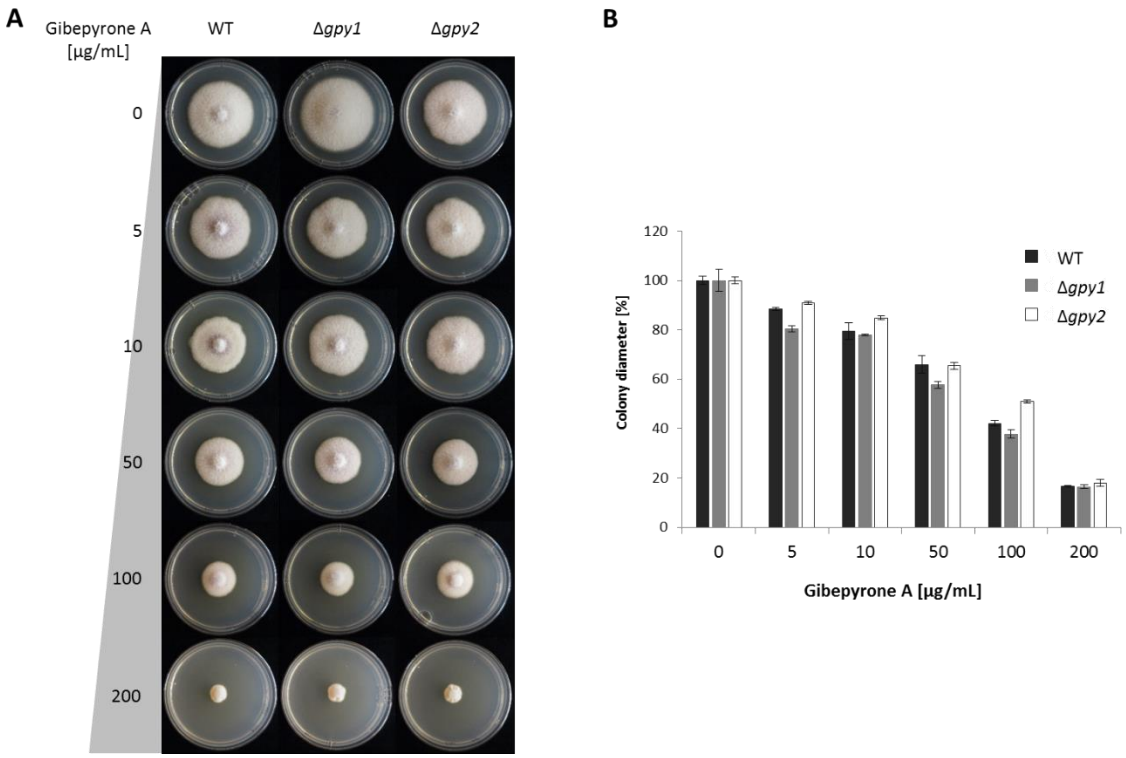

Figure S13. Vegetative growth of the wild type (WT), Δ*gpy1* and Δ*gpy2* mutants upon addition of gibepyrone A. *A*, 0-200 µg/mL synthetic gibepyrone A was supplemented to CM solid medium and the strains were incubated in triplicates for four days. *B*, The colony diameter (without mycelial plug) on CM without supplement was set to 100% for each strain.

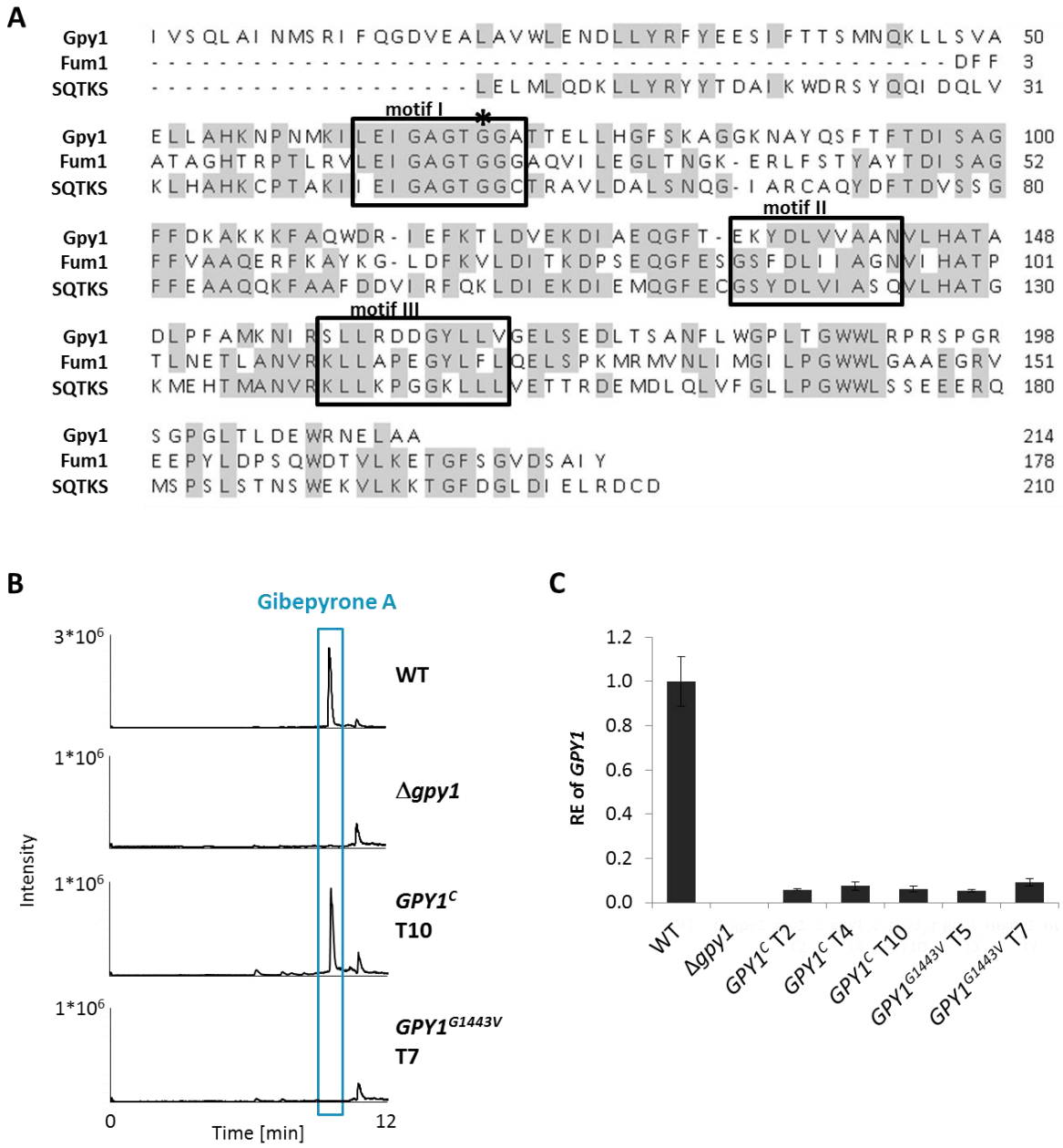

Figure S14. Loss of function mutation of the Gpy1 *C*-methyltransferase (*C*-MT) domain. *A*, Amino acid alignment of *C*-MT domains of Gpy1 (FFUJ_12020), Fum1 (*F. verticillioides* M-3125; GenBank accession no. AAD43562.2) and SQTKS (*Phoma* sp. C2932) (1). *C*-MT domains were identified with the InterPro database (IPR029063, *S*-adenosyl-L-methionine (SAM)-dependent methyltransferase) and were aligned using the ClustalW algorithm. Identical amino acids are highlighted in gray and *C*-MT motifs I, II and III according to Kagan and Clarke (2) are indicated. The introduced loss of function mutation of the Gpy1 *C*-MT domain, G1443V (*), lies within motif I that, together with residues within motif II, is directly involved in SAM substrate binding (1). *B*, HPLC-MS/MS analysis of culture fluids of the wild type (WT), Δ*gpy1* as well as transformants (T) complemented with the full-length gene ($GPY1^{C}$) or with the point-mutated variant ($GPY1^{G1443V}$). The strains were grown in the presence of 6 mM glutamine for seven days. *C*, qRT-PCR analysis of the relative expression (RE) of *GPY1* (PKS) using the ΔΔCt method. The WT, Δ*gpy1*, $GPY1^{C}$ and $GPY1^{G1443V}$ strains were cultivated in the presence of 6 mM glutamine for three days whereupon total RNA was isolated from the harvested mycelium. Error bars (±SD) originate from a technical replicate and expression of the WT was arbitrarily set to 1.

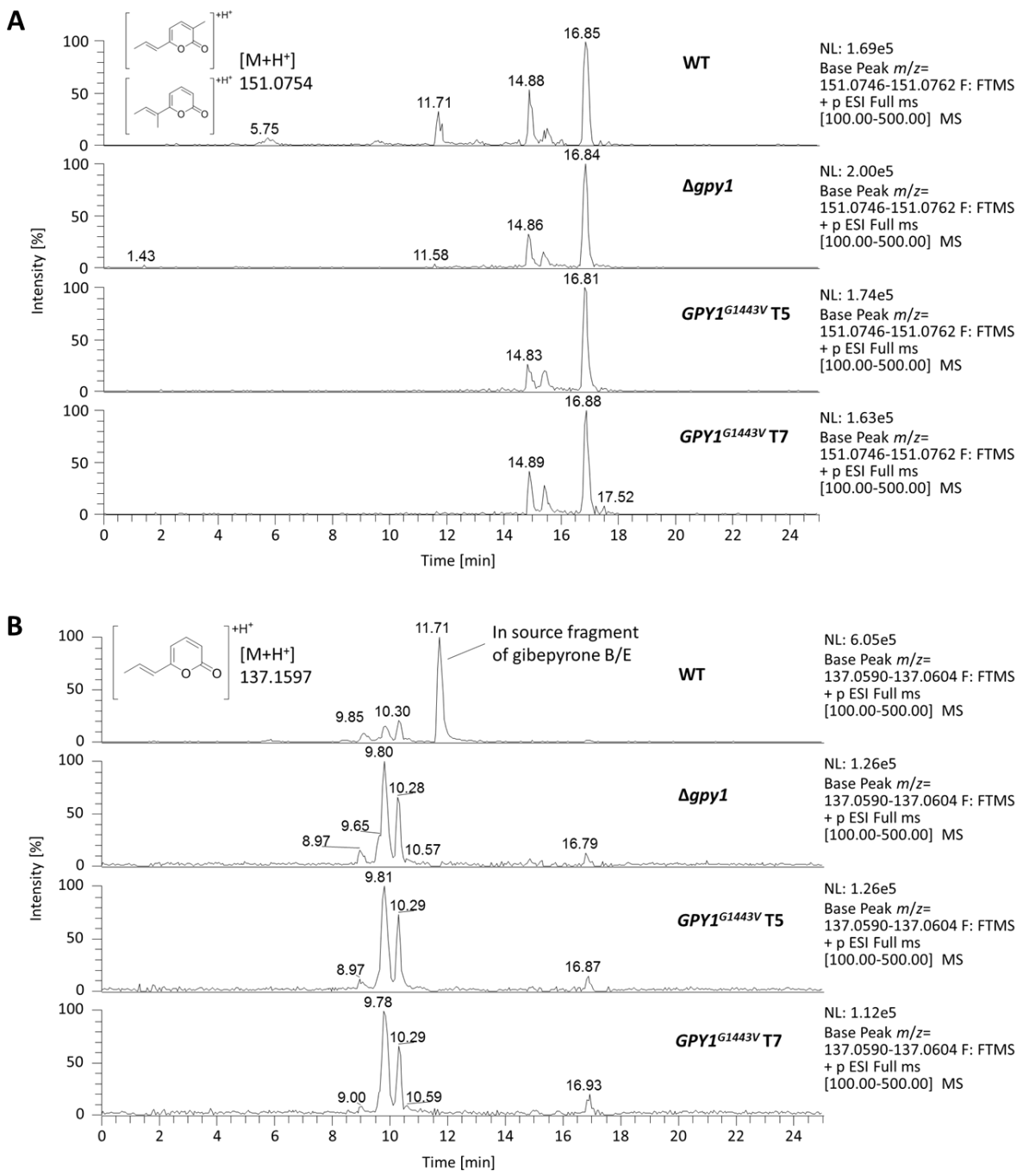

Figure S15. Analysis of non-methylated gibepyrone A derivatives in *GPY1*^{G1443V} mutants. HPLC-HRMS analysis of culture fluids of the wild type (WT), Δ*gpy1* and two independent transformants (T) of *GPY1*^{G1443V}. The strains were grown in the presence of 6 mM glutamine for seven days and the supernatant was analyzed without further processing. Shown are extracted ion chromatograms for the calculated masses of single-methylated (*A*) and completely non-methylated (*B*) gibepyrone A derivatives. No novel peak can be identified for the complemented mutants.

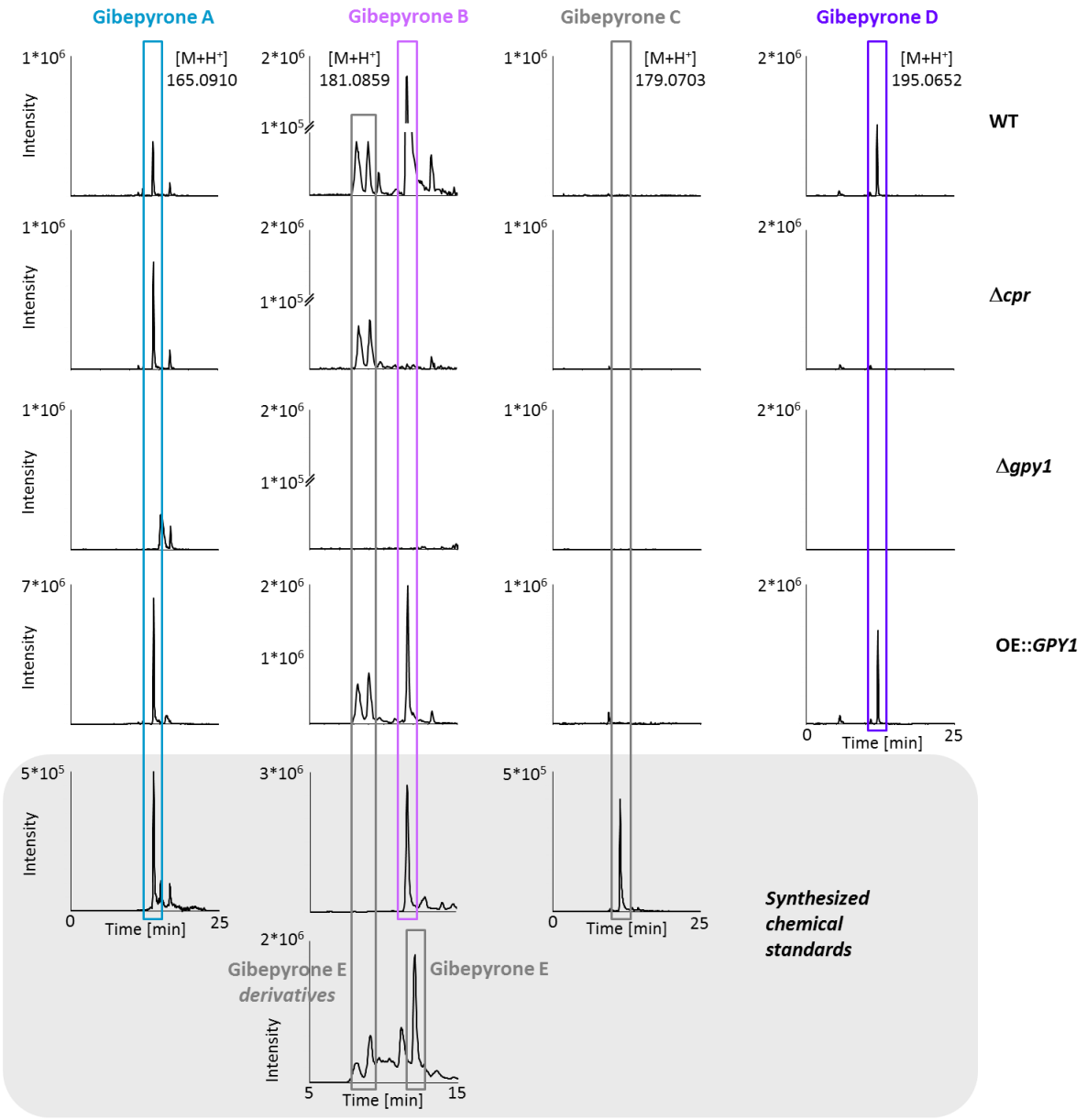

Figure S16. Production of gibepyrone A derivatives, gibepyrones B-E. HPLC-HRMS analysis of culture fluids of the wild type (WT) as well as the Δ*cpr*, Δ*gpy1* and OE::*GPY1* mutants. The strains were grown in the presence of 6 mM glutamine for seven days and the supernatant was analyzed without further processing. Shown are extracted ion chromatograms for the calculated masses of gibepyrones A-E for the four strains as well as for the synthesized chemical standards. The gibepyrone E peak cannot be found in the cultures. However, in the presence of water, both the cultures and the standard show an identical double peak, designated gibepyrone E derivatives.

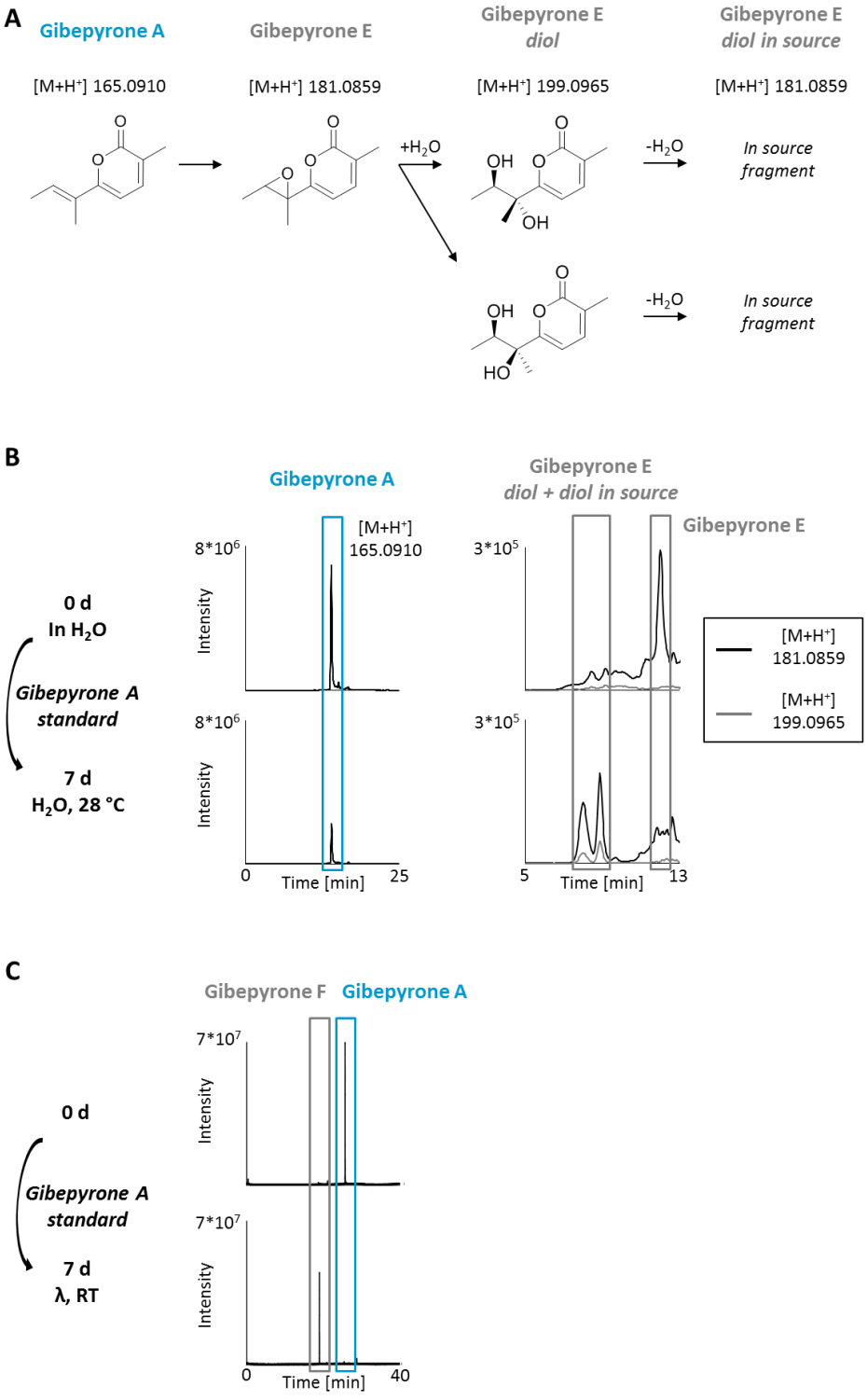

Figure S17. Spontaneous degradation of gibepyrone A to gibepyrones E and F. *A*, Proposed degradation of gibepyrone A to gibepyrone E and further conversion to gibepyrone E diols (in the presence of water) as well as diol in source fragments (during MS analysis). *B*, The synthetic gibepyrone A standard was incubated in water at 28 °C for seven days (d) and measured (in the presence of water) *via* HPLC-HRMS. Shown are extracted ion chromatograms for the calculated masses of gibepyrone A ([M+H$^+$] 165.0910) and gibepyrone E ([M+H$^+$] 181.0859) as well as gibepyrone E diols ([M+H$^+$] 199.0965). The gibepyrone E peak was verified through comparison with the synthesized chemical standard. *C*, The synthetic gibepyrone A standard was incubated in the presence of light (λ) at room temperature (RT) for seven days (d) and measured *via* GC-MS. Shown are extracted ion chromatograms for the calculated masses of gibepyrones A and F.

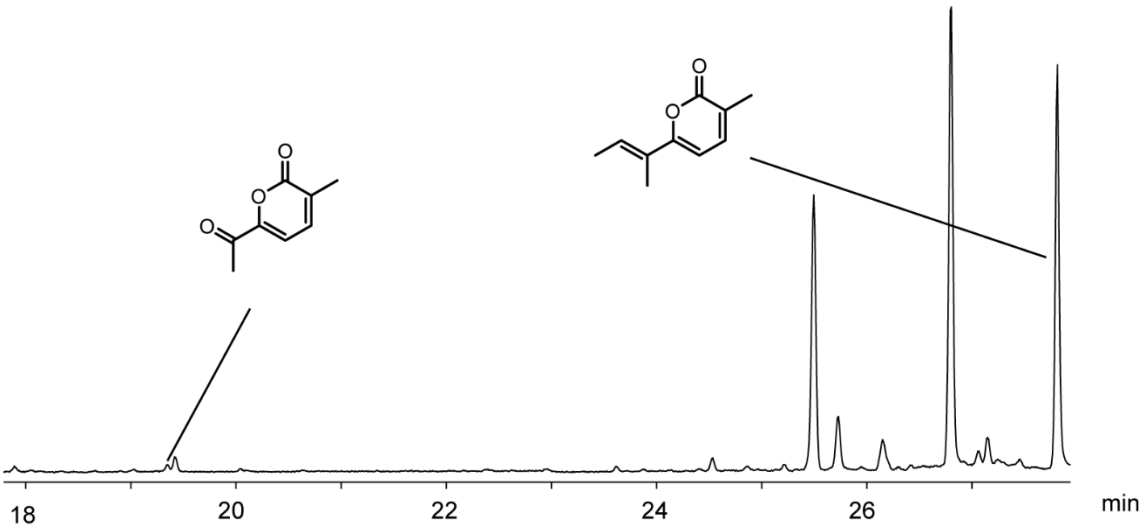

Figure S18. CLSA/GC-MS analysis of the Δ*cpr* mutant. Besides the parent compound gibepyrone A, also the oxidation product gibepyrone F is visible.

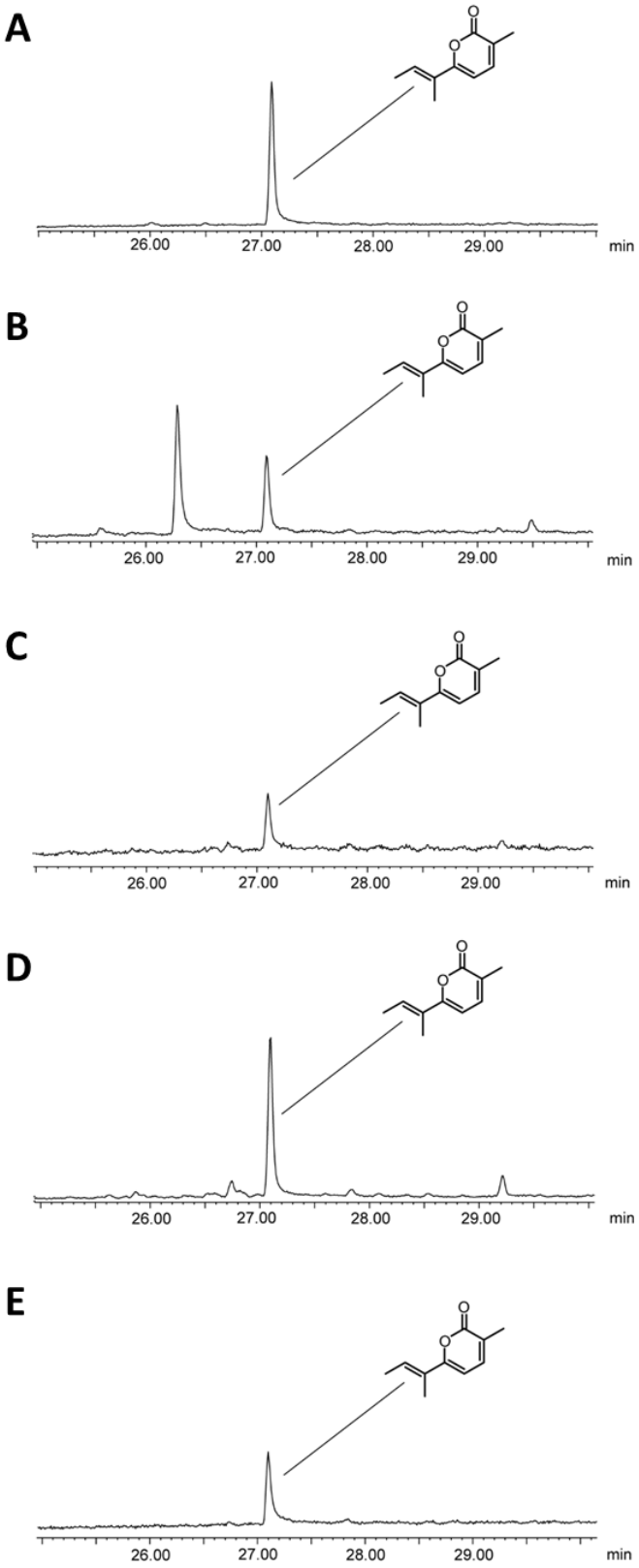

Figure S19. Total ion chromatograms obtained from *F. fujikuroi* and *F. solani* liquid culture extracts. All show production of the same compound, which is identified as gibepyrone A by comparison to the synthetic standard. *A*, *F. fujikuroi* IMI58289 grown in Abraham medium. *B*, *F. solani* DSM 62416 grown in Abraham medium. *C*, *F. fujikuroi* IMI58289 grown in ICI medium (6 mM glutamine). *D*, *F. solani* DSM 62416 grown in ICI medium (6 mM glutamine). *E*, Synthetic gibepyrone A standard.

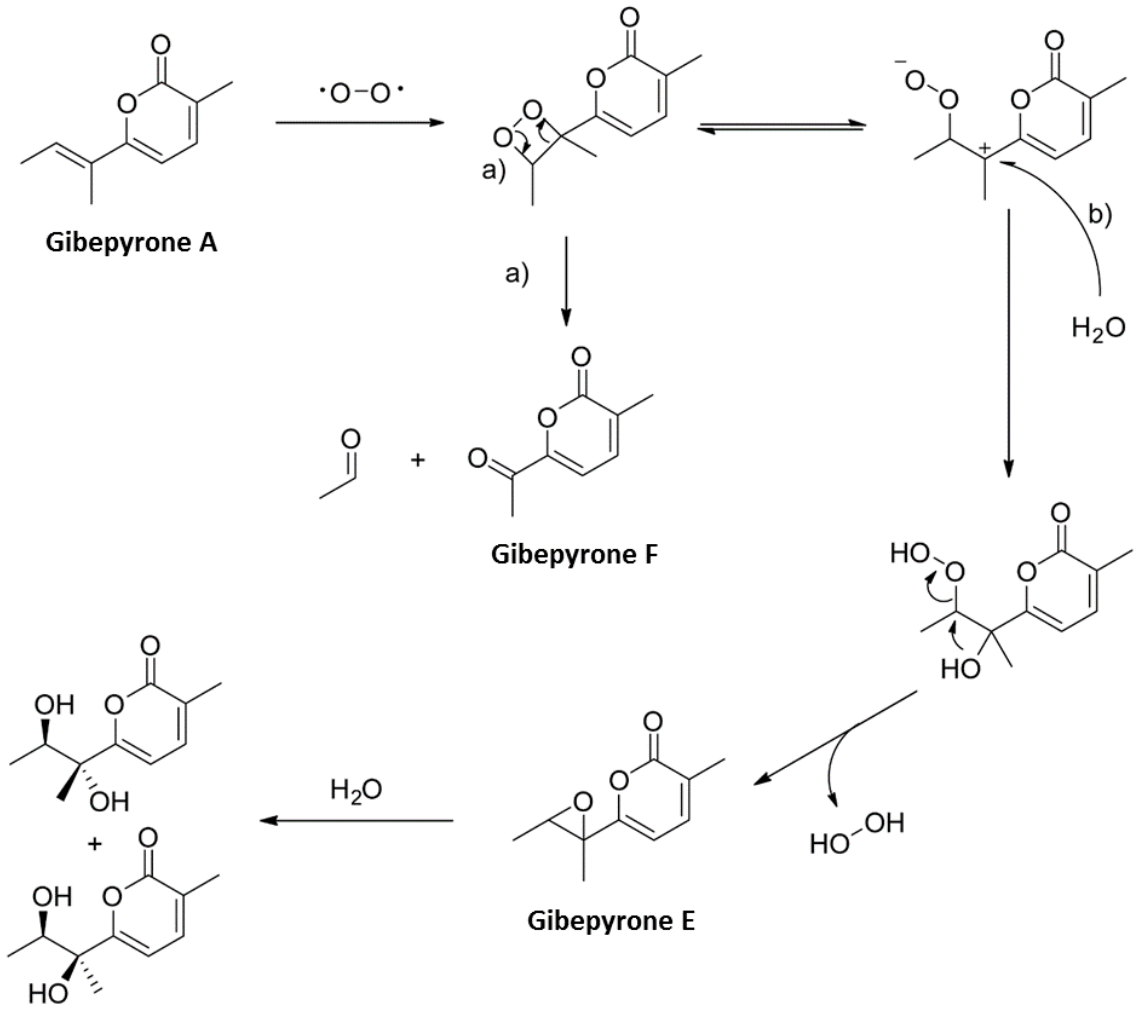

Figure S20. Putative reaction pathways for the oxidation of gibeyrone A towards gibepyrone F and gibepyrone E. The first step could be an addition of oxygen to the exocyclic double bond, giving a dioxetane structure. Without the presence of water, this compound may undergo a reversed [2+2] cycloaddition, giving gibepyrone F and acetaldehyde (path a). In an aqueous environment (path b), the dioxetane ring can open under attack of a water molecule, and subsequent elimination of hydrogen peroxide gives gibepyrone E. Gibepyrone E itself reacts fast in the presence of water to yield two diastereomeric diols.

Table S1. Primer sequences used for the generation of deletion constructs, verification of their homologous integration as well as for probe generation. Introduced overhangs required for yeast recombinational cloning are underlined.

Gene	Primer	Sequence 5' → 3'
12019	12019_5F	GTAACGCCAGGGTTTTCCCAGTCACGACGTAGCTATAGAGGTCCGATG
	12019_5R	ATCCACTTAACGTTACTGAAATCTCCAACTTTCGTTGCTAATAAACACG
	12019_3F	CTCCTTCAATATCATCTTCTGTCTCCGACTAGACCCTTTGATGGGAC
	12019_3R	GCGGATAACAATTTCACACAGGAAACAGCATCCAAGCTTCCCTCTTGTC
	12019_5diag	ATTCTGACTTCTCTAGTGG
	12019_3diag	CAACAGCCTTCTCAACCAAGACC
	12019_WT_F	GGACAACAATGAACGCGACTCG
	12019_WT_R	GCCATGAGATTCCTTCAGAACG
GPY1 (*12020*)	12020_5F	GTAACGCCAGGGTTTTCCCAGTCACGACGCGGTACCGTATTGGTTGGAGTC
	12020_5R	ATCCACTTAACGTTACTGAAATCTCCAACGGATAGTTCATGACACCACCGG
	12020_3F	CTCCTTCAATATCATCTTCTGTCTCCGACGGGTATACCACAGATTGGG
	12020_3R	GCGGATAACAATTTCACACAGGAAACAGCGGCGACATTGGAGACAAGAAG
	12020_5diag	CGGATCTGCTGATGTTTGCTGC
	12020_3diag	CATTGAACCAGTCCATCCACC
	12020_WT_F	CCAGCTCTATTACCCGTGCC
	12020_WT_R	CGCAATAAGCGAGTCCATTCC
GPY2 (*12021*)	12021_5F	GTAACGCCAGGGTTTTCCCAGTCACGACGTTAAGGTCTGTTACGAGACG
	12021_5R	ATCCACTTAACGTTACTGAAATCTCCAACCTGATTCGATCAGAGACAAAC
	12021_3F	CTCCTTCAATATCATCTTCTGTCTCCGACCTCGAGGATAAGATTATGC
	12021_3R	GCGGATAACAATTTCACACAGGAAACAGCTGCCTCAGGAGGACAGTGC
	12021_5diag	ACGTCTGTAAAGACTTGGACG
	12021_3diag	TAGCATAACGGGTGATACG
	12021_WT_F	TAGTCAATTCATTGCTCGG
	12021_WT_R	TGGAGCAGTTCCTTGGGATC
12023	12023_5F	GTAACGCCAGGGTTTTCCCAGTCACGACGGTGAGGCAGTTCAATTG
	12023_5R	ATCCACTTAACGTTACTGAAATCTCCAACGTCTGTGCCGTTGG
	12023_3F	CTCCTTCAATATCATCTTCTGTCTCCGACCGTCAGCGGATCCTGG
	12023_3R	GCGGATAACAATTTCACACAGGAAACAGCCGTTAAGCGATAGAG
	12023_5diag	CGGATAATGCTAGTAGC
	12023_3diag	CGAGGAGATTCAGACC
	12023_WT_F	GCTTGGATCCTCAAGCGG
	12023_WT_R	GTAGCACACAACGCAAGG
hphR	hph_F	GTCGGAGACAGAAGATGATATTGAAGGAGC
	hph_R	GTTGGAGATTTCAGTAACGTTAAGTGGAT
	trpC_T	GGAATAGAGTAGATGCCGACCGG
	trpC_P2	GTGATCCGCCTGGACGACTAAACC

Table S2. Primer sequences used for the generation and analysis of complementation and overexpression vectors. Introduced overhangs required for yeast recombinational cloning are underlined.

Gene	Primer	Sequence 5' → 3'
GPY1 (*12020*)	12020_c_F1	GCTGCCGGTGGTGTCATGAACTATCC
	12020_c_R1	GGAAGGGATTTGACAATCTCGGATG
	12020_c_F2	CATCCGAGATTGTCAAATCCCTTCC
	12020_c_R2	CCAATCTAGAGATCGGGTCATCATGC
	12020_c_F3	GCATGATGACCCGATCTCTAGATTGG
	12020_c_R3	TAATCATACATCTTATCTACATACGTCATCCGGCAATCATTCTAG
	12020_G1443V_F	GGTGCTGGAACTGTTGGTGCAACG
	12020_G1443V_R	CGTTGCACCAACAGTTCCAGCACC
	12020_OE_F	CCATCACATCACAATCGATCCAACCATGCCCTCCCAGATTCCAC
	12020_OE_R	GTAACGCCAGGGTTTTCCCAGTCACGACGCTAGACCCTTTGATGGGAC
	12020_c_Seq	CCGAGCGAGCGTATCACGG
	12020_Seq1	ACTGCAACAGCTATGGATCC
	12020_Seq2	AGATGGTGACAGCATTCGG
	12020_Seq3	TCATCAAGGTGGTCTTGGC
	12020_Seq4	CTCAAGGTTGGAGCAGGCCC
	12020_Seq5	CATCCCAGACAACGACAATGCC
	12020_Seq6	GAACACGGACGTCGCGTCTTG
	12020_Seq7	GGACGCGGCTGCGATTCC
	12020_Seq8	CATGGTTGAGAAGCGAGAGGTCG
	12020_Seq9	CAACAGCCTTCTCAACCAAGACC
	12020_Seq10	CGAGCTTATCACACTCGCGCC
	12020_Seq11	GCCAGAACAACTGACCGCCC
	12020_c_diag	GCCTGGGAGACGACATGCC
	12020_OE_diag	CTATTGCGCGCCACAGGAAAC
GPY2 (*12021*)	12021_c_R1	CGCTCGTACCACCAACAGAACTCTCATCTG
	12021_c_F2	CAGATGAGAGTTCTGTTGGTGGTACGAGCG
	12021_c_R2	TAATCATACATCTTATCTACATACGTCAAAGCTCGCCAGCCGAGT
	12021_OE_F	TCTTATCCCCGTATCACAACCACATTCACAATGCCGCCTCCCAATTGTC
	12021_OE_R	GTAACGCCAGGGTTTTCCCAGTCACGACGATGAGCCATAGTCCAATTGC
	12021_Seq1	TCAATTGCAGCGGGAGCCC
	12021_Seq2	GCGCACCTCGTCCATCTTGG
	12021_Seq3	GGGCTCTGGTGAGAGAGGCG
	12021_Seq4	CGGCGCCAGCGATAAAGACC
	12021_Seq5	CGTGTTGGGCGATCTTGCACC
	12021_Seq6	ATACGCCGAGATTGCACCGC
	12021_Seq7	CCCAGACGGATAGTGGAGTCACG
	12021_Seq8	GGACAGTCGGTCAAGGGTGTCG
	12021_Seq9	GAGCAGGAGATCATCCAAGGCC
	12021_c_diag	CGACAACGCTCGCTTGCG
	12021_OE_diag	GCGCGTCCAGACCAGTACCC
Tgluc	BcGlu_Term_F2	GCGGCCGCTTAGCGTATGTAGATAAGATGTATG
	Tgluc_Nat1_R	CCACTTAACGTTACTGAAATCTCCAACATCTTGTTGGGGGGAAGGGGT
natR	hph_R2	GTTGGAGATTTCAGTAACGTTAAGTGGATCGTATCTTATCGAGATCCTGAACACC
	nat1_R1	CAGTGCCTCGATGGCCTCGGCGTC
12023	12023_OE_F	CCATCACATCACAATCGATCCAACCATGGAACCTTCTTCATCCTC
	12023_OE_R	TAATCATACATCTTATCTACATACGTTAAGTATTGTCCGGGCTTC
	12023_Seq1	ACATCAGGTAGTGAAGTCTGG
	12023_Seq2	TGGATCAGACCAAGAAGCG
	12023_Seq3	AAAGTAGCCAGGTGCTCGG
	12023_Seq4	AGTAATTCGCCGTAAGCAACC
	12023_Seq5	TGAAGATAACGATACAGCGC
	12023_Seq6	ACATCGTCCAAACCGTCGC
PoliC	PoliC_Seq_F2	GGGAGACGTATTTAGGTGCTAGGG
PglnA	GS_Prom_M	ATGTCGAAGTATCTTCCCTGTGC

Table S3. Primer sequences used for expressional analysis by qRT-PCR. Reference genes: *GMT*, GDP mannose transporter gene; *RAC*, related actin gene; *UBI*, ubiquitin gene.

Gene	Primer	Sequence 5' → 3'
12019	12019_RT_F	GAGACGAGACACGGAGCGCC
	12019_RT_R	GTTGATGATCCAGGTGCCGGC
GPY1 (*12020*)	12020_RT_F	CGCTCGACACATCATTCTGGCC
	12020_RT_R	CCGACAGGTGTATCGATGGAAGC
GPY2 (*12021*)	12021_RT_F	GCTGCGCCAGGCAGTATTCG
	12021_RT_R	GAAGCGAGAGGTTGGCTGATGG
12022	12022_RT_F	CCCTTCCTCGGTCTCGAGACTG
	12022_RT_R	GCGGTAGCTTGTCGATGCGG
12023	12023_RT_F	AGGATATAGCGGCGTGTAGCGG
	12023_RT_R	GTTGTAGTGCCCCCGACAACG
GMT (*07710*)	FGMTRTPCRFW	CGGGCCATTCTCTATTCTTTC
	FGMTRTPCRRV	ATGCTGTGATGGCAACAATG
RAC (*05652*)	FRACRTPCRFW	GAGAACGAGCGTGTCTTGATTGAGCC
	FRACRTPCRRV	TTTCCTCCGCAGAATGAAGAAGGACTC
UBI (*08398*)	FUBRTPCRFW	CCAACCCTGACGATCCTCTTGTGC
	FUBRTPCRRV	TACTTTCGAGTCCACTCCCGAGCTG

References

1. Skellam, E.J., Hurley, D., Davison, J., Lazarus, C.M., Simpson, T.J., and Cox, R.J. (2010) Mutation of key residues in the *C*-methyltransferase domain of a fungal highly reducing polyketide synthase. *Mol.Biosyst*. **6,** 680-682

2. Kagan, R.M., and Clarke, S. (1994) Widespread occurrence of three sequences motifs in diverse *S*-adenosylmethionine-dependent methyltransferases suggests a common structure for these enzymes. *Arch.Biochem.Biophys*. **310,** 417-427

Gibepyrone biosynthesis in the rice pathogen Fusarium fujikuroi is facilitated by a small polyketide synthase gene cluster

Slavica Janevska, Birgit Arndt, Eva-Maria Niehaus, Immo Burkhardt, Sarah M. Rösler, Nelson L. Brock, Hans-Ulrich Humpf, Jeroen S. Dickschat and Bettina Tudzynski

J. Biol. Chem. published online November 17, 2016
